Modeling the magnetized interstellar medium in Star Forming Galaxies

Dieter Breitschwerdt

Zentrum für Astronomie und Astrophysik
Technische Universität Berlin

ZAA

Collaborators

* Miguel de Avillez (Evora, Portugal)
* Ernst Dorfi (Vienna, Austria)
* Ingo Philipp (Vienna, Austria)
* Michael Schulreich (Berlin, Germany)
* Georg Zwettler (Vienna, Austria)

Overview

* Introduction
* Halo Dynamics
* Plasma Models of Galactic Halos
* Galactic Wind Theory & Models
* Self-consistent modeling of galactic outflows & ionization structure
* Electron transport in NGC 891 and NGC 253
* Diffuse radial γ-ray gradient in the Milky Way
* Cosmic Ray Acceleration Beyond the "Knee"
* Summary

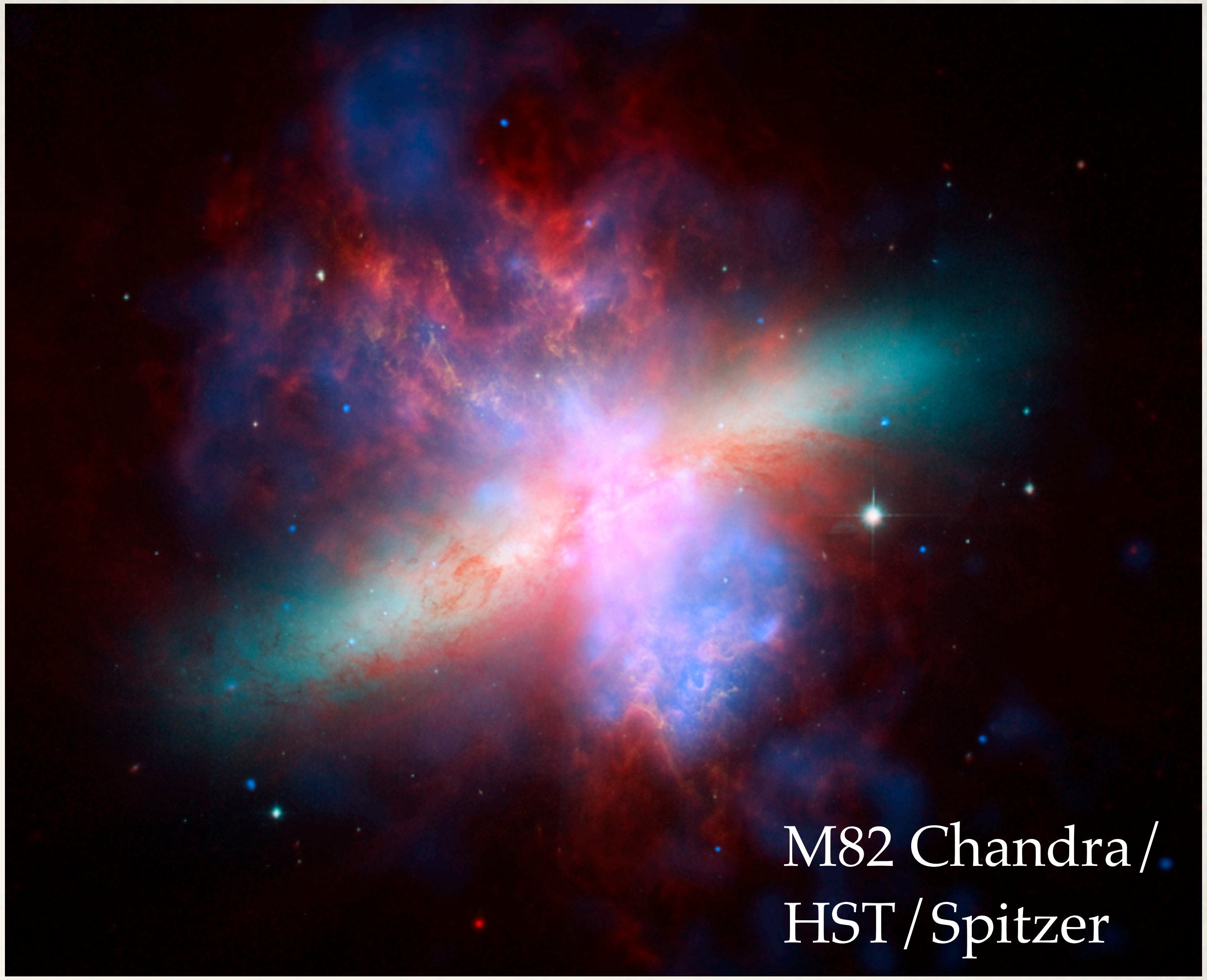

- **Galaxies** are essential building blocks of the Universe
- they presumably form by hierarchical merging events
- **feedback processes** in the disk and halo become ever more important for their appearance and evolution ➔ **Galactic Cosmic Matter Cycle**
- **star formation** generates hot plasma, "metals", CRs, B-fields in disk & halo
- no hydrostatic halo ➔ **superbubbles**, **outflows** (fountain & winds)

ISM in Galaxies

- Morphology of Galaxies: **Bulge**, **Disk**, **Halo**
- Active star formation in disk galaxies ➔ gas and dust
- Important components to consider: **Magnetic fields, cosmic rays**

	Gas Phase	T [K]	n[cm^{-3}]	f_V	f_M
I	MM1) = Molecular Medium (H_2)	~ 20	~ 10^3	0.01	0.3-0.6
II	CNM = cold neutral medium	~ 100	20 – 60	0.05	
III	WNM = warm neutral medium	~ 6000	~ 0.05 – 0.3	0.3 – 0.4	
IV	WIM = warm ionized medium	~ 8000	~ 0.1 – 0.5	0.1 – 0.2	
V	HIM2) = hot ionized medium	~ 10^6	~ 10^{-3}	0.5	~ 0.01

1) not in pressure equilibrium (gravitationally bound)
2) no phase transition, heated by SNRs and superbubbles

- According to classical theory gas exists in various stable **phases** in the p-V-diagramm
- Transitions possible by **heating** and **cooling**
- **star formation** drives matter cycle

➔ **how does the interstellar gas evolve?**

High Resolution ISM Simulations

- Solve full **HD/MHD equations** on a large grid: **1 kpc × 1kpc × ± 10 kpc** (Δx=0.625 pc or less)
- Type Ia,b,c/II SNe random + clustered in disk
- background heating due to diffuse UV photon field
- gravitational field by stars + self-gravity
- SFR ∝ local density/temp.: **n >10 cm^{-3}/T<100 K**
- formation and motion of OB associations (**➔** random velocity of stars)
- Evolution of computational volume for τ ~ 400 My
- ➔ sufficiently long to erase memory of initial conditions!
- 3D calculations on parallel processors with adaptive mesh refinement (**AMR**)

High Resolution ISM Simulations

- Numerical solution of HD/MHD-Eqs.

$$\frac{\partial \rho}{\partial t} + \nabla \cdot \vec{u} = q$$

$$\frac{\partial \rho \vec{u}}{\partial t} + \nabla \cdot \underline{\mathrm{T}} = \rho \vec{f} + \vec{m}$$

$$\frac{\partial W}{\partial t} + \nabla \cdot \vec{S} = \rho \vec{u}(\vec{f} + \vec{m}) + W_0$$

$$\vec{E} = -\frac{1}{c}\left[\vec{u} \times \vec{B}\right]$$

$$\frac{\partial \vec{B}}{\partial t} = -c\left[\nabla \times \vec{E}\right]$$

$$\nabla \cdot \vec{B} = 0 \,(\text{as initial condition})$$

- ideal MHD ($\sigma \to 0$)

- with

$$\underline{\mathrm{T}} = \rho \vec{u} \otimes \vec{u} + \left[P + \frac{B^2}{8\pi}\right] \cdot \underline{\mathrm{I}} - \frac{\vec{B} \otimes \vec{B}}{4\pi}$$

$$W = \frac{1}{2}\rho u^2 + \frac{P}{\gamma - 1} + \frac{B^2}{8\pi}$$

$$\vec{S} = \left(\frac{1}{2}u^2 + \frac{\gamma}{\gamma - 1}\frac{P}{\rho}\right)\rho \vec{u} + \frac{\vec{E} \times \vec{B}}{4\pi}$$

- Realistic **boundary conditions**: mass, momentum, energy input by SNe and stellar winds
- **source terms**: $q=M_{ej}/(V_{ej}\ t_0)$, $m=q\ V_{ej}$, $dW_0/dt=(W_{k0}+W_{th})/t_0$
- external body force: gravitational field
- background heating, interstellar cooling

SNR/SB Driven Outflows

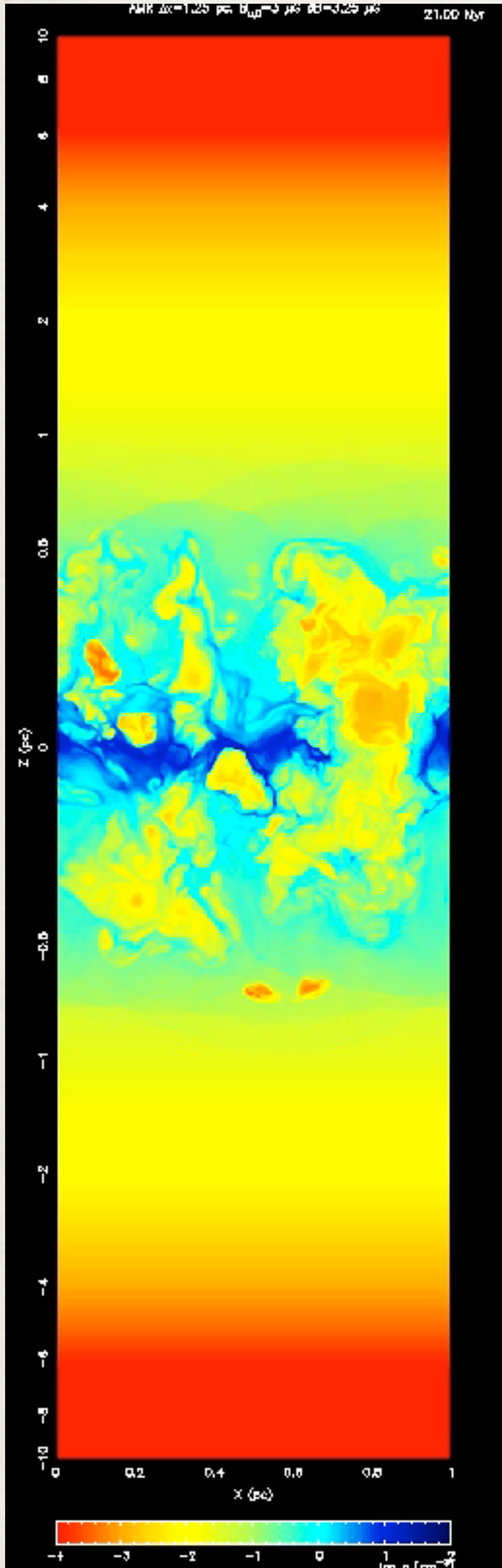

Avillez & Breitschwerdt (2004)

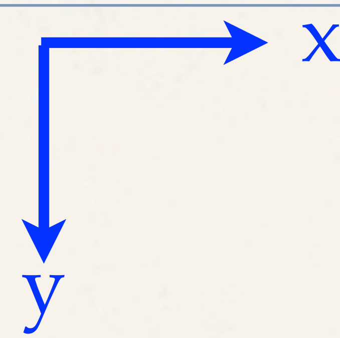

SNR/SB Driven Outflows

Avillez & Breitschwerdt (2004)

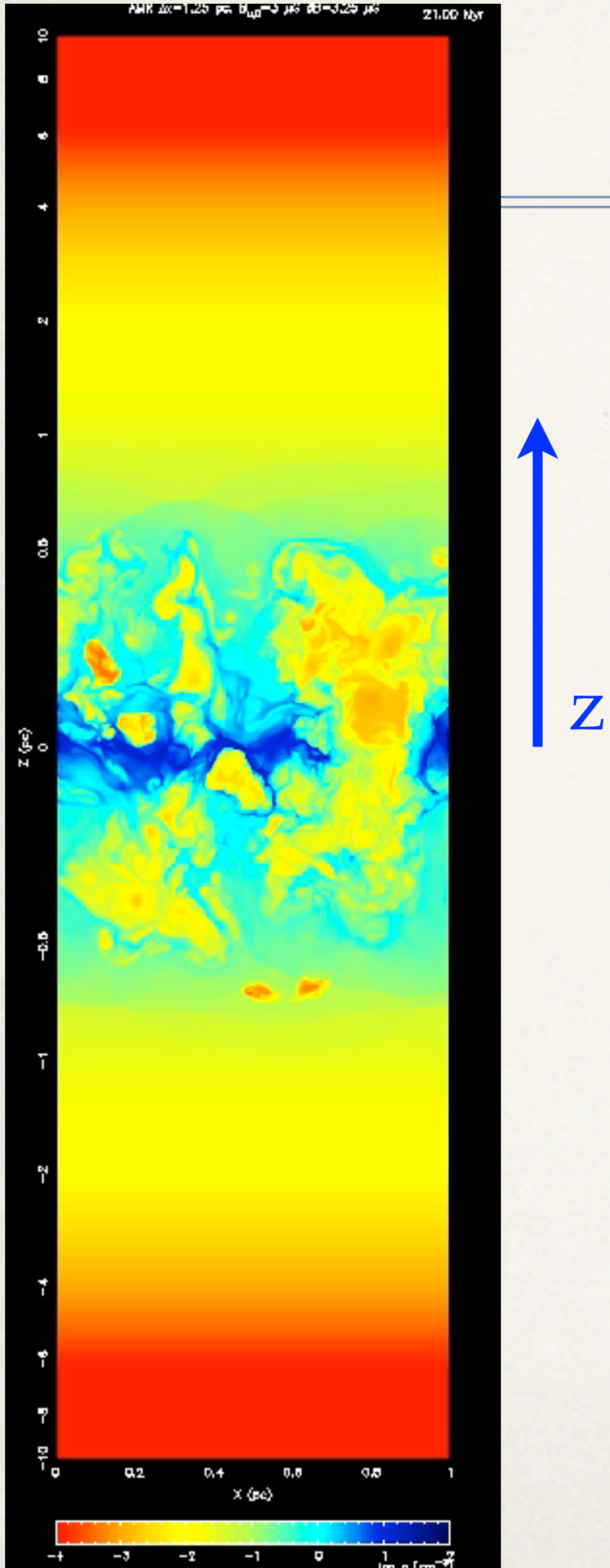

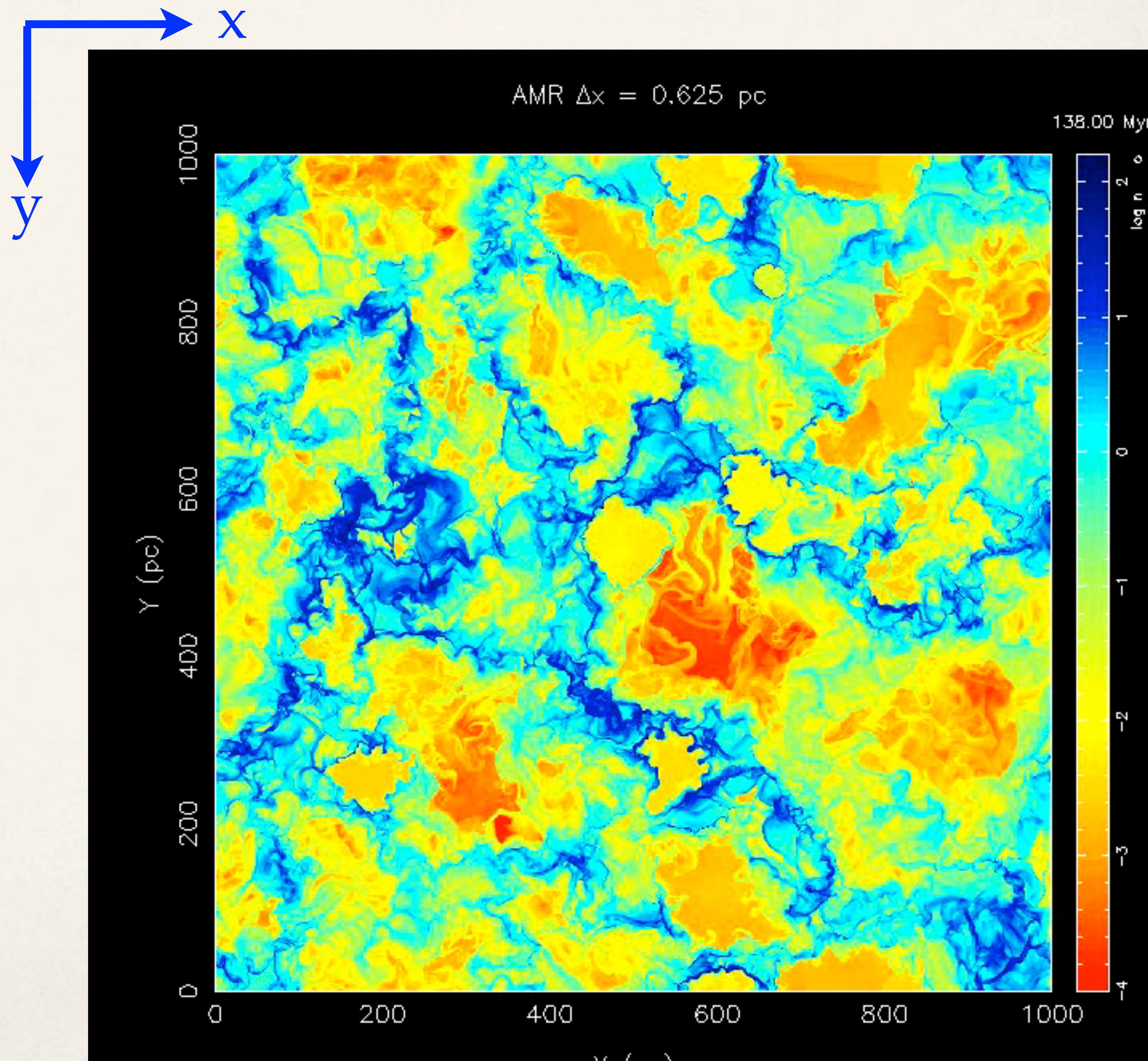

HD-Evolution of ISM II

Results

Avillez & Breitschwerdt, 2010

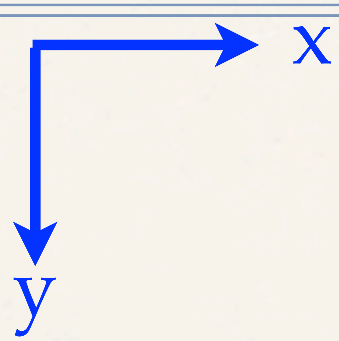

- **Collective** effect of SNe induces **break-out** of ISM disk gas ➔ "**gal-actic fountain**" (cf. intermediate vel-ocity clouds) ➔ reduce disk pressure
- Density and temperature distribu-tion shows **structures on all scales** (cf. observation of filaments)
- **shear flow** due to expanding SNRs generate high level of **turbulence** ➔ **coupling of scales**
- Cloud formation by **shock compres-sed layers** ➔ clouds are **transient** features ➔ generation of new stars
- large amount of gas in **thermally unstable** phases
- **volume filling factor** of HIM ~ 20%
- **no pressure equilibrium!**

HD-Evolution of ISM II

Results

Avillez & Breitschwerdt, 2010

- **Collective** effect of SNe induces **break-out** of ISM disk gas ➔ “**gal-actic fountain**” (cf. intermediate vel-ocity clouds) ➔ reduce disk pressure
- Density and temperature distribu-tion shows **structures on all scales** (cf. observation of filaments)
- **shear flow** due to expanding SNRs generate high level of **turbulence** ➔ **coupling of scales**
- Cloud formation by **shock compres-sed layers** ➔ clouds are **transient** features ➔ generation of new stars
- large amount of gas in **thermally unstable** phases
- **volume filling factor** of HIM ~ 20%
- **no pressure equilibrium!**

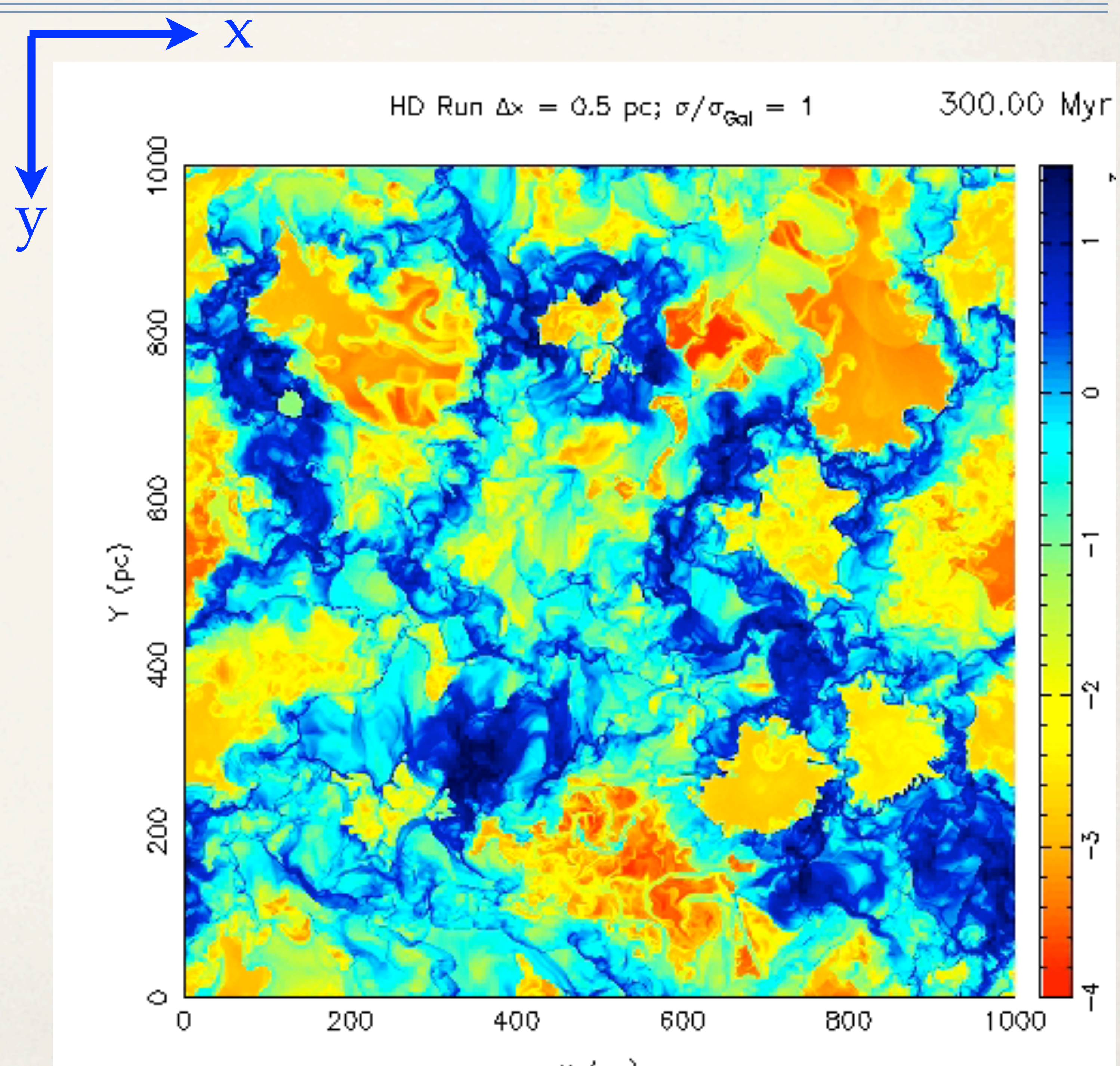

Turbulence I

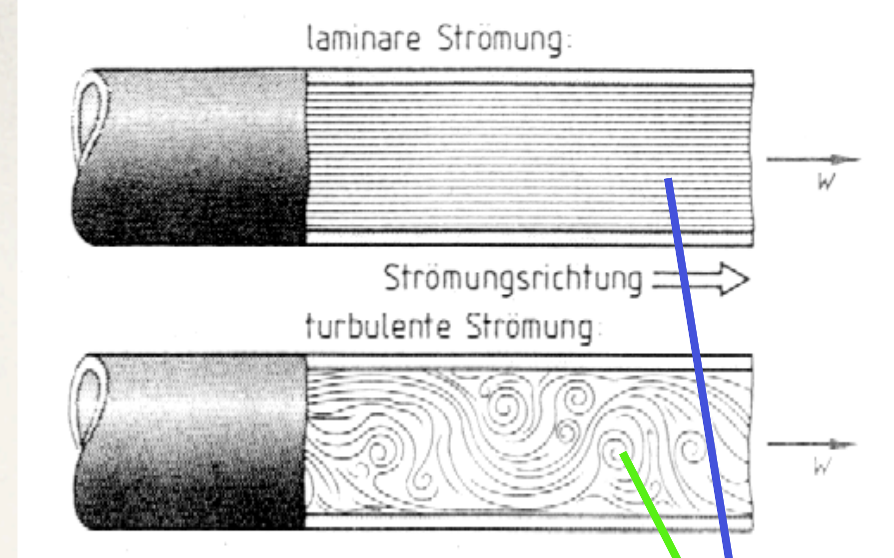

- ISM is highly **compressible** and **turbulent** medium (C.F. v. Weizsäcker 1951)
- Reynolds number **Re**=u L/ν ~**10^6 - 10^7** high
- Term (u∇)u is **non-linearity in Navier-Stokes (NS) equations**

$$\nabla\left(\frac{u^2}{2}\right) = (\vec{u}\nabla)\vec{u} + \vec{u}\times\vec{\omega},\ \vec{\omega} = \nabla\times\vec{u}$$

write NS eqs. as function of **vorticity** ω:

$$\frac{\partial\vec{\omega}}{\partial t} = \nabla\times[\vec{u}\times\vec{\omega}] + \nu\Delta\vec{\omega}$$

and since

$\nabla\times[\vec{u}\times\vec{\omega}] = (\vec{\omega}\cdot\nabla)\vec{u} - (\vec{u}\cdot\nabla)\vec{\omega}$ we get:

$$\frac{D\vec{\omega}}{Dt} \equiv \frac{\partial\vec{\omega}}{\partial t} + (\vec{u}\cdot\nabla)\vec{u} = (\vec{\omega}\cdot\nabla)\vec{u} + \nu\Delta\vec{\omega}$$

Change of vorticity due to:

Change of moment of inertia by stretching of fluid element (b))

Viscous torques spin up or slow down fluid element (a) and change vorticity

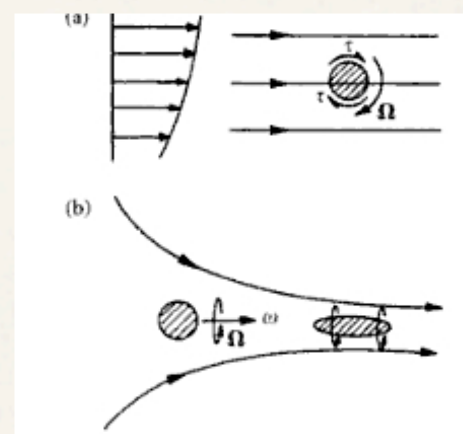

Figure 2.8 Vorticity can change because: (a) viscous forces spin up (or slow down) a fluid element or (b) because the moment of inertia of that element is changed.

$$\overbrace{\rho\left(\underbrace{\frac{\partial\mathbf{v}}{\partial t}}_{\text{Unsteady acceleration}} + \underbrace{\mathbf{v}\cdot\nabla\mathbf{v}}_{\text{Convective acceleration}}\right)}^{\text{Inertia (per volume)}} = \overbrace{\underbrace{-\nabla p}_{\text{Pressure gradient}} + \underbrace{\mu\nabla^2\mathbf{v}}_{\text{Viscosity}}}^{\text{Divergence of stress}} + \underbrace{\mathbf{f}}_{\text{Other body forces}}$$

Navier-Stokes Eq. for Newtonian fluids

Turbulence II

- **Turbulence**: 3D chaotic solution of Navier-Stokes eq.
- Stretching of fluid elements leads to increase of vorticity
  ➔ **“vortex tubes”**

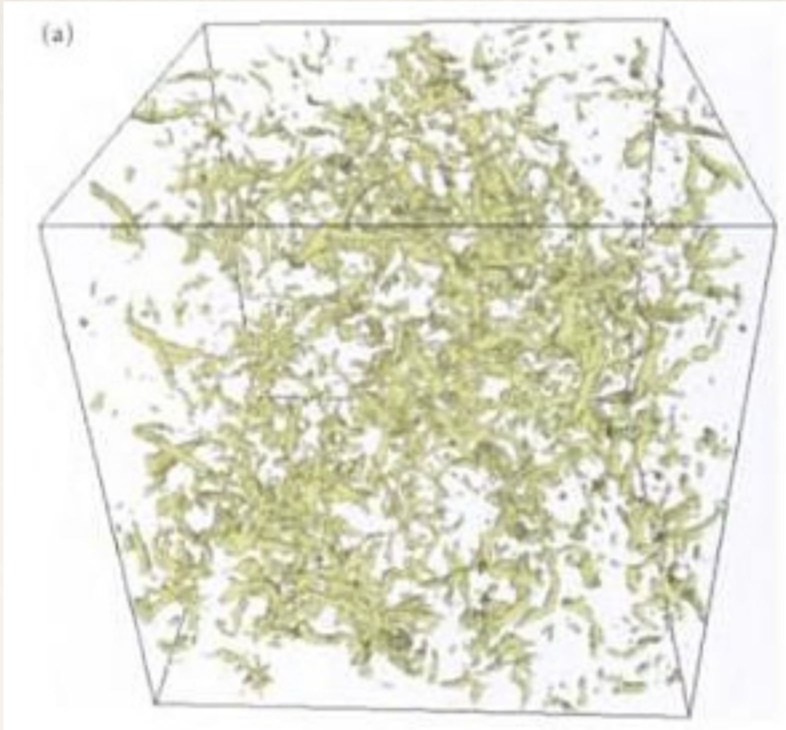

Large Eddy Simulation of isotropic turbulence in a periodic box; shown are contours of vorticity

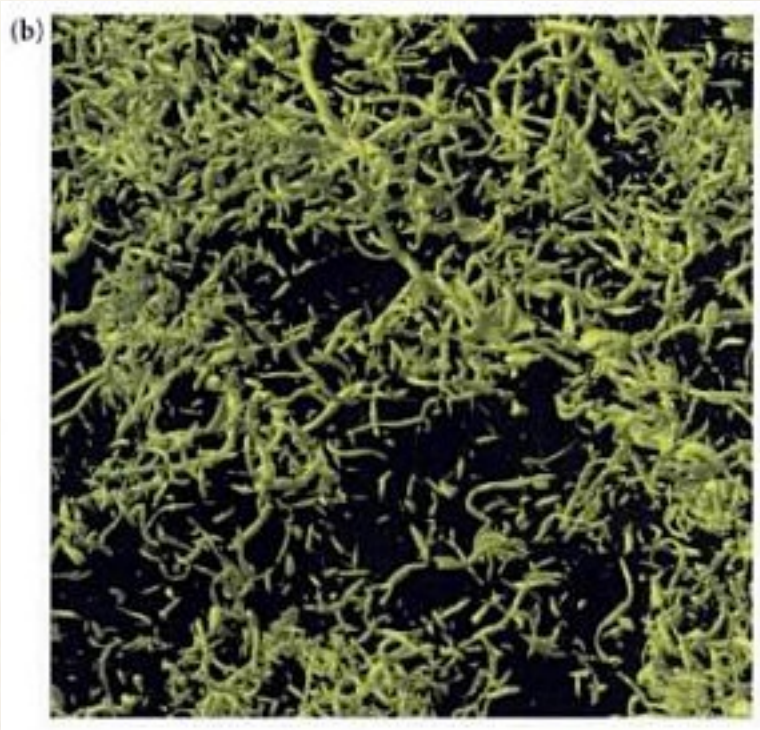

Direct Numerical Simulation of isotropic turbulence (s.a.); Re ~1200 (Credit: Davidson)

3D-Simulation of a laboratory jet in a non-reactive gas, Re ~21000; 2D-Projektion; Credit: D. Glaze (Purdue University); velocity field is marked by arrows

Turbulence II

- **Turbulence**: 3D chaotic solution of Navier-Stokes eq.
- Stretching of fluid elements leads to increase of vorticity
  ➔ **"vortex tubes"**

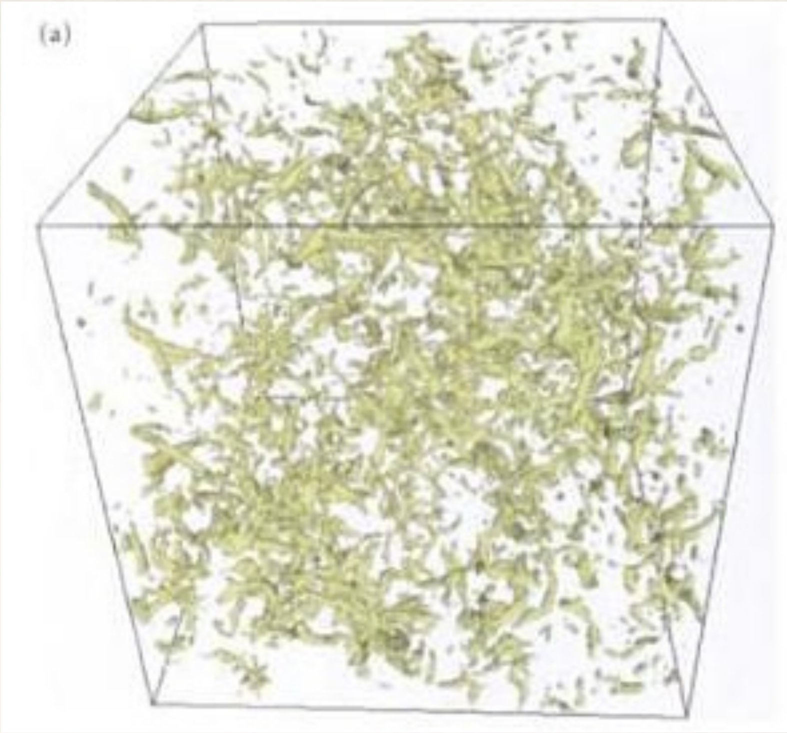

Large Eddy Simulation of isotropic turbulence in a periodic box; shown are contours of vorticity

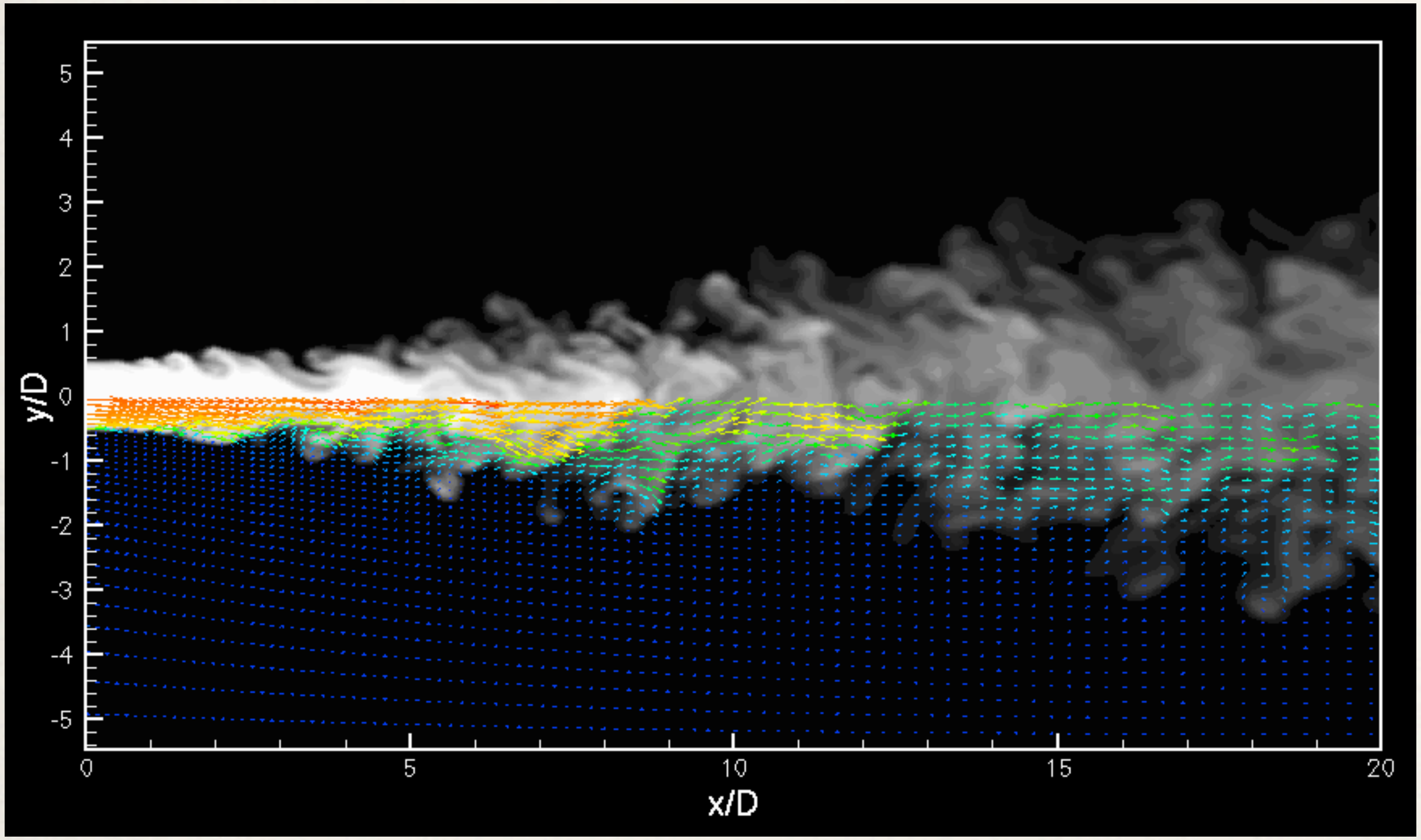

3D-Simulation of a laboratory jet in a non-reactive gas, Re ~21000; 2D-Projektion; Credit: D. Glaze (Purdue University); velocity field is marked by arrows

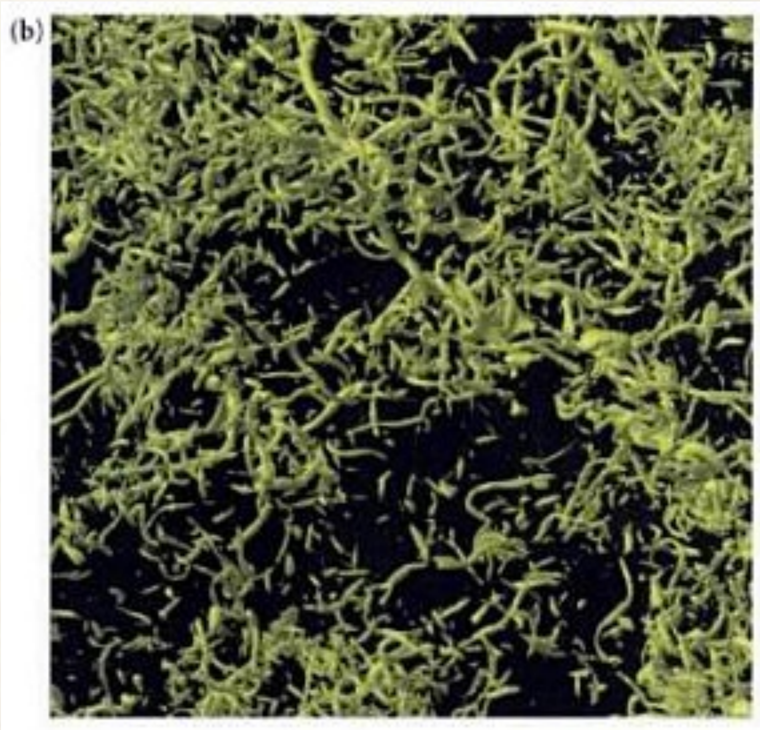

Direct Numerical Simulation of isotropic turbulence (s.a.); Re ~1200 (Credit: Davidson)

MHD-Evolution of ISM (I)

Avillez & Breitschwerdt, 2005a

MHD-Evolution of ISM (I)

Avillez & Breitschwerdt, 2005a

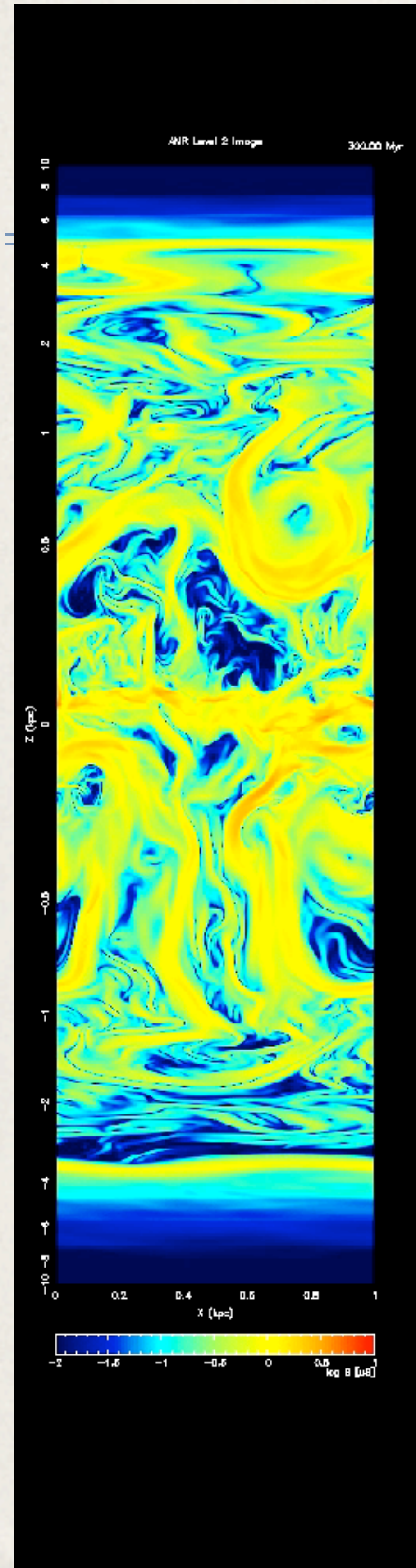

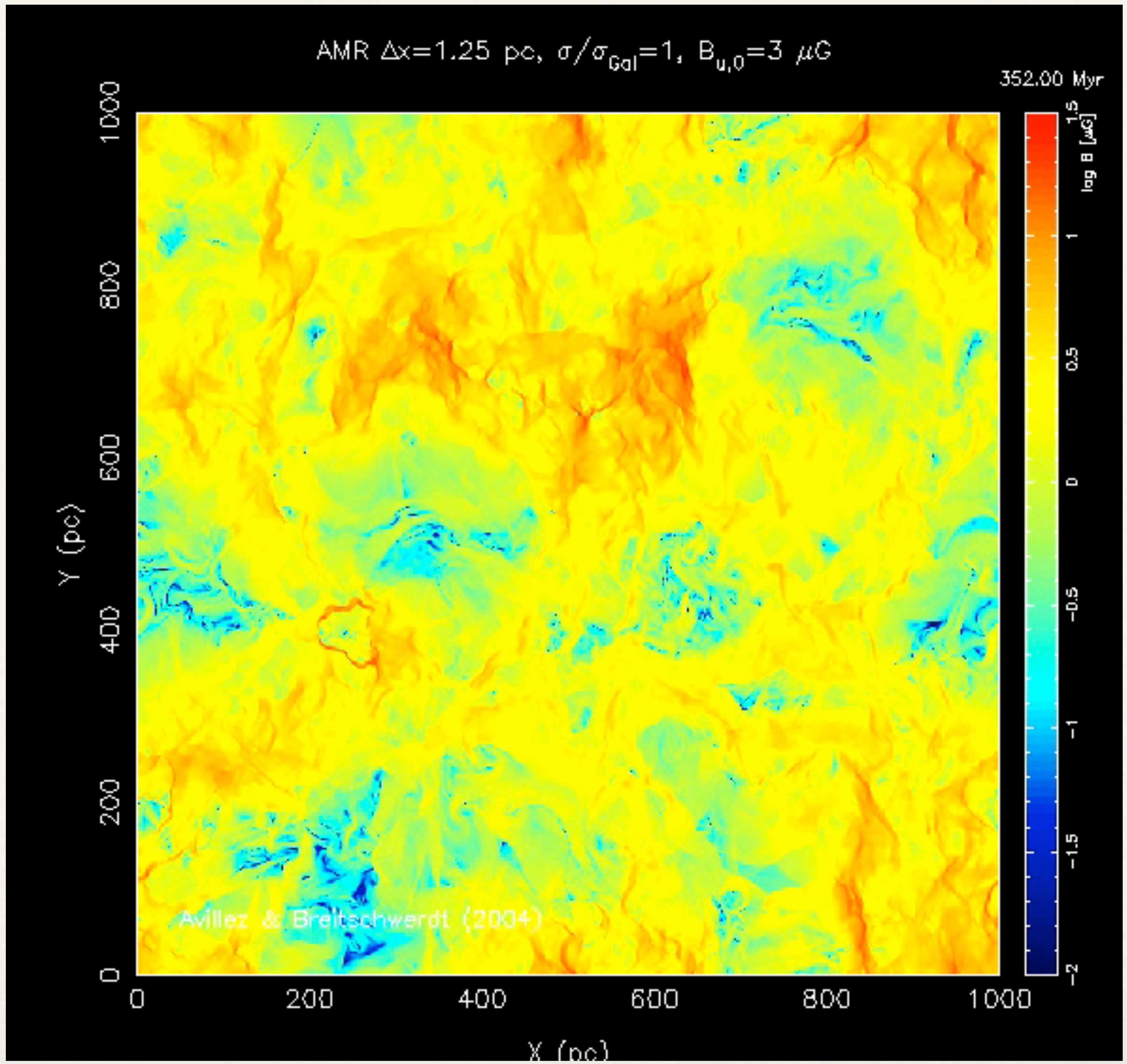

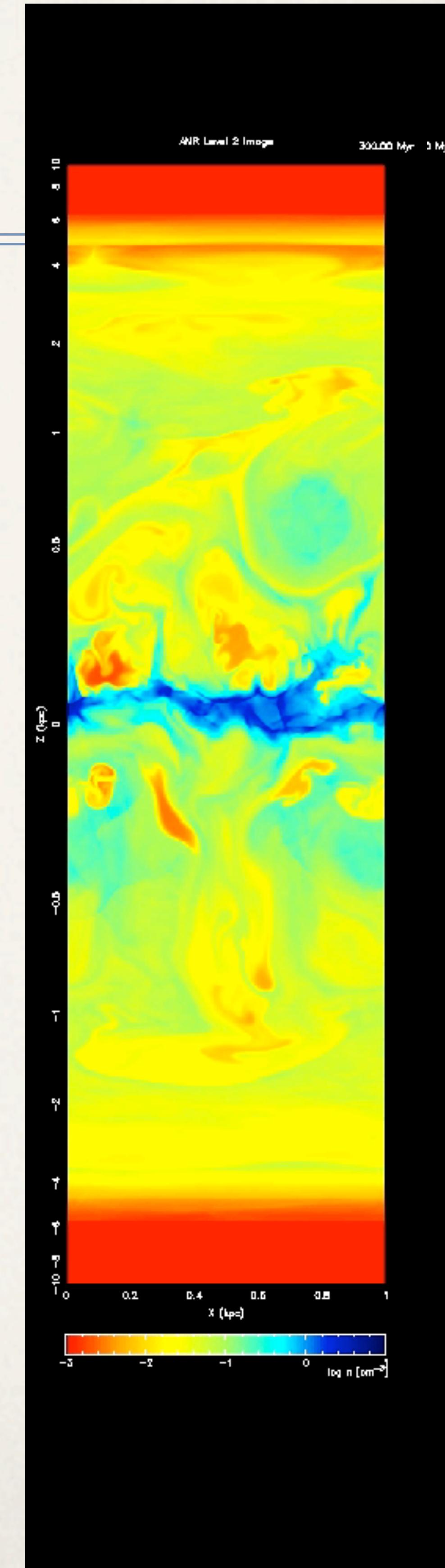

MHD-Evolution of ISM (I)

Avillez & Breitschwerdt, 2005a

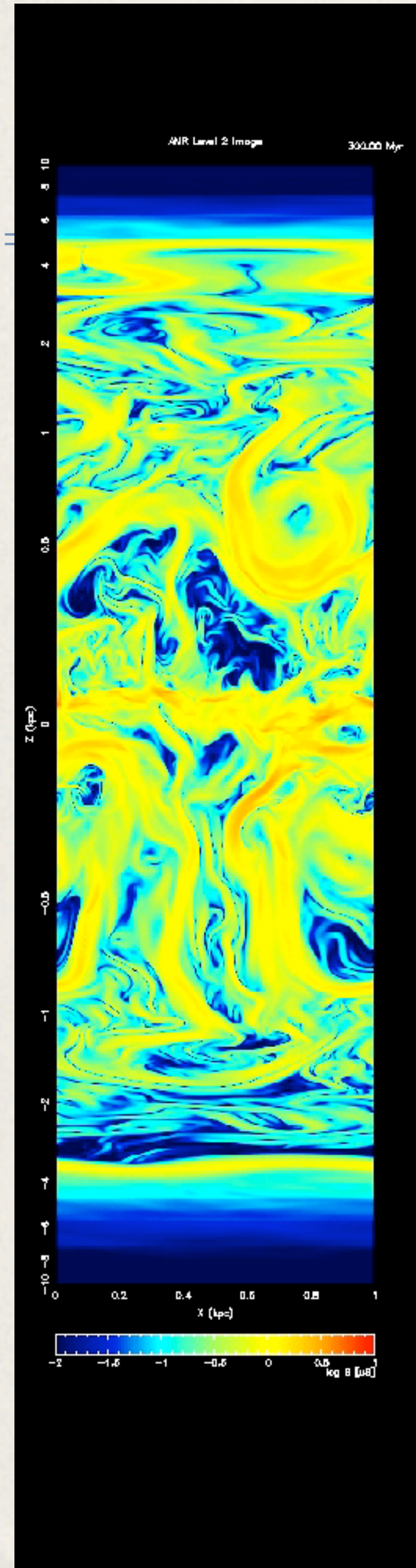

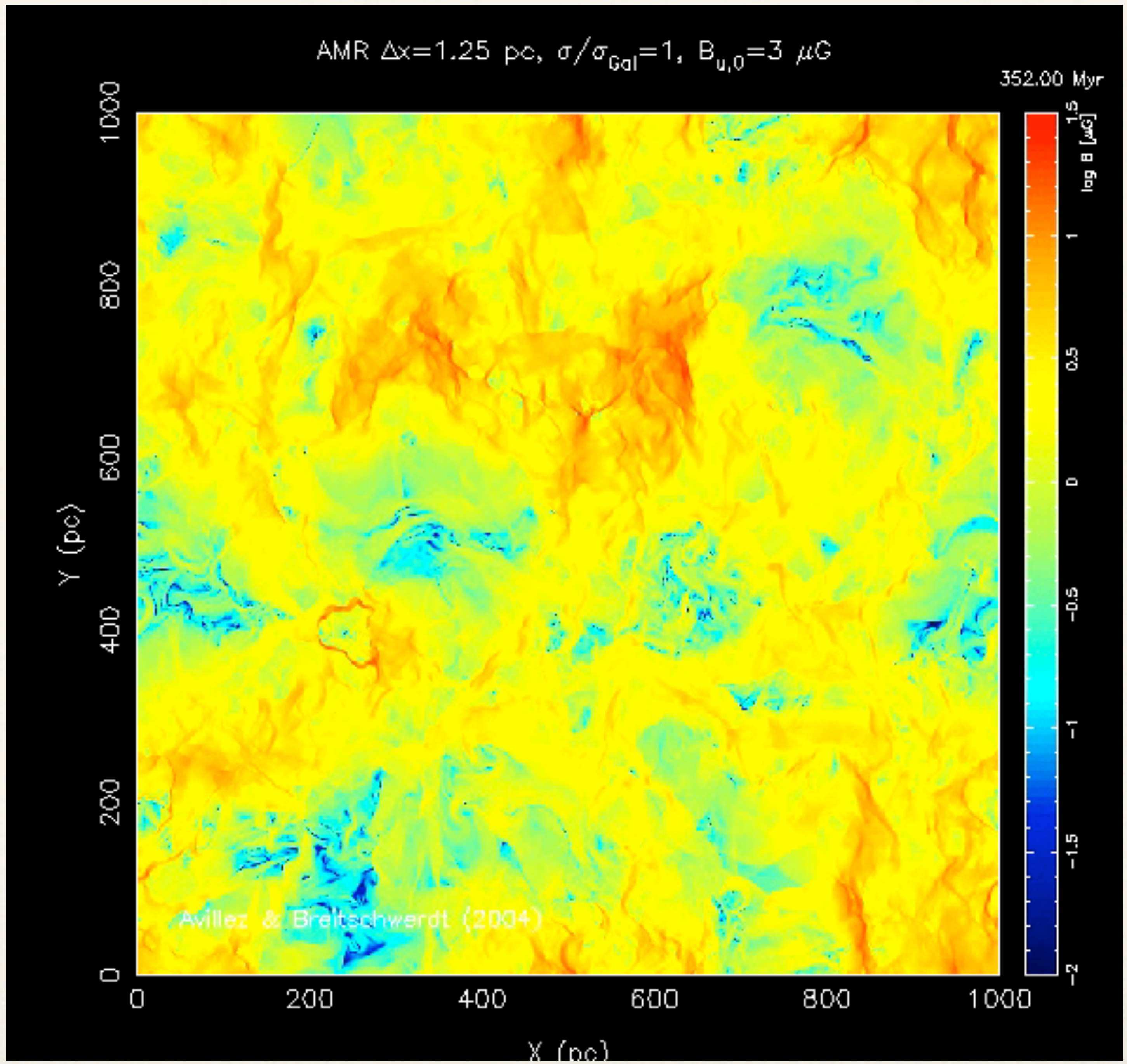

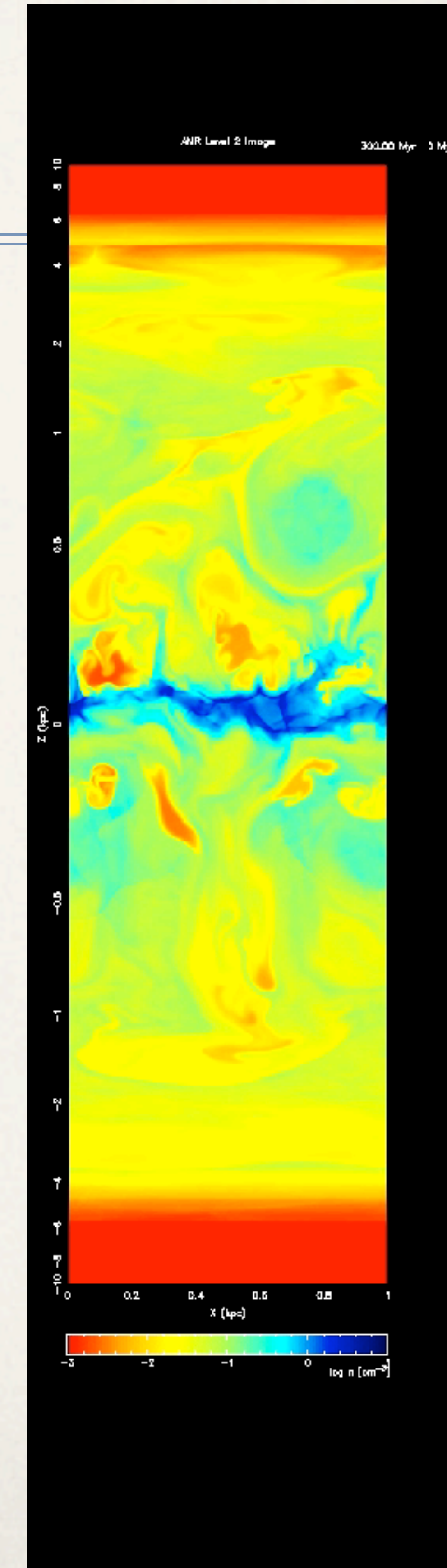

MHD-Evolution of ISM (I)

Avillez & Breitschwerdt, 2005a

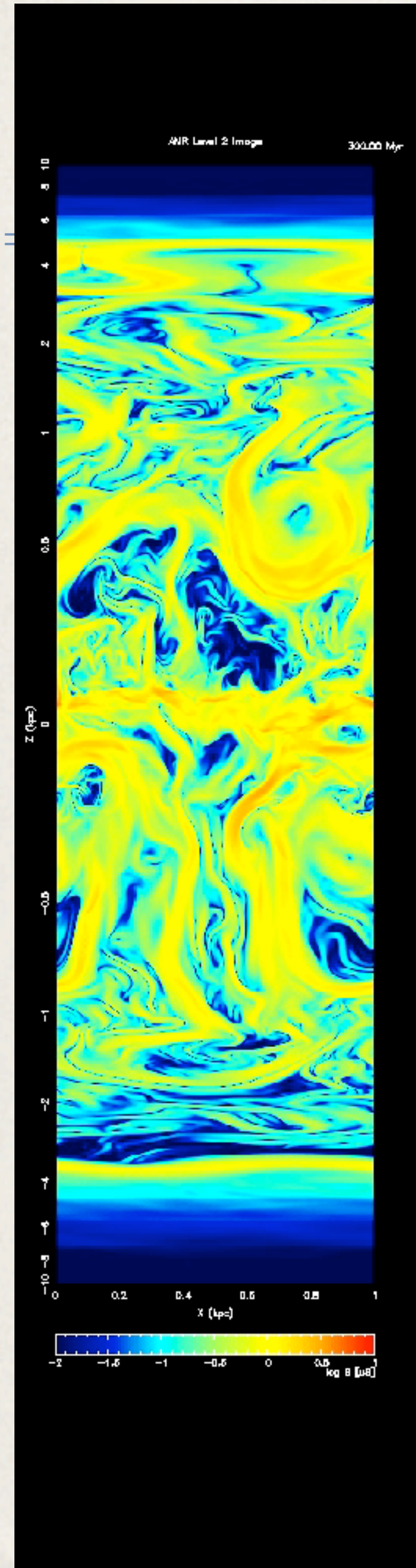

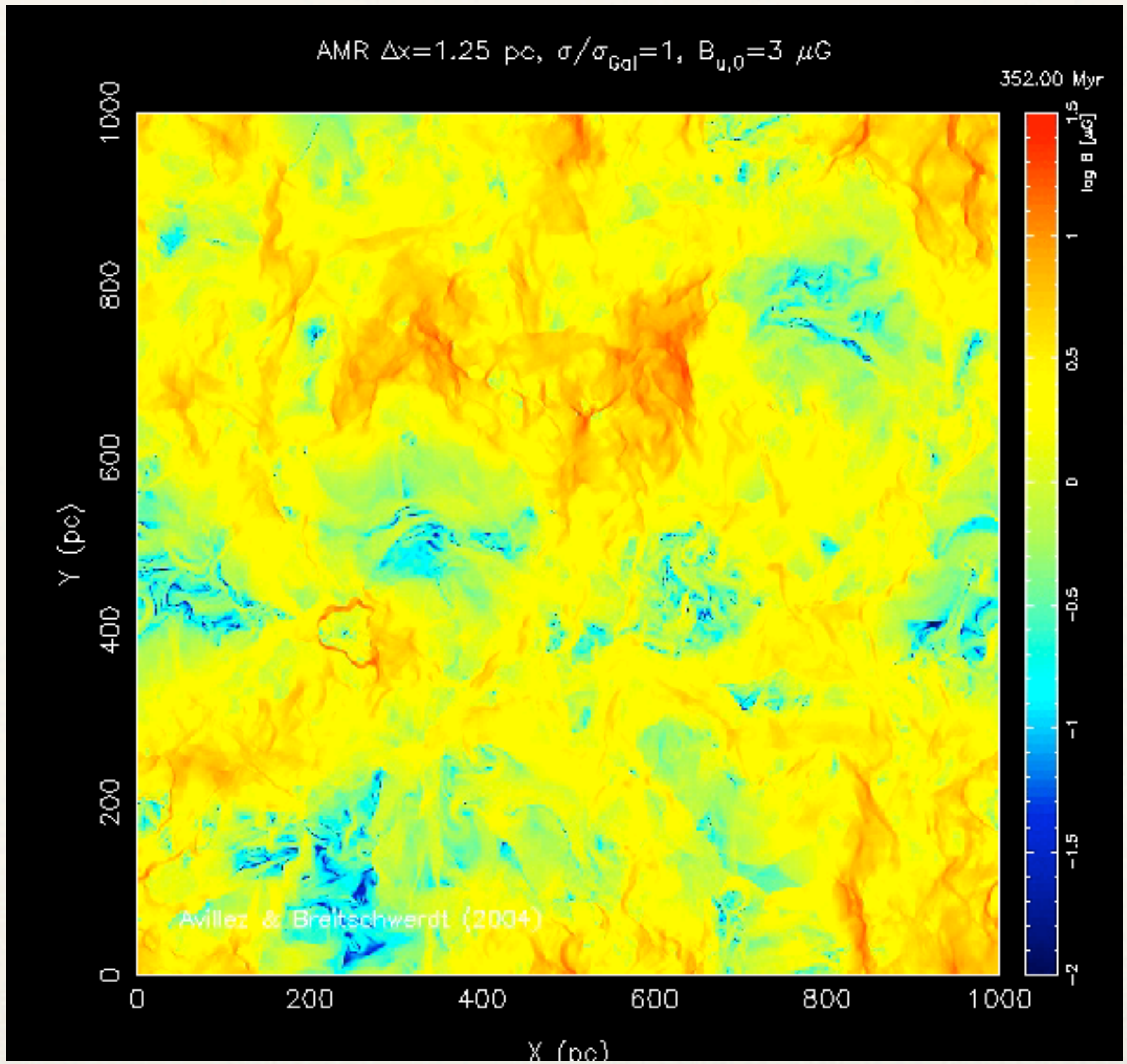

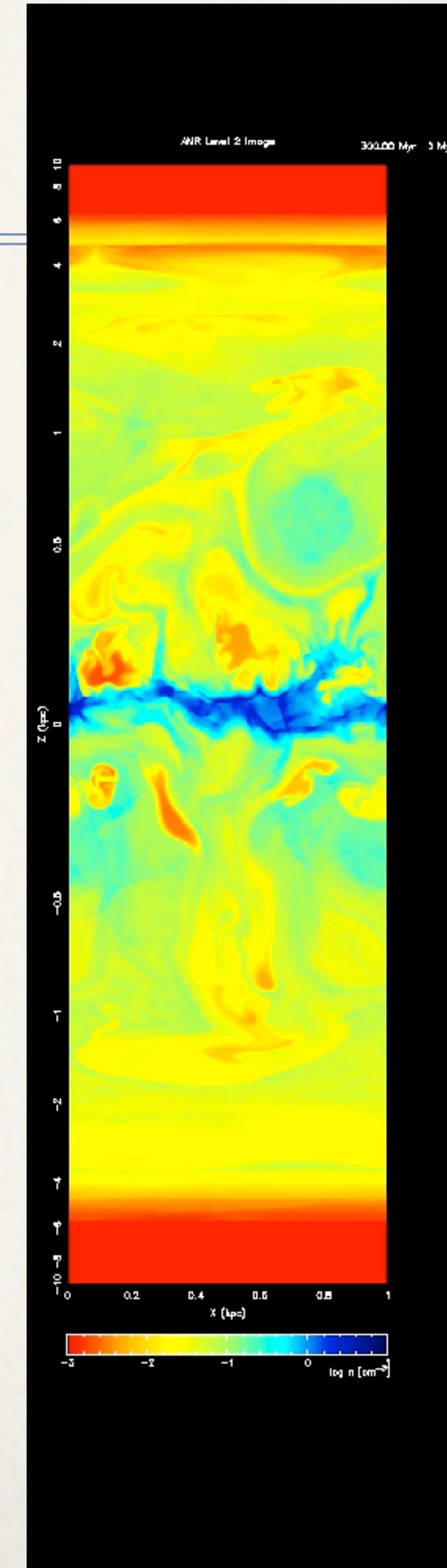

MHD-Evolution of ISM (I)

Avillez & Breitschwerdt, 2005a

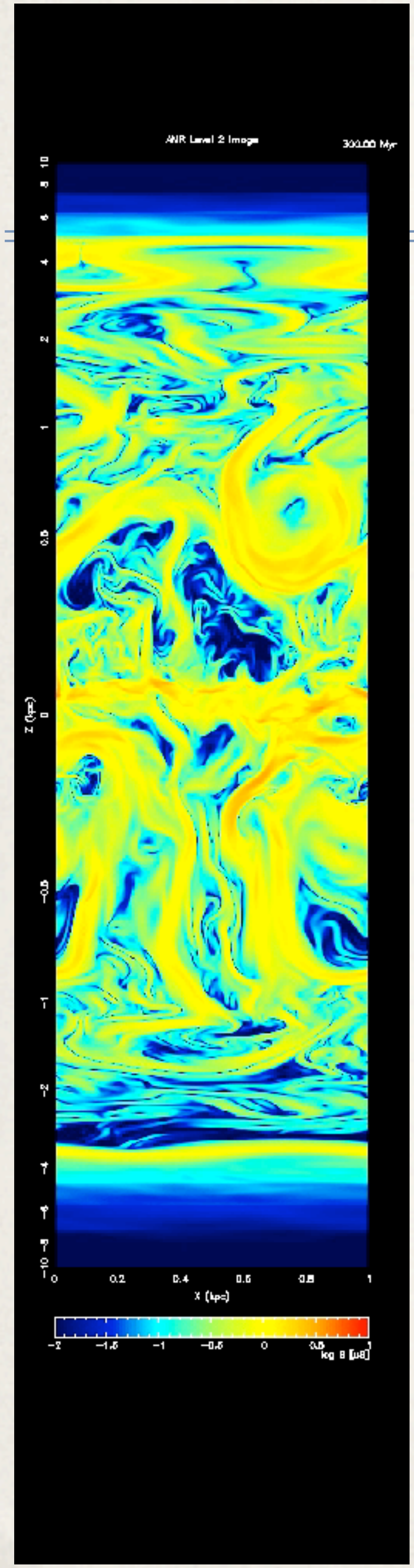

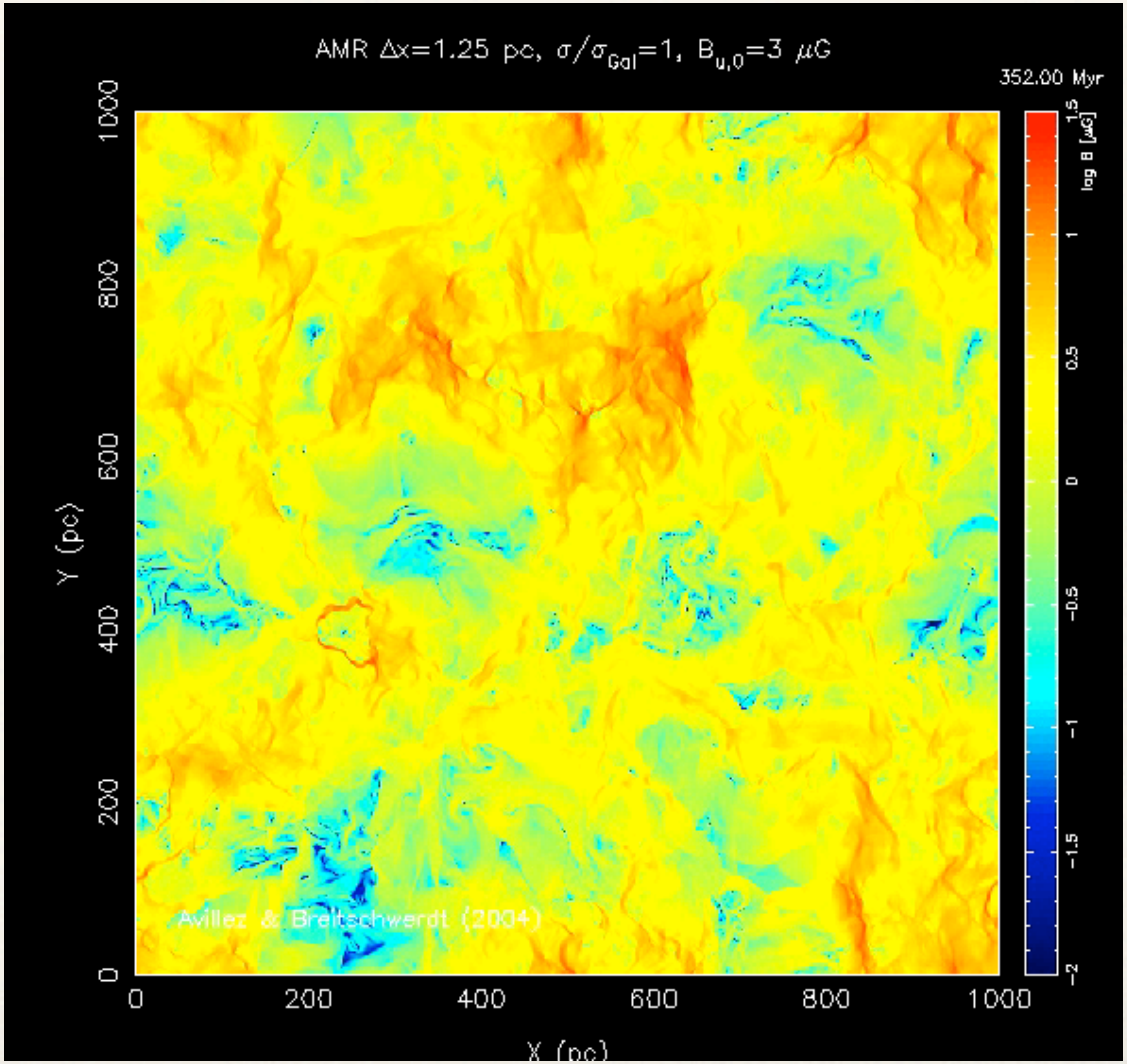

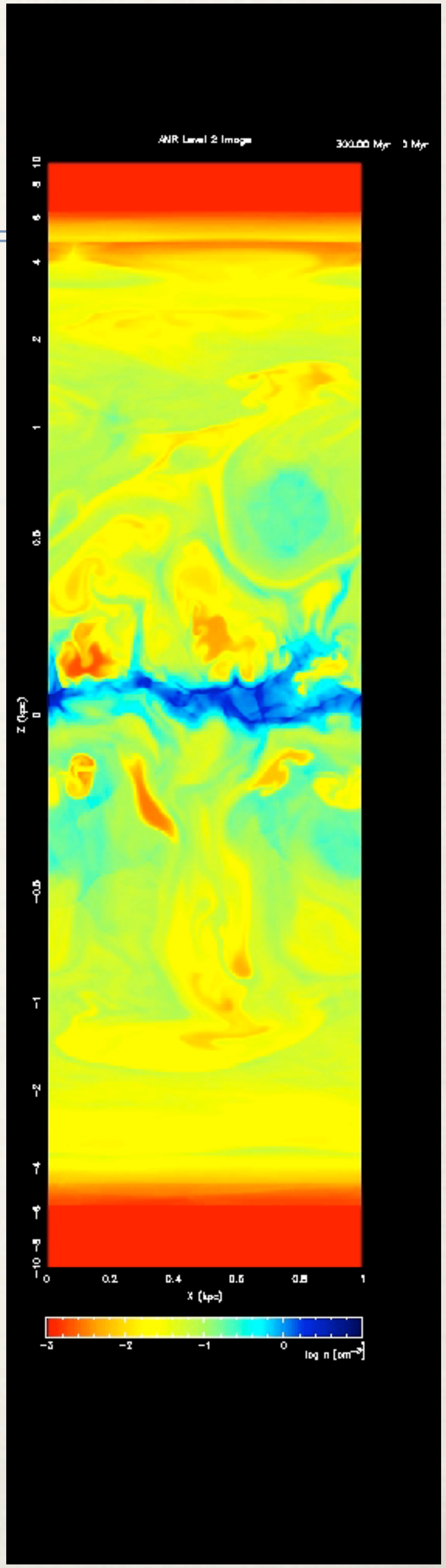

MHD-Evolution of ISM (II)

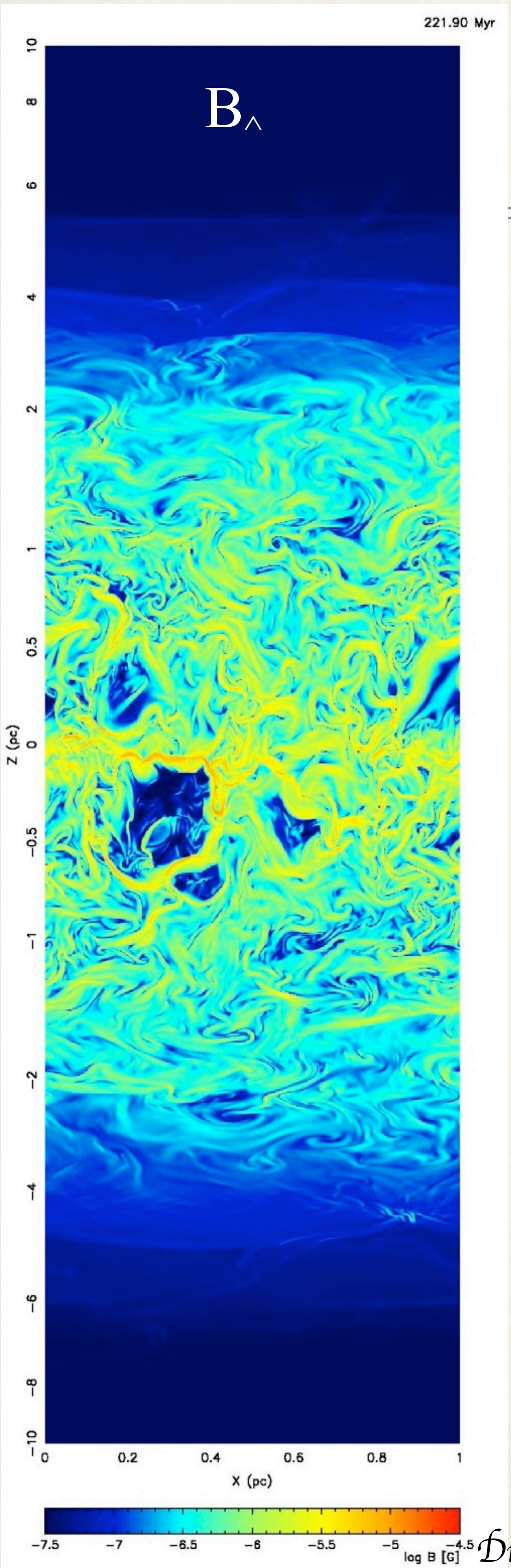

Avillez & Breitschwerdt, 2005

B-field // to disk cannot prevent outflow into halo; Halo density is **inhomogeneous (Fountain)**

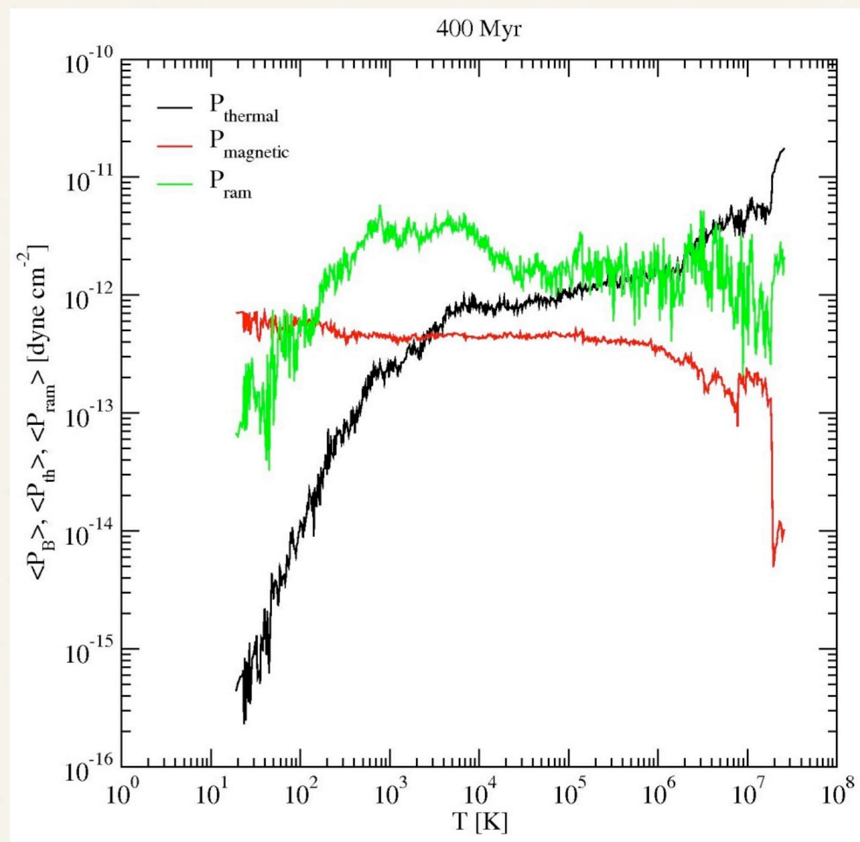

Which pressure determines ISM dynamics?

- For T < 200 K: **magnetic** pressure dominates,
- for 200 K < T < 10^6 K **ram pressure** dominates,
- for T>10^6 K **thermal pressure** dominates

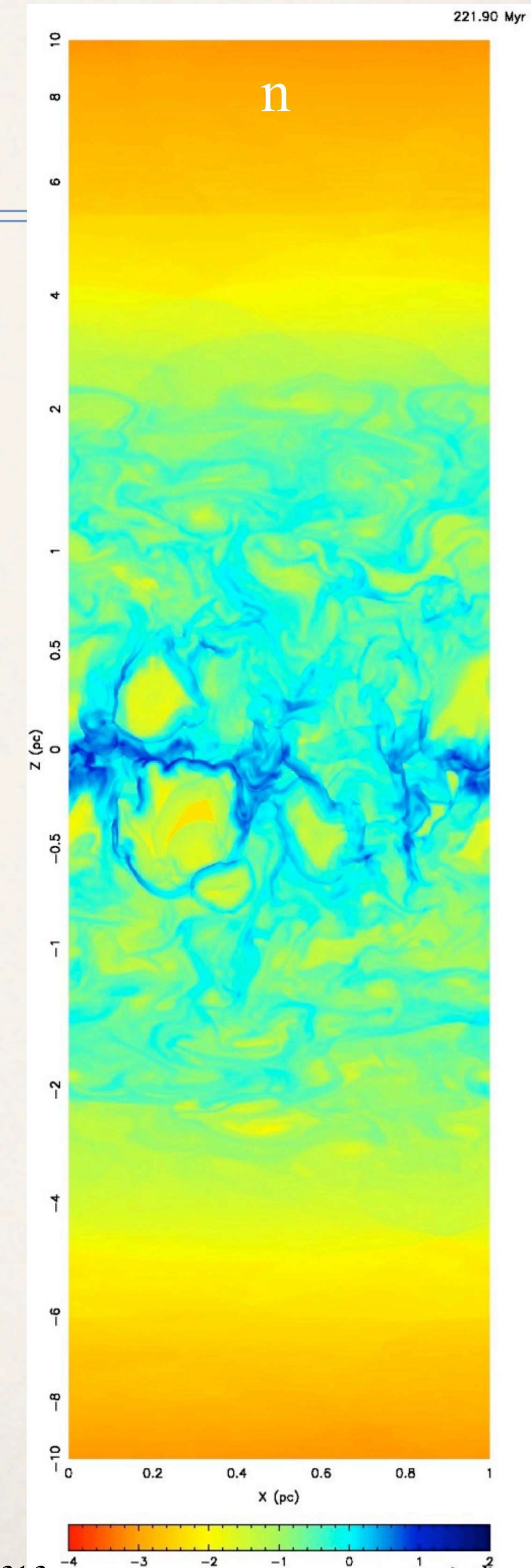

Plasma Models: CIE vs. NEI

- **optically thin hot plasmas**: continuum + line spectrum
- **collisional ionization equilibrium (CIE)**: ionization by collisions (3-body process) is balanced by **radiative recombination ➔** no detailed balancing, because atomic time scales are different
- plasma is driven out of CIE ➔ **non-equilibium ionization (NEI)** structure
- particularly striking effect: **fast adiabatic cooling** like in a galactic fountain or wind (Breitschwerdt & Schmutzler, 1994)

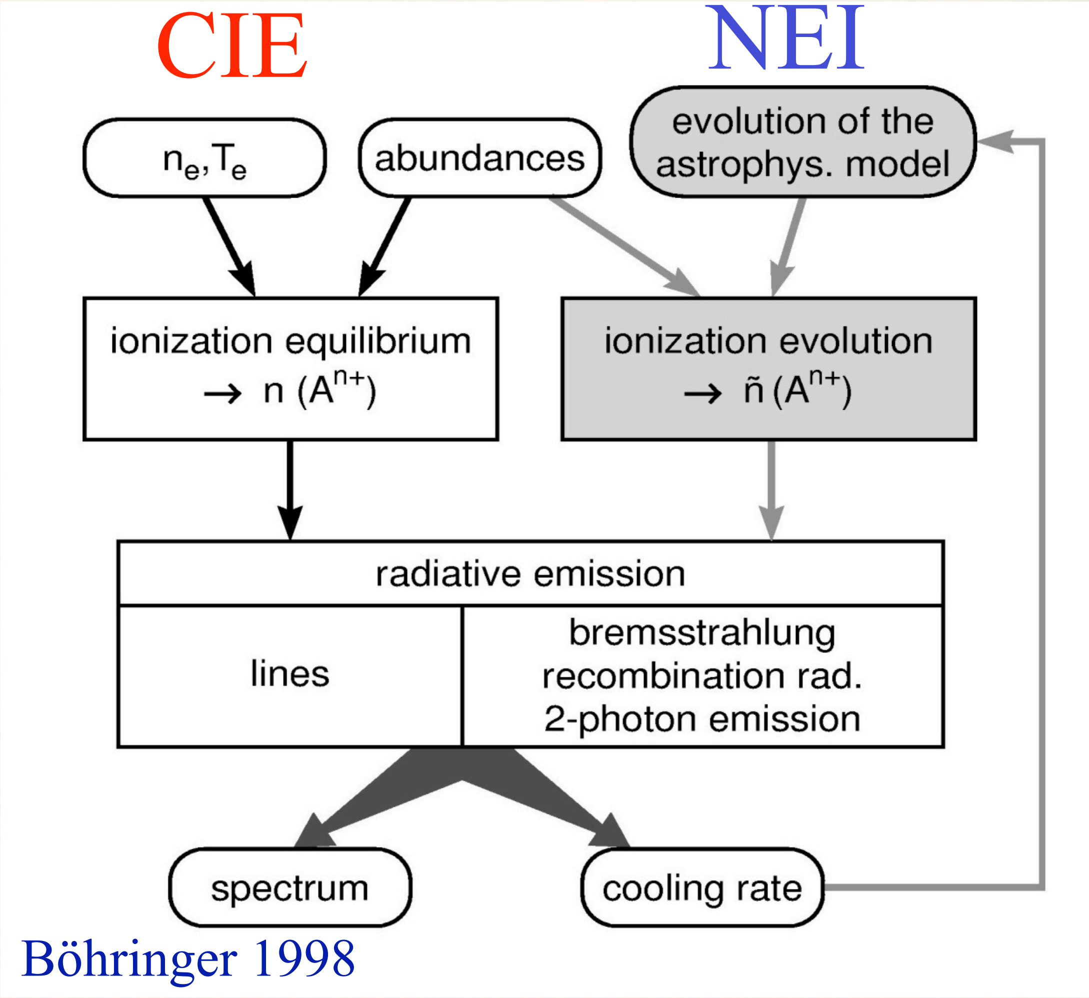

***Top**: CIE vs. NEI plasma emission codes; in **CIE**, plasma emission can be calculated (in coronal approx., i.e. $n_e < 10^4$ cm^{-3}) once and for all if n_e, T_e and Z are given; in **NEI** Z + astrophysical model for dynamical evolution is required!*
***Left**: Animation of collisional ionization by electrons*

radiative recombination *collisional ionization*

Plasma Models: CIE vs. NEI

- **optically thin hot plasmas**: continuum + line spectrum
- **collisional ionization equilibrium (CIE)**: ionization by collisions (3-body process) is balanced by **radiative recombination ➔** no detailed balancing, because atomic time scales are different
- plasma is driven out of CIE ➔ **non-equilibium ionization (NEI)** structure
- particularly striking effect: **fast adiabatic cooling** like in a galactic fountain or wind (Breitschwerdt & Schmutzler, 1994)

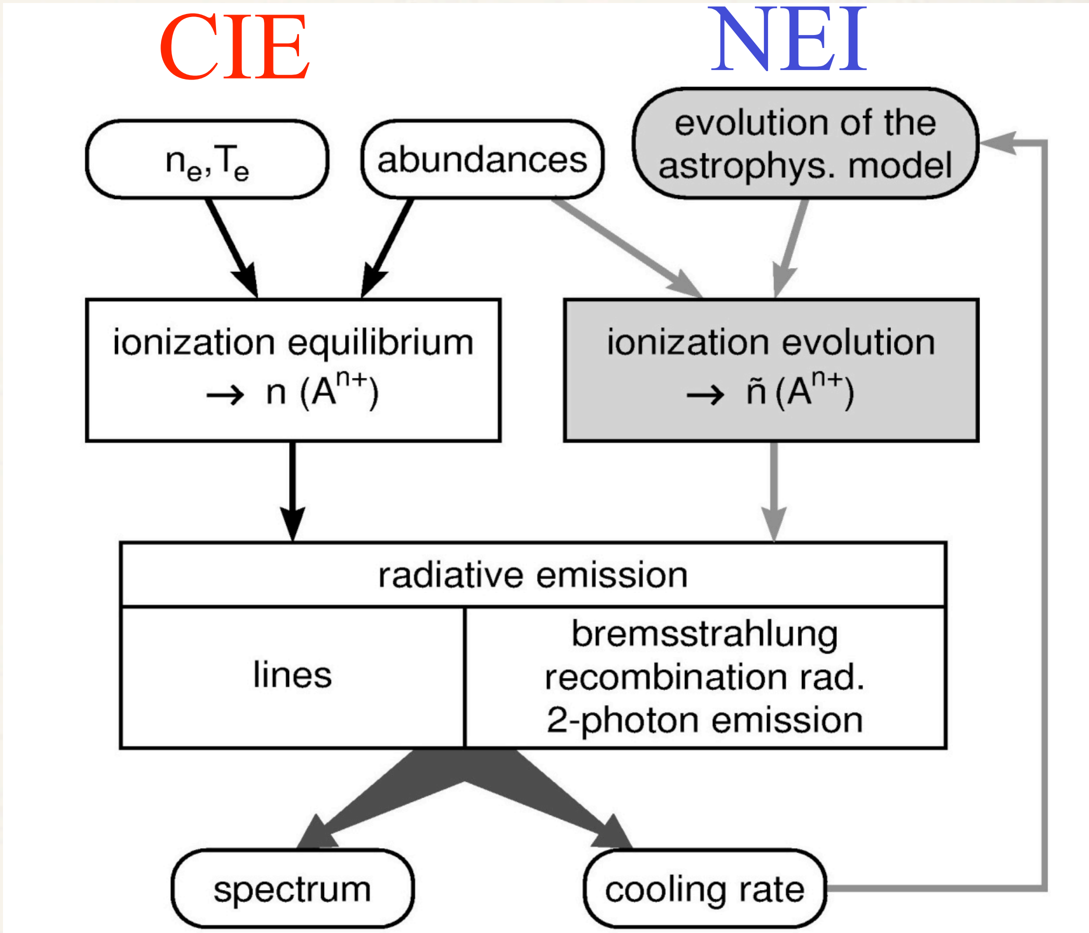

Böhringer 1998

Top: *CIE vs. NEI plasma emission codes; in **CIE**, plasma emission can be calculated (in coronal approx., i.e.* $n_e < 10^4$ cm^{-3}*) once and for all if* n_e*,* T_e *and Z are given; in **NEI** Z + astrophysical model for dynamical evolution is required!*
Left: *Animation of collisional ionization by electrons*

radiative recombination *collisional ionization*

Plasma Models: CIE vs. NEI

- **optically thin hot plasmas**: continuum + line spectrum
- **collisional ionization equilibrium (CIE)**: ionization by collisions (3-body process) is balanced by **radiative recombination ➔** no detailed balancing, because atomic time scales are different
- plasma is driven out of CIE ➔ **non-equilibium ionization (NEI)** structure
- particularly striking effect: **fast adiabatic cooling** like in a galactic fountain or wind (Breitschwerdt & Schmutzler, 1994)

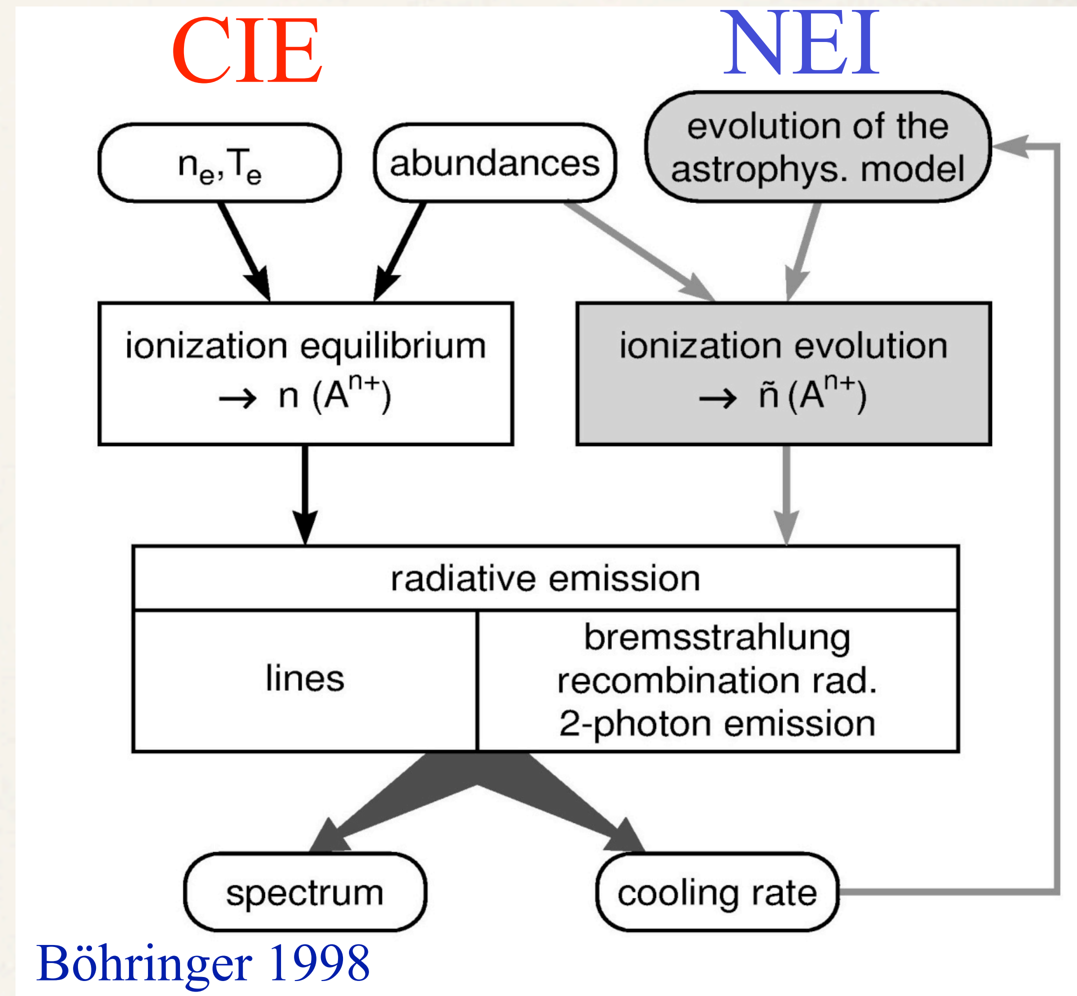

__Top__: CIE vs. NEI plasma emission codes; in __CIE__, plasma emission can be calculated (in coronal approx., i.e. $n_e < 10^4$ cm^{-3}) once and for all if n_e, T_e and Z are given; in __NEI__ Z + astrophysical model for dynamical evolution is required!
__Left__: Animation of collisional ionization by electrons

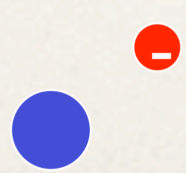

radiative recombination *collisional ionization*

Plasma Models: CIE vs. NEI

- **optically thin hot plasmas**: continuum + line spectrum
- **collisional ionization equilibrium (CIE)**: ionization by collisions (3-body process) is balanced by **radiative recombination ➔** no detailed balancing, because atomic time scales are different
- plasma is driven out of CIE ➔ **non-equilibium ionization (NEI)** structure
- particularly striking effect: **fast adiabatic cooling** like in a galactic fountain or wind (Breitschwerdt & Schmutzler, 1994)

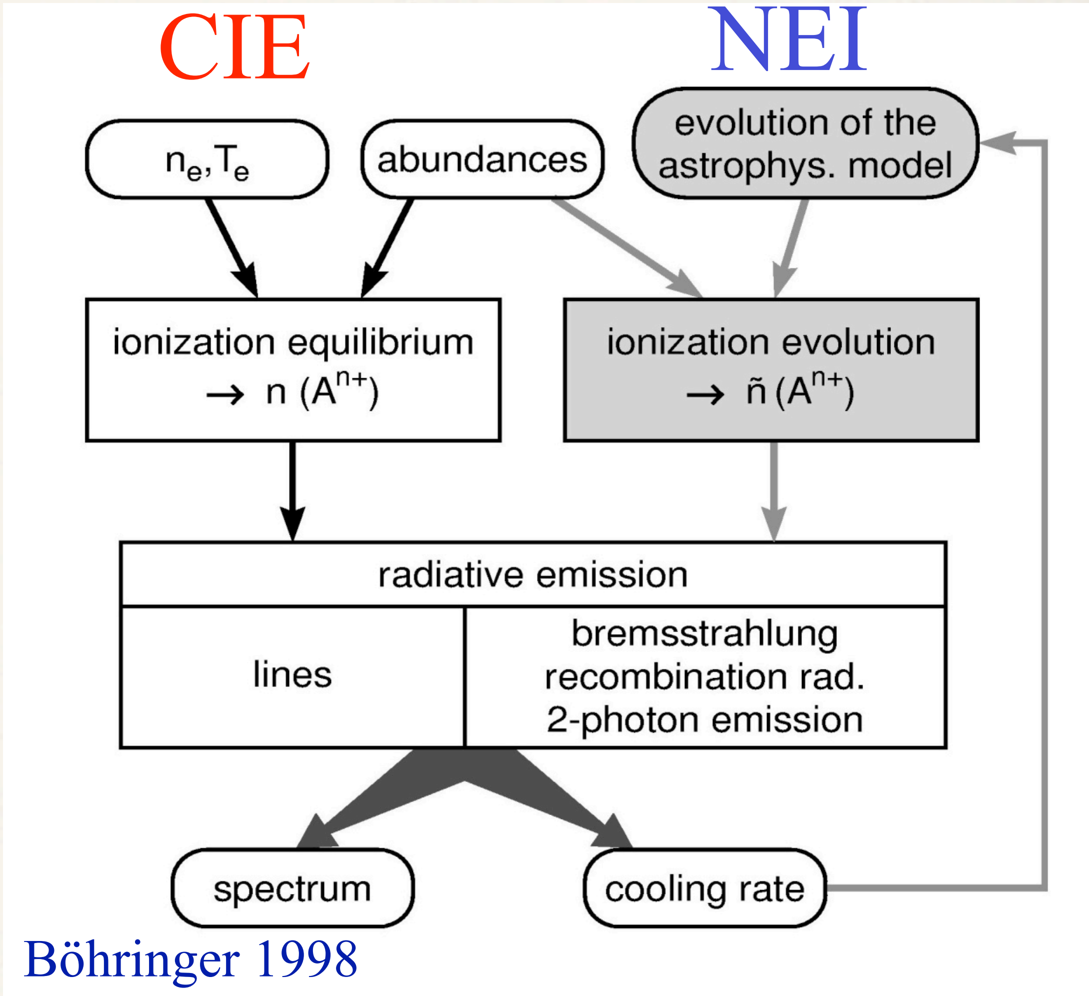

__Top__: CIE vs. NEI plasma emission codes; in __CIE__, plasma emission can be calculated (in coronal approx., i.e. $n_e < 10^4$ cm^{-3}) once and for all if n_e, T_e and Z are given; in __NEI__ Z + astrophysical model for dynamical evolution is required!
__Left__: Animation of collisional ionization by electrons

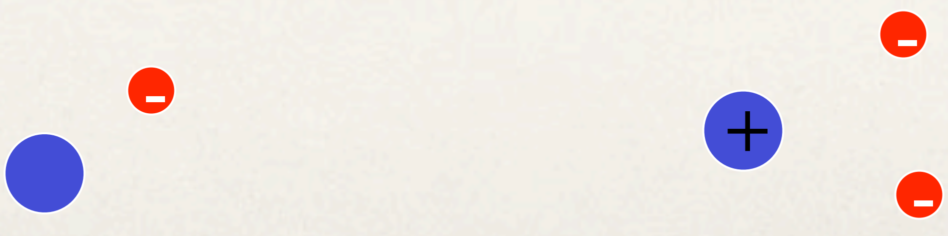

radiative recombination *collisional ionization*

Plasma Models: CIE vs. NEI

- **optically thin hot plasmas**: continuum + line spectrum
- **collisional ionization equilibrium (CIE)**: ionization by collisions (3-body process) is balanced by **radiative recombination ➔** no detailed balancing, because atomic time scales are different
- plasma is driven out of CIE ➔ **non-equilibium ionization (NEI)** structure
- particularly striking effect: **fast adiabatic cooling** like in a galactic fountain or wind (Breitschwerdt & Schmutzler, 1994)

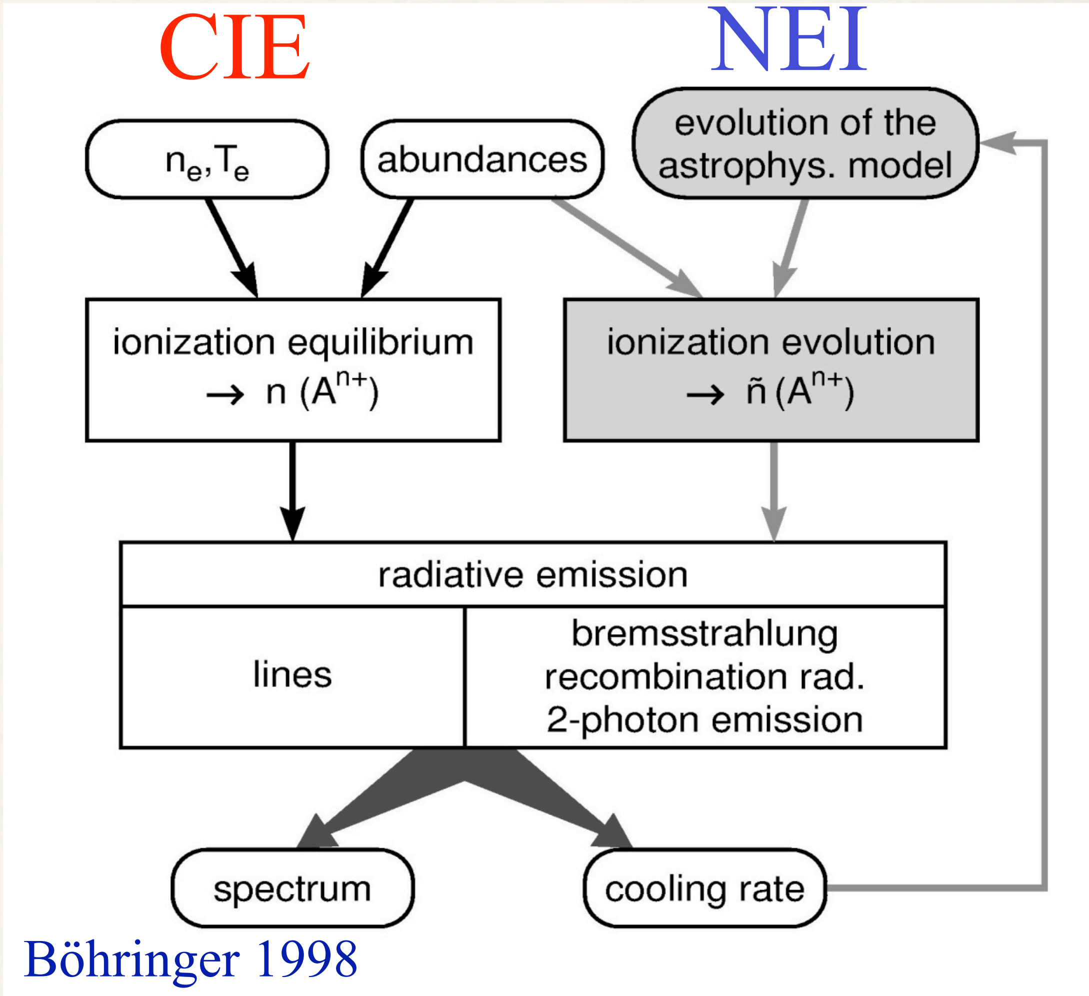

__Top__: CIE vs. NEI plasma emission codes; in __CIE__, plasma emission can be calculated (in coronal approx., i.e. $n_e < 10^4$ cm^{-3}) once and for all if n_e, T_e and Z are given; in __NEI__ Z + astrophysical model for dynamical evolution is required!
__Left__: Animation of collisional ionization by electrons

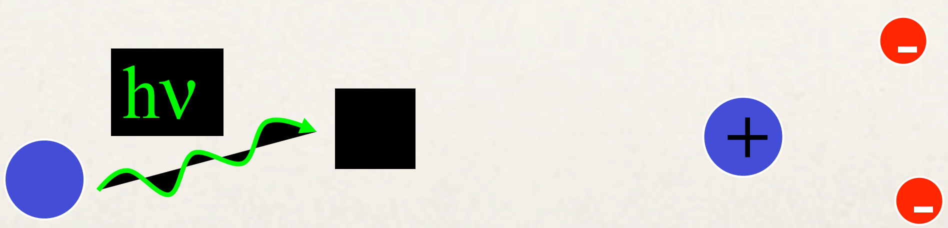

radiative recombination *collisional ionization*

Example: ionization structure of oxygen in CIE and NEI

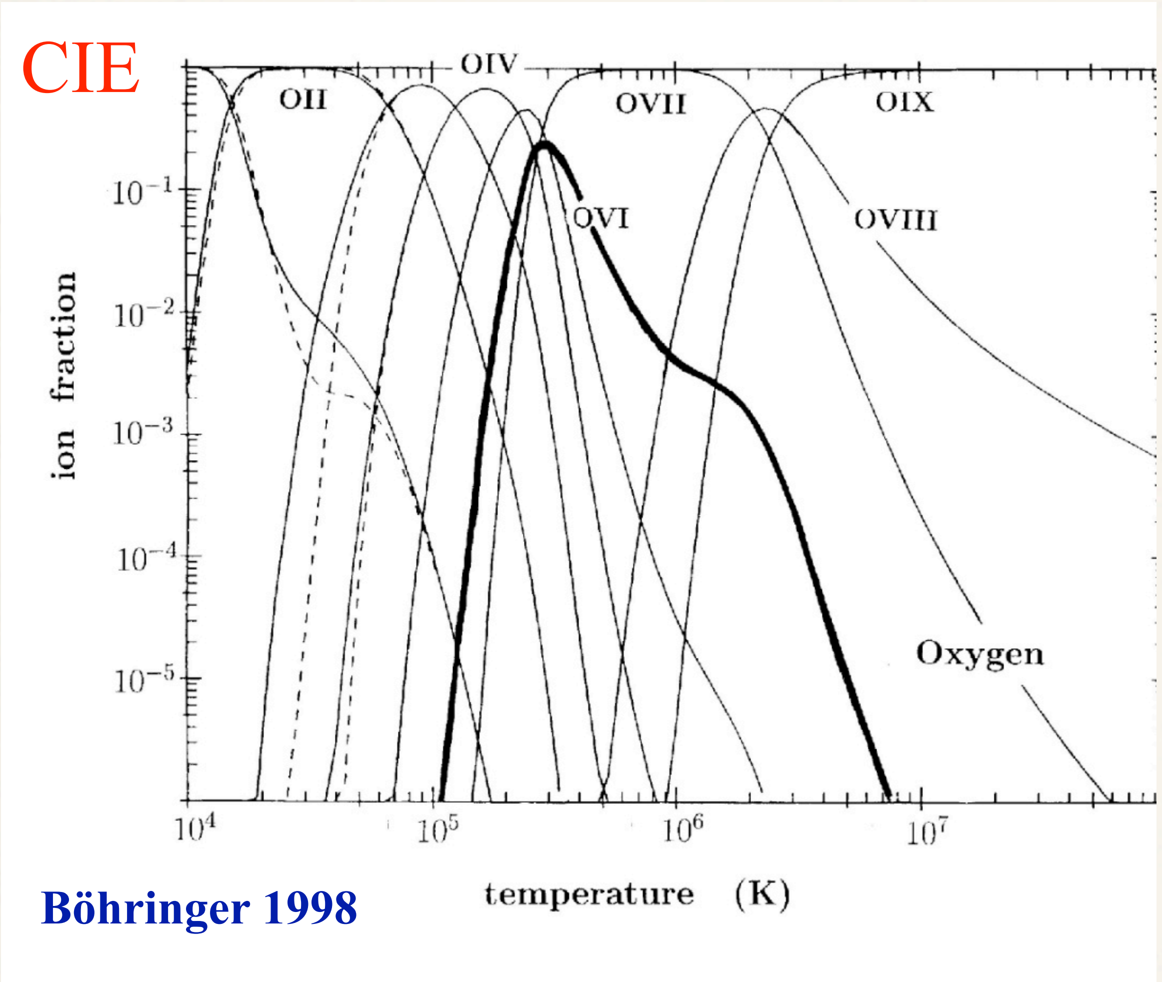

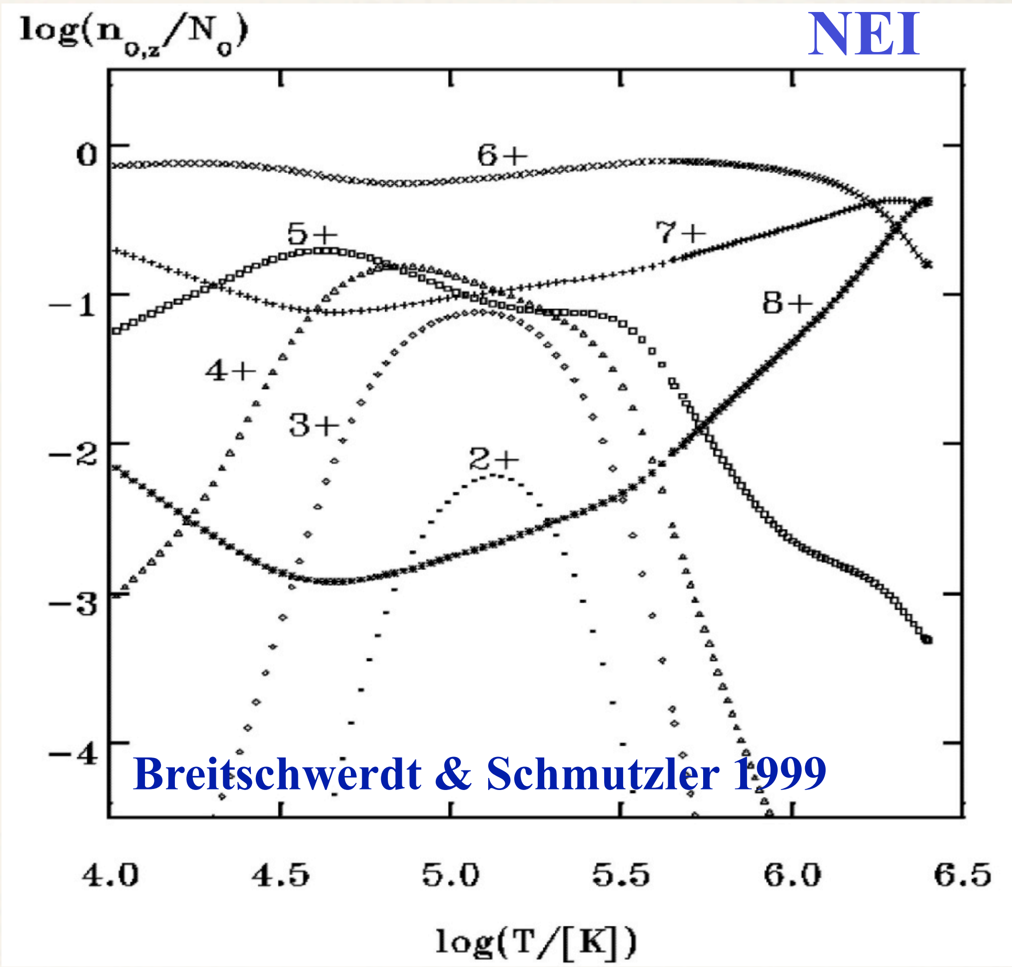

- **CIE:** ionization fraction x of O depend only on temperature T (for given Z) ➔ sharply peaked ➔ convenient diagnostic tool for determining T
- **NEI**: x depends on dynamical and thermal history of plasma ➔ more difficult to fit spectrum, but: **evolution of plasma can be inferred!**

Modeling galactic halos with outflow (I)

- **model edge-on (starburst) galaxies:** e.g. NGC 253, NGC 3079
- underlying **galactic wind** model: **steady-state outflow** driven by **thermal gas, CR and wave pressures** (cf. Breitschwerdt et al. 1991)
- **dynamically and thermally self-consistent** modelling:
- Outflow changes ϱ and T
- this modifies ionization structure
- which in turn modifies cooling function $\Lambda(\varrho,T)$
- which changes outflow
- flow is described in a flux tube given by:

$$A(z) = A_0 \left[1 + \left(\frac{z}{H}\right)^2\right]$$

Mass-loaded wind flow!!!

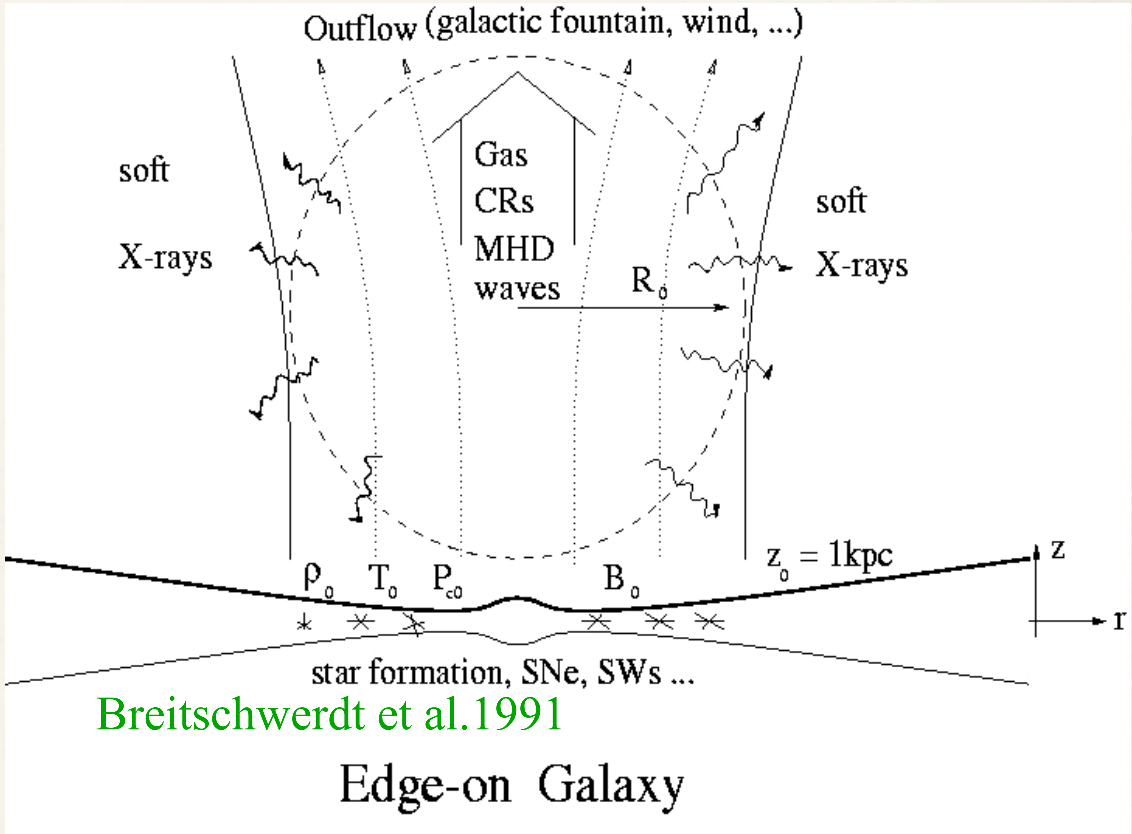

__Top__: steady-state galactic wind model, in which gas, CRs and waves drive an outflow with a smooth subsonic-supersonic transition

ZAA

Modeling galactic halos with outflow (I)

- **model edge-on (starburst) galaxies:** e.g. NGC 253, NGC 3079
- underlying **galactic wind** model: **steady-state outflow** driven by **thermal gas, CR and wave pressures** (cf. Breitschwerdt et al. 1991)
- **dynamically and thermally self-consistent** modelling:
  - Outflow changes ϱ and T
  - this modifies ionization structure
  - which in turn modifies cooling function $\Lambda(\varrho,T)$
  - which changes outflow
- flow is described in a flux tube given by:

$$A(z) = A_0 \left[1 + \left(\frac{z}{H}\right)^2\right]$$

[Mass-loaded wind flow!!!](#)

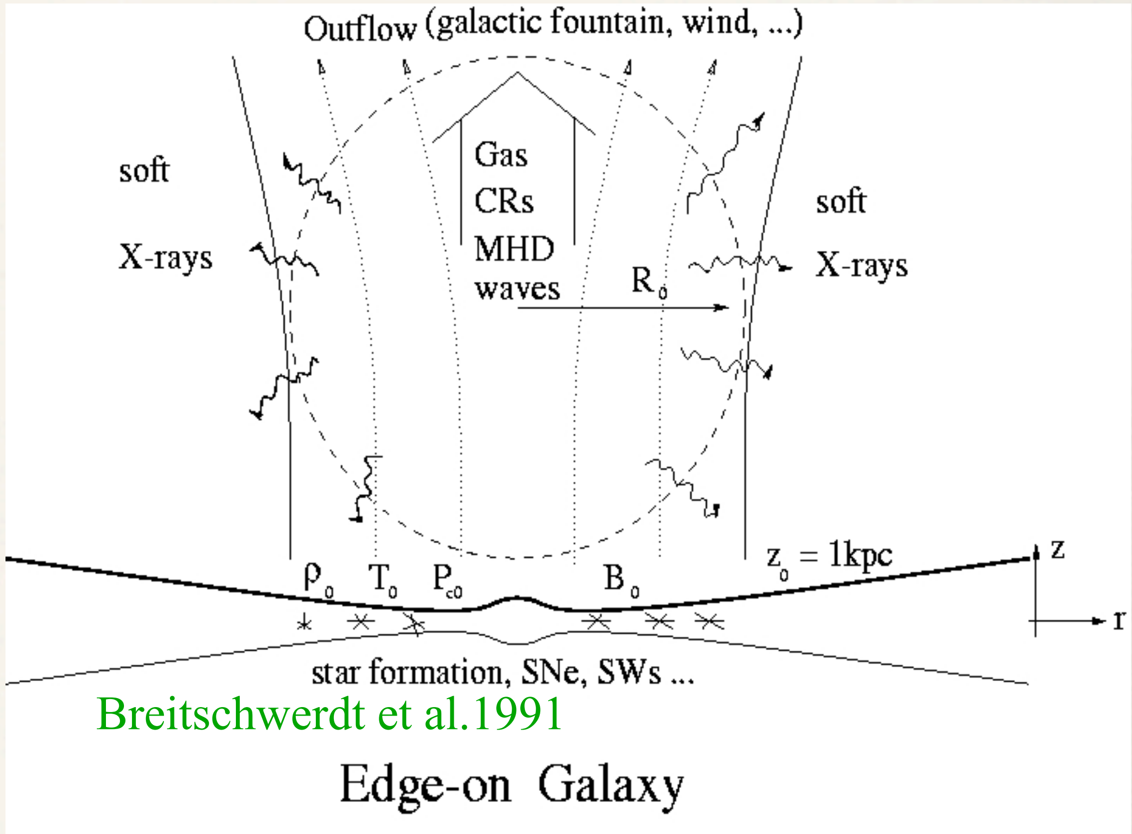

***Top**: steady-state galactic wind model, in which gas, CRs and waves drive an outflow with a smooth subsonic-supersonic transition*

Modeling galactic halos with outflow (II)

Procedure:

- **Generating** an outflow model and follow time-dependent evolution of ions (NEI)
- **Binning** of high-resolution unabsorbed synthetic (model) spectrum into e.g. EPIC pn channels (for XMM-Newton)
- **Folding** spectrum through detector response matrix

→ Treating observed and synthetic spectrum equally!

- **Fitting** synthetic spectrum in XSPEC (X-ray spectral fitting routine) to observational data
- **Comparing** with observed spectrum and iterate outflow model if necessary until convergence

Modeling galactic halos with outflow (III): NCG 253

Modeling galactic halos with outflow (III): NCG 253

Modeling galactic halos with outflow (III): NCG 253

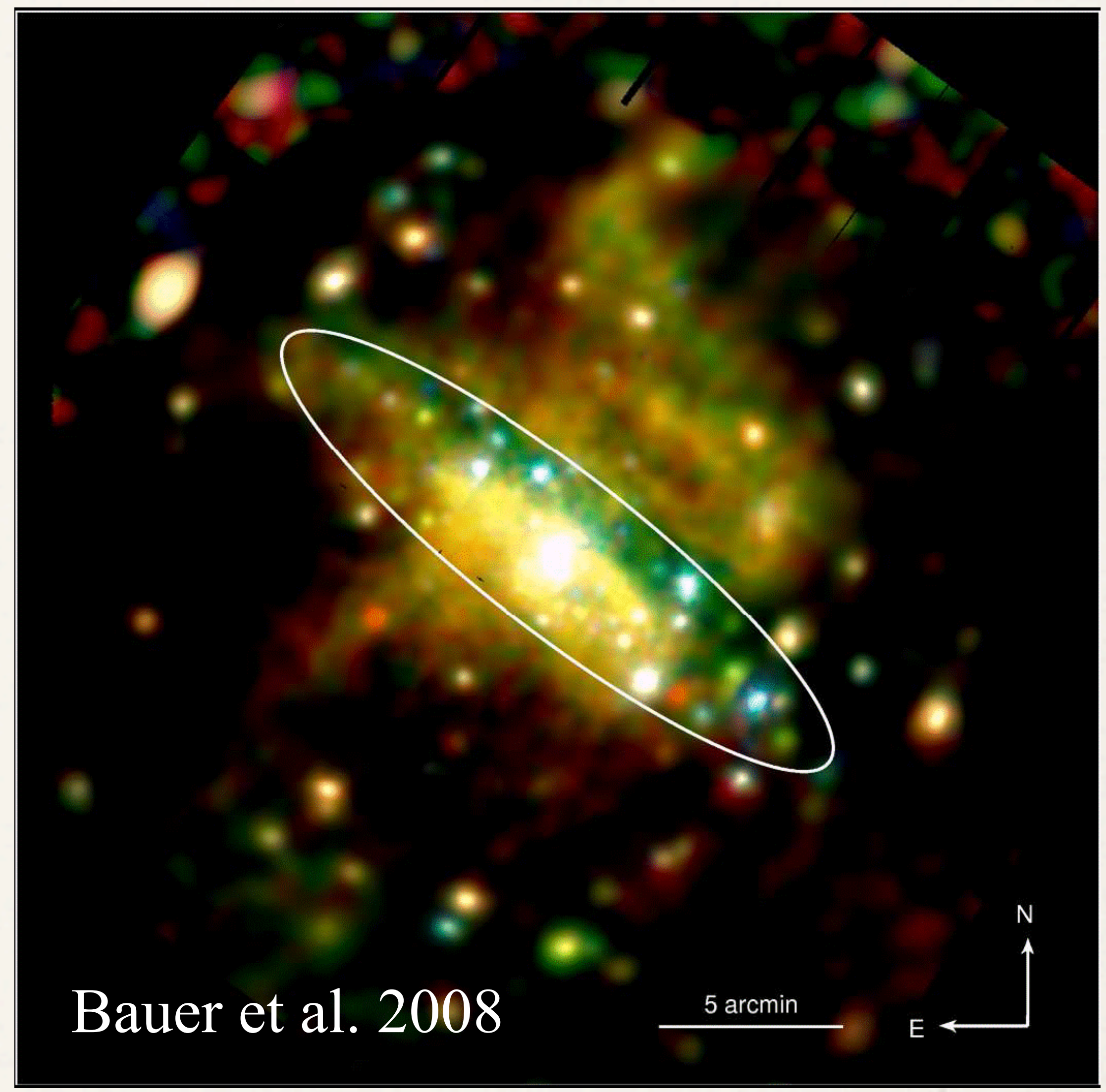

Modeling galactic halos with outflow (III): NCG 253

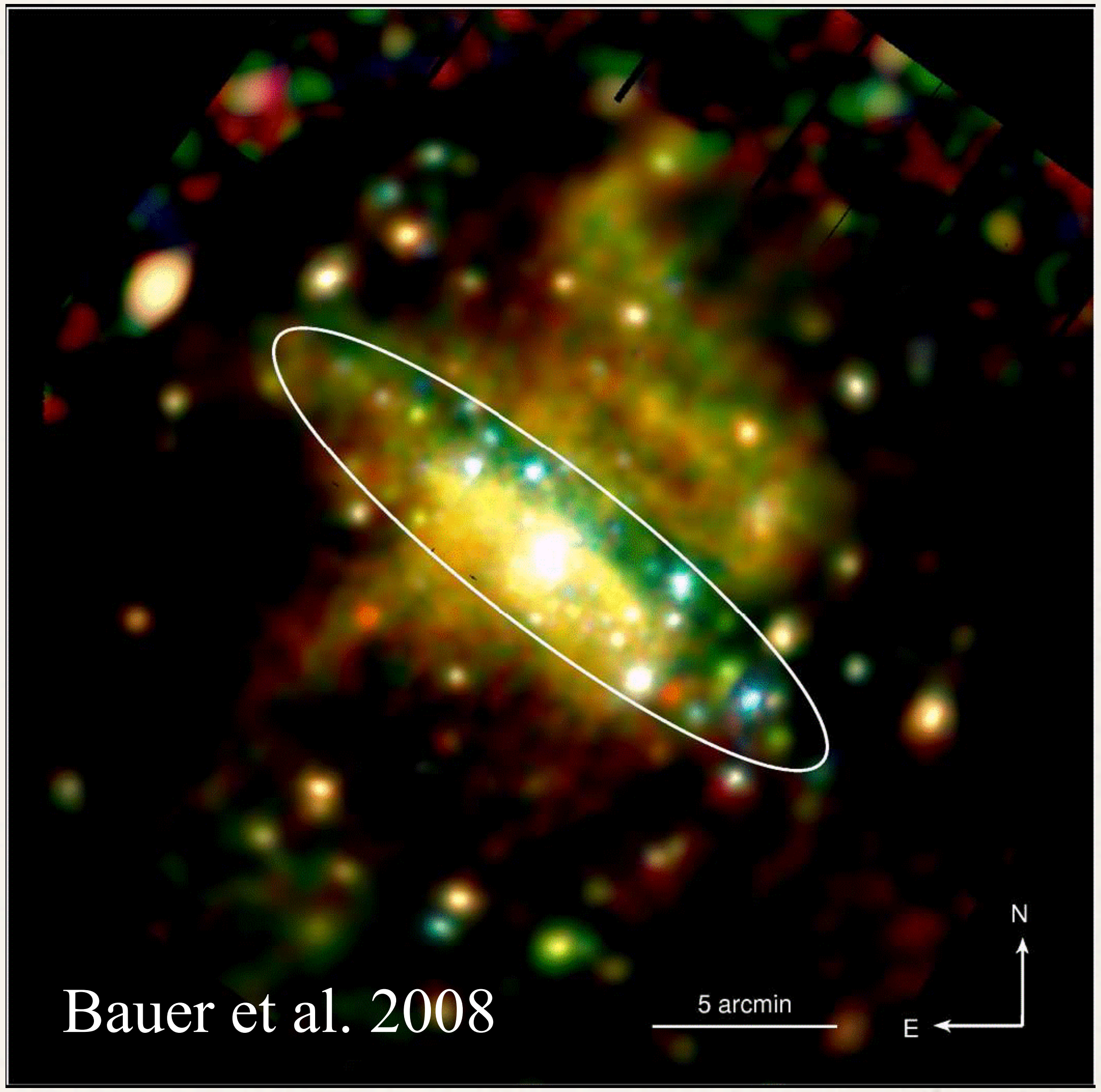

- 2MASS mosaic of NGC253
- Shows also extranuclear SB

Modeling galactic halos with outflow (III): NCG 253

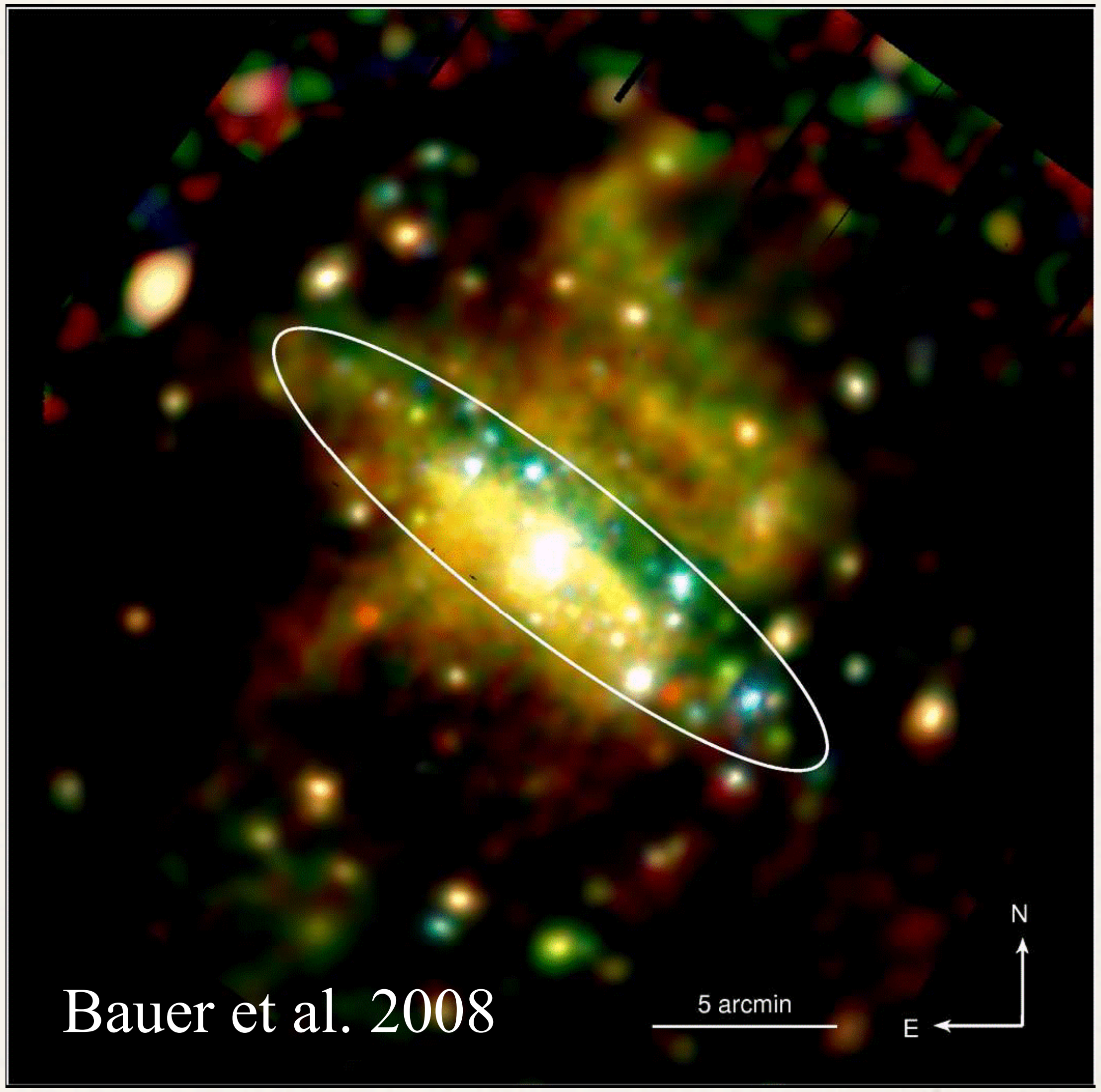

- 2MASS mosaic of NGC253
- Shows also extranuclear SB

- XMM EPIC pn: Soft X-ray halo of NGC253 (0.2 – 0.5 keV)

Modeling galactic halos with outflow (IV): NCG 253

- **NEI spectrum** mimics a "multitemperatu-re" halo by its characteristic lines, but is physically radically different from it
- **Reason**: Sum of CIE spectra cannot represent the specific **thermodynamic** path of a true NEI spectrum

NEI Model (Breitschwerdt & Freyberg 2003)

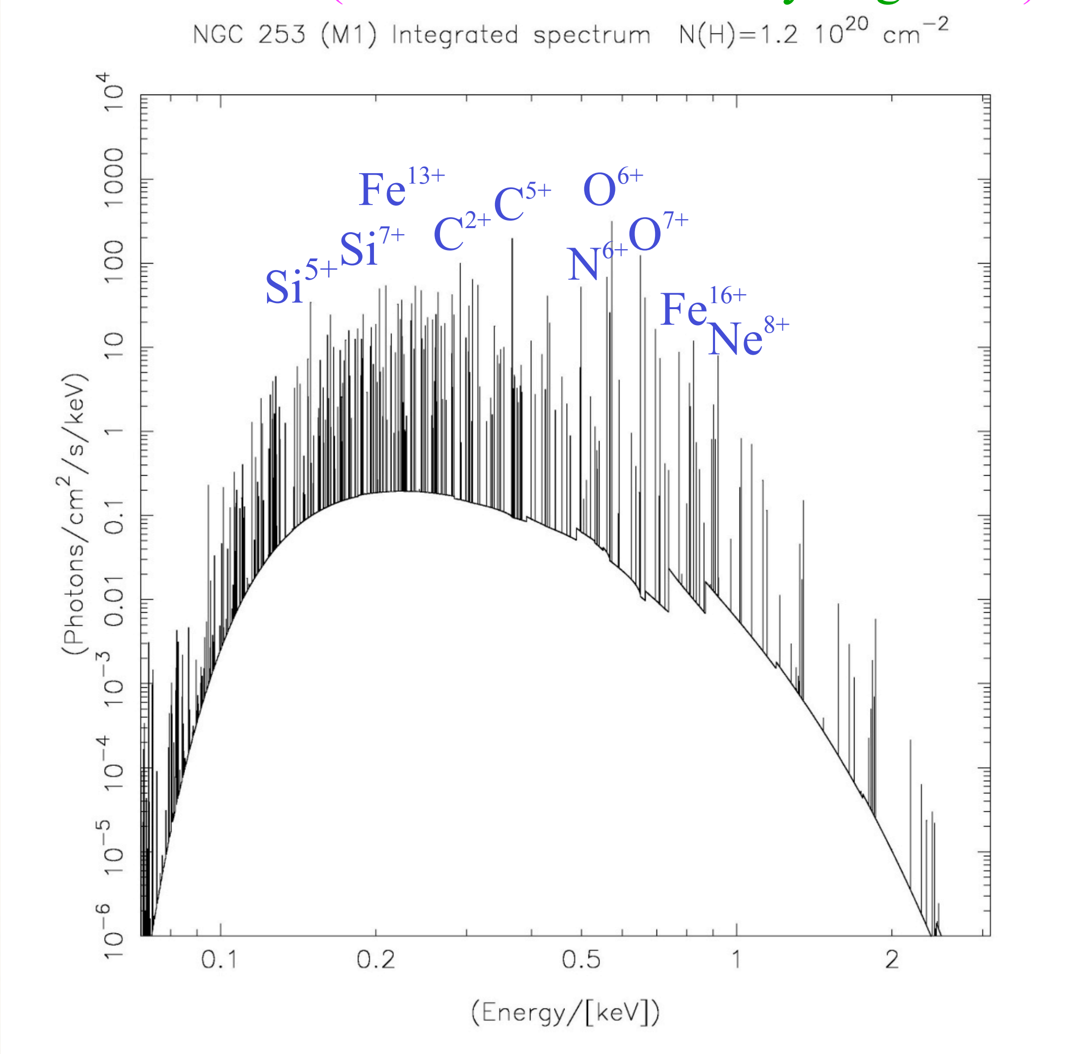

__Top__: Integrated spectrum of a dynamically and thermally self-consistent NEI simulation; the spectrum is a composite of continuum and lines, which are characteristic for the plasma history ➔ spectrum will be folded through detector response

Modeling galactic halos with outflow (V): NCG 3079

- **NGC 3079**: starburst LINER SBc galaxy
- Distance ~ 17 Mpc, Inclination ~ 85°
- **Low foreground absorption** Log(N(H))= 19.9 ➔ important for recording soft X-ray photons since photoelectric absorption ~ E^{-3}
-

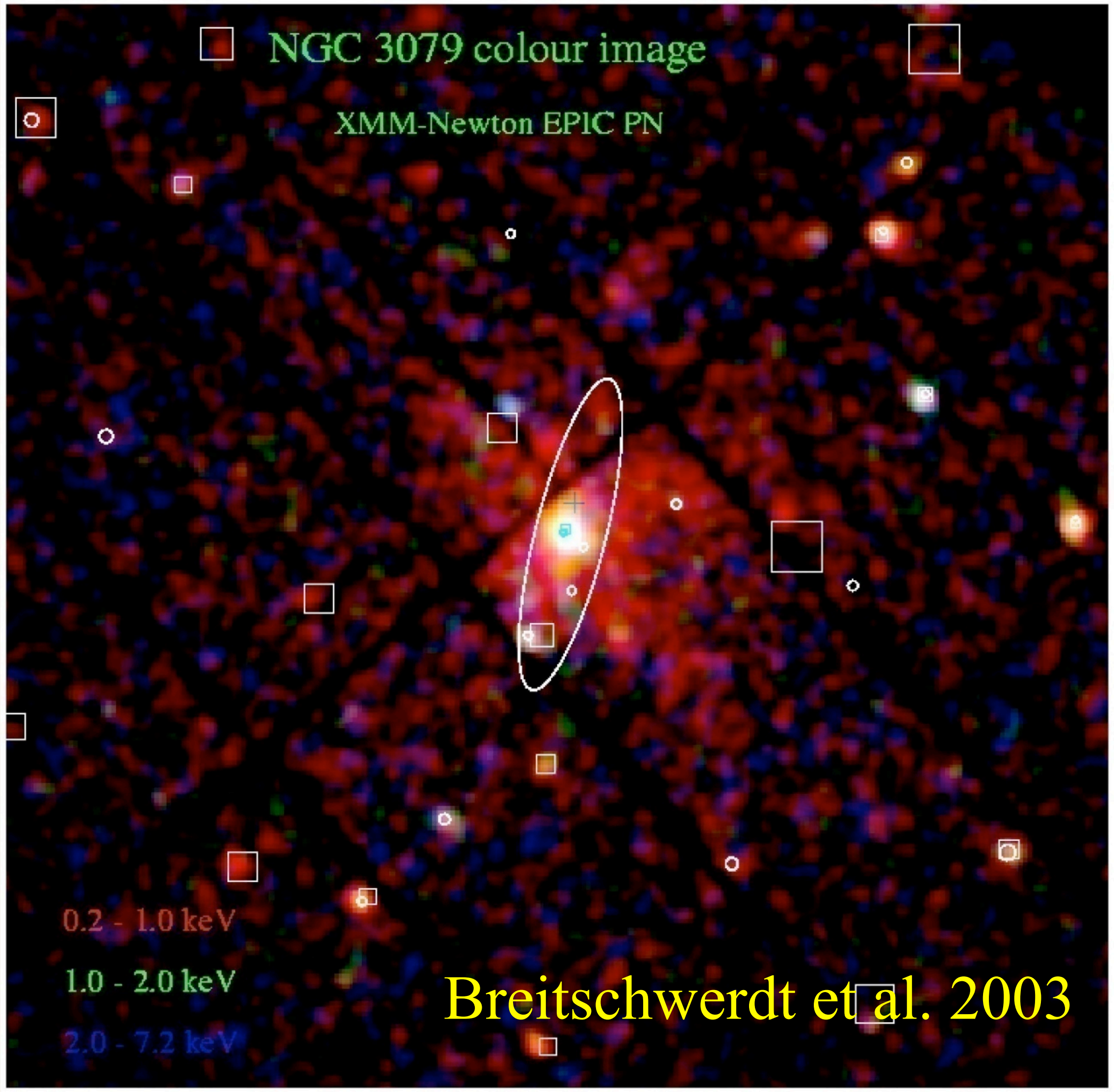

Top: *NGC 3079, XMM-Newton image (EPIC pn camera); the optical disk is indicated by the D_{25} ellipse; the exposure was 25 ksec.*

Modeling galactic halos with outflow (VI): NCG 3079

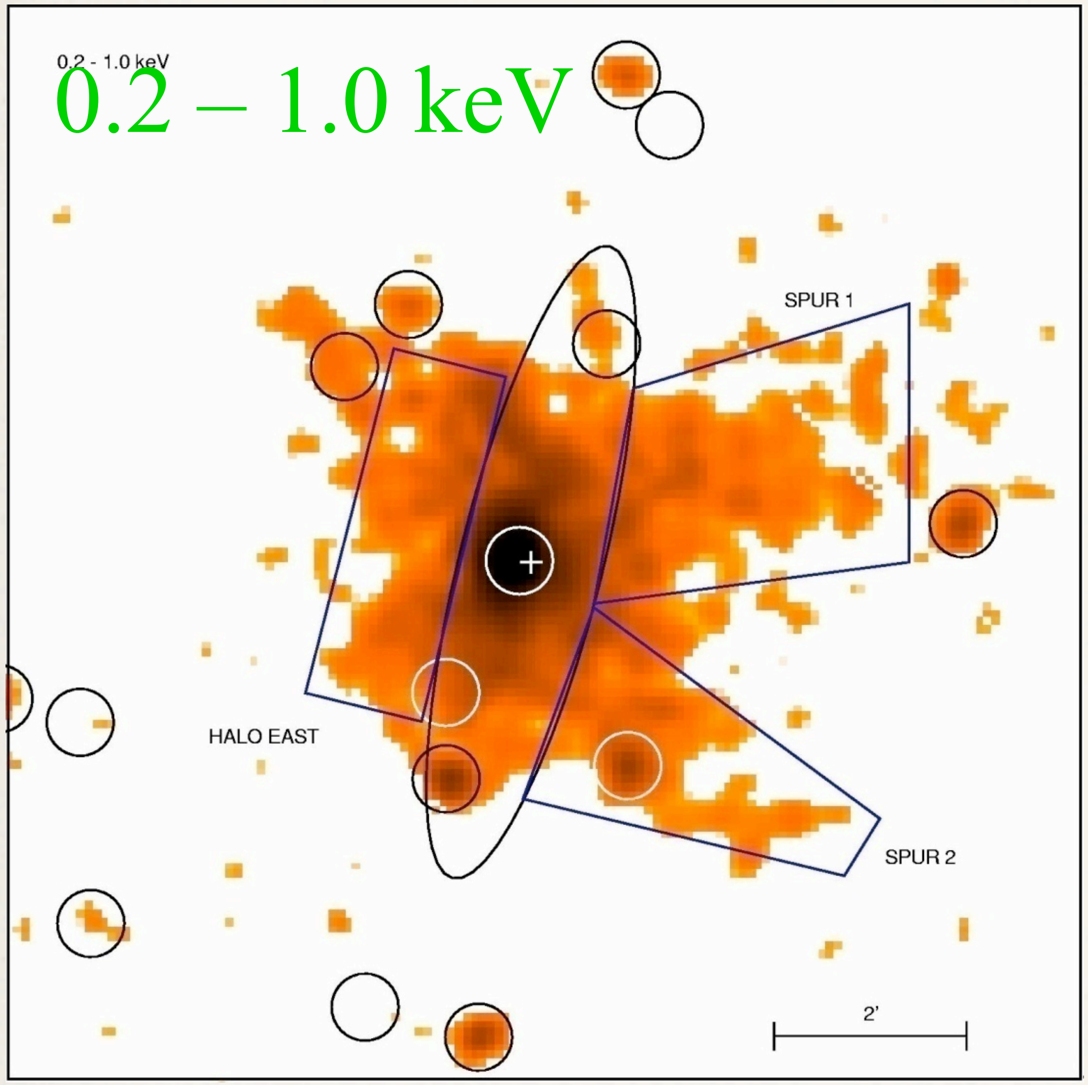

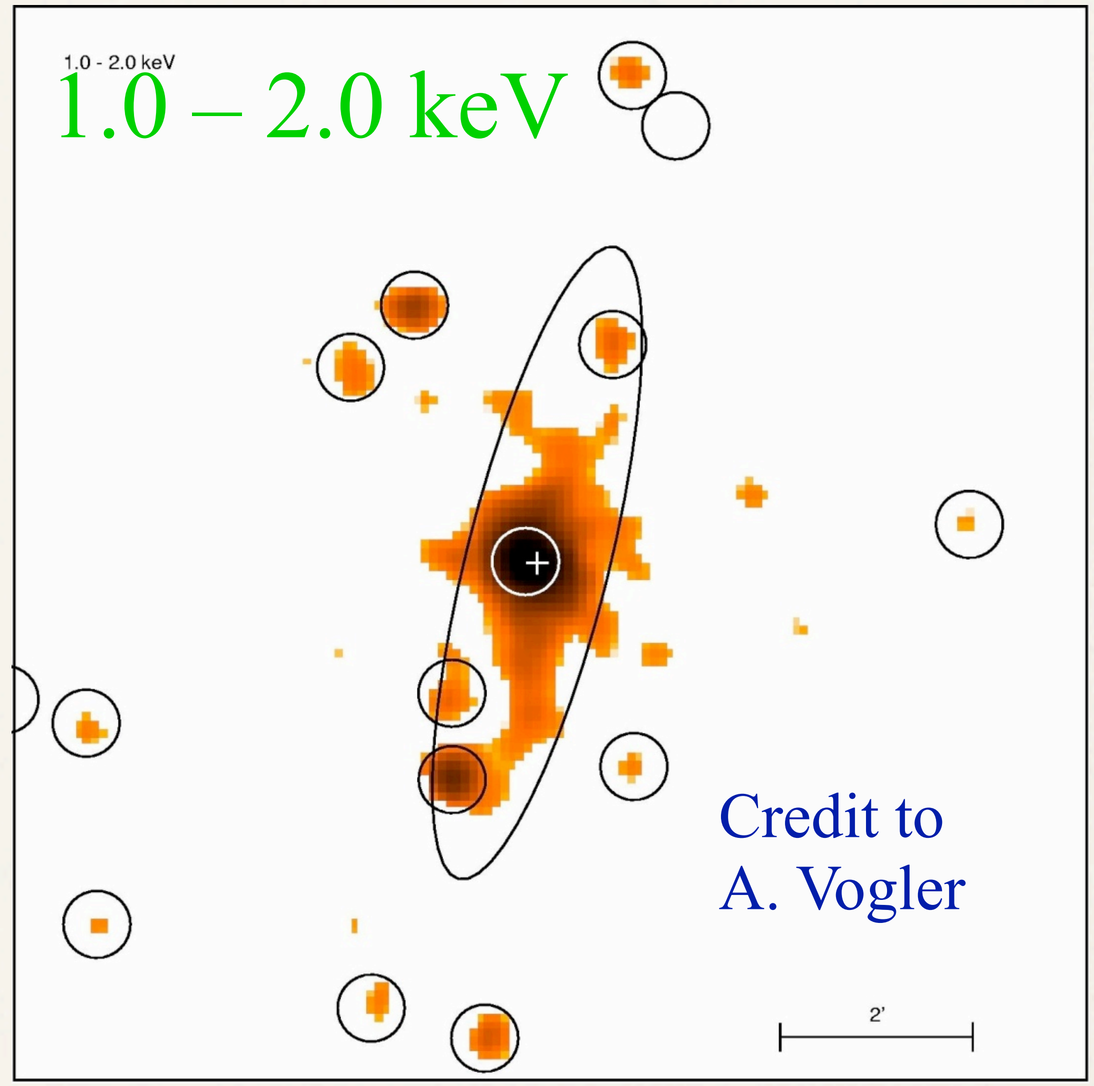

- large extended soft halo emission
- $0.2 \leq E \leq 1.0$ keV

- morphology: soft X-ray spurs
- hard emission largely confined to disk

Modeling galactic halos with outflow (VII): NCG 3079

Model	n_0 [cm^{-3}]	T_0 [10^6 K]	B_0 [μG]	u_0 [km/s]
M1	$3\ 10^{-3}$	3.0	2.0	200.3
M2	$3\ 10^{-3}$	5.0	5.0	312.9
M3	$3\ 10^{-3}$	4.0	5.0	260.4
M4	$4.2\ 10^{-3}$	3.7	5.0	234.1
M5	$5\ 10^{-3}$	3.6	5.0	220.0

- changing inner boundary conditions, where wind is emanating

Modeling galactic halos with outflow (VII): NCG 3079

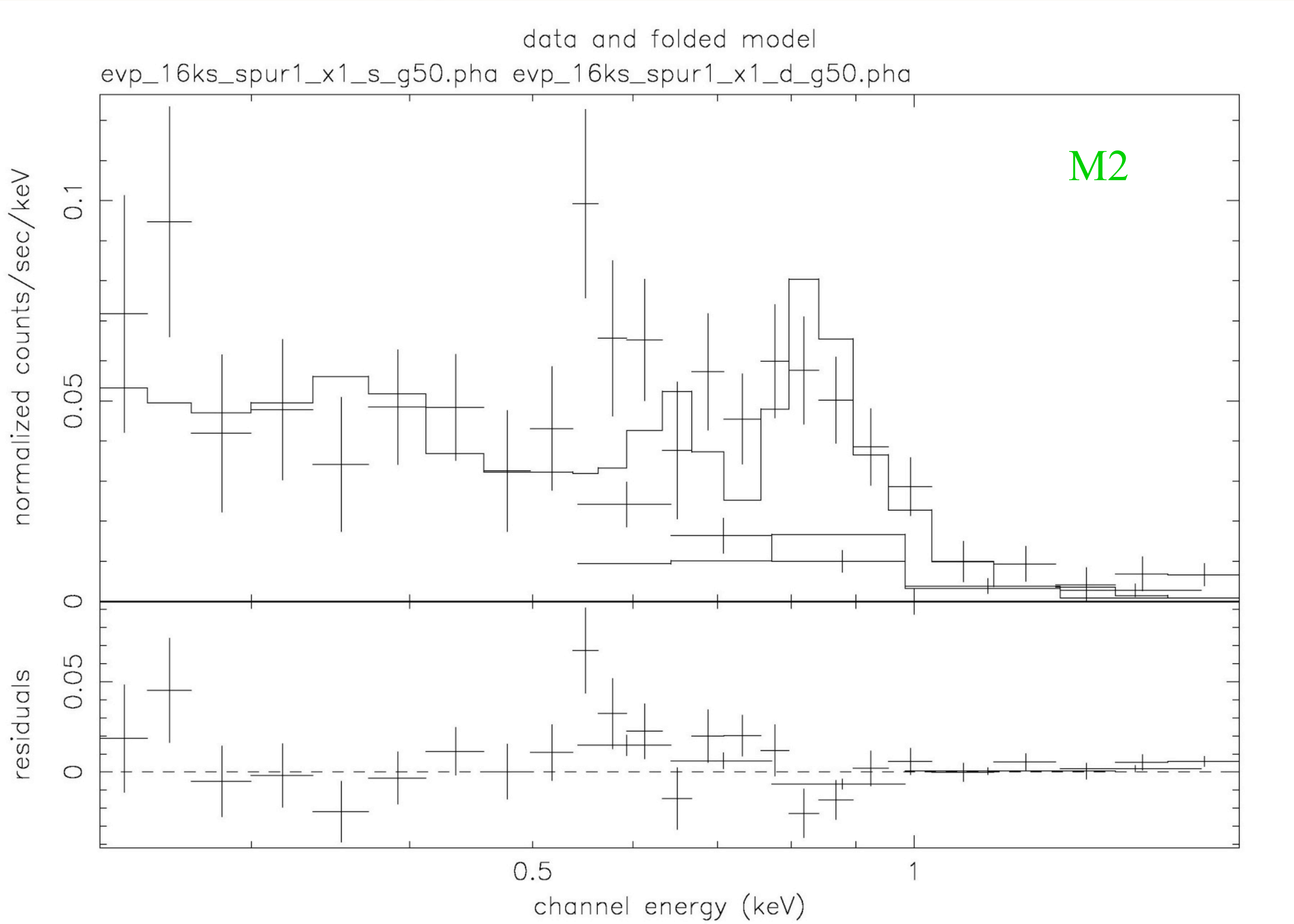

- bad fit in the 0.5 - 0.8 keV region
- too much emission in the 0.8 - 1 keV region ➔ T too high

Modeling galactic halos with outflow (VII): NCG 3079

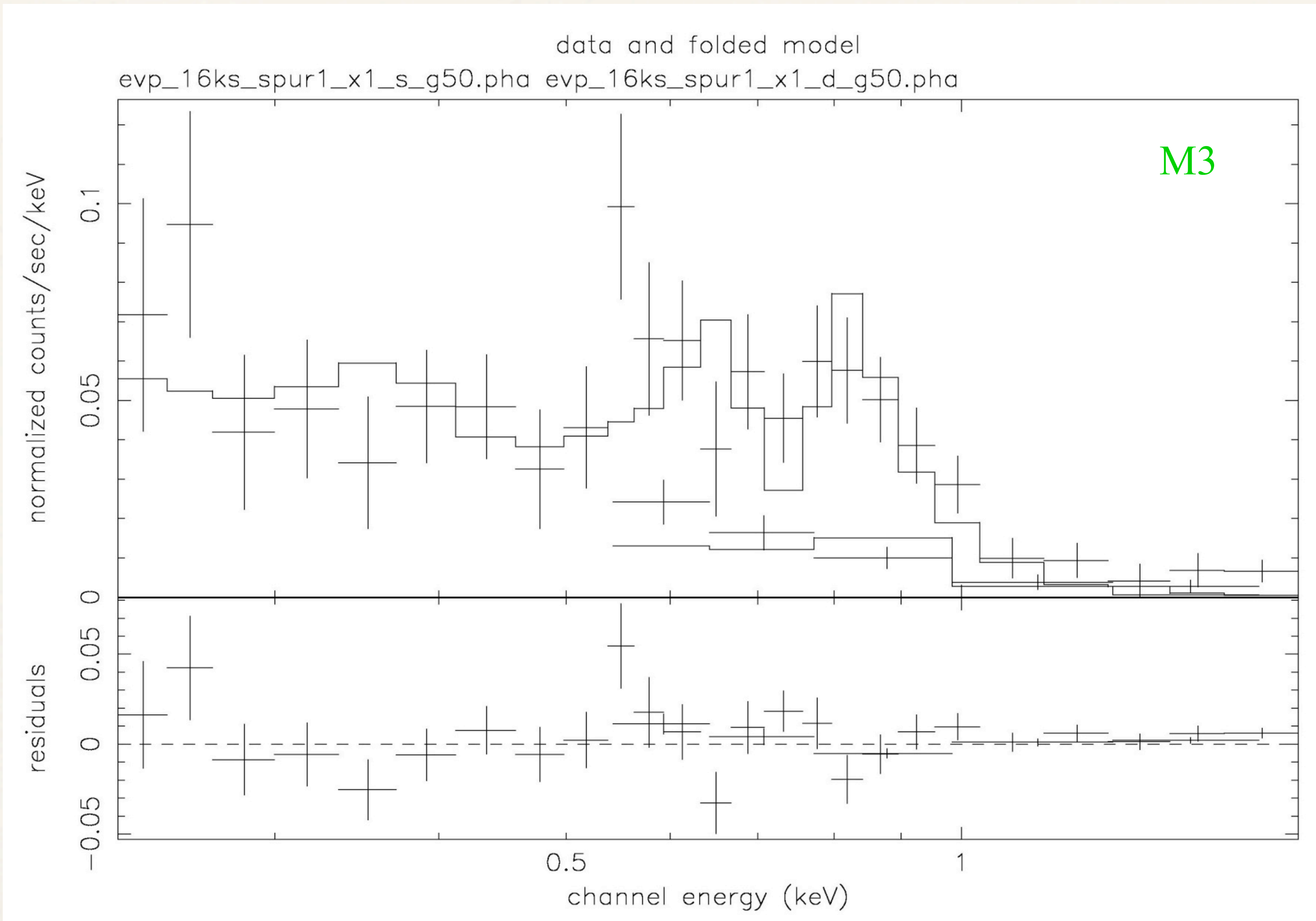

Dieter Breitschwerdt - Workshop on "Magnetic Fields on scales from kpc to km" - Cracow, 18.5.2010

ZAA

Modeling galactic halos with outflow (VII): NCG 3079

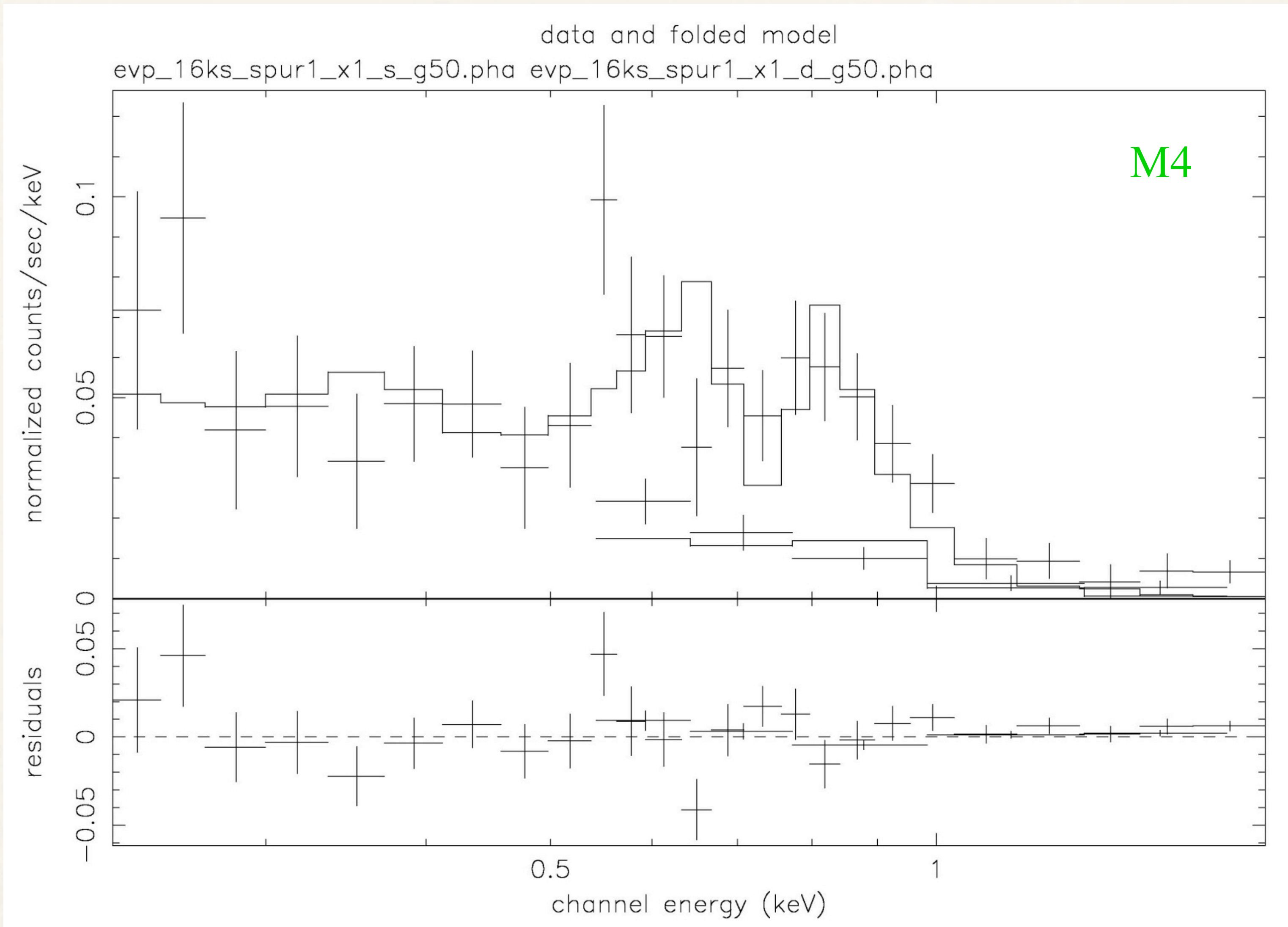

- better fit: T still slightly too high

Modeling galactic halos with outflow (VII): NCG 3079

- **best fit model:**
- galactic wind with gravitational potential (including dark matter halo)
- **$n_0 = 5\ 10^{-3}\ cm^{-3}$, $T_0 = 3.6\ 10^6$ K, $B_0 = 5\mu G$, $u_0 = 220$ km/s**
- foreground absorption: $N(H) = 3.9\ 10^{20}\ cm^{-2}$
- goodness of fit: $X^2_{red} = 1.2$
- derived mass loss rate:
- $dm/dt = \varrho_0\ u_0 = 0.055\ M_{sol}/yr/kpc^2$
- **mass loss rate in "spur" region** ($R = 8kpc$): $dM/dt = \pi/2\ R^2\ \varrho_0\ u_0 =$ **$3.5\ M_{sol}/yr$**

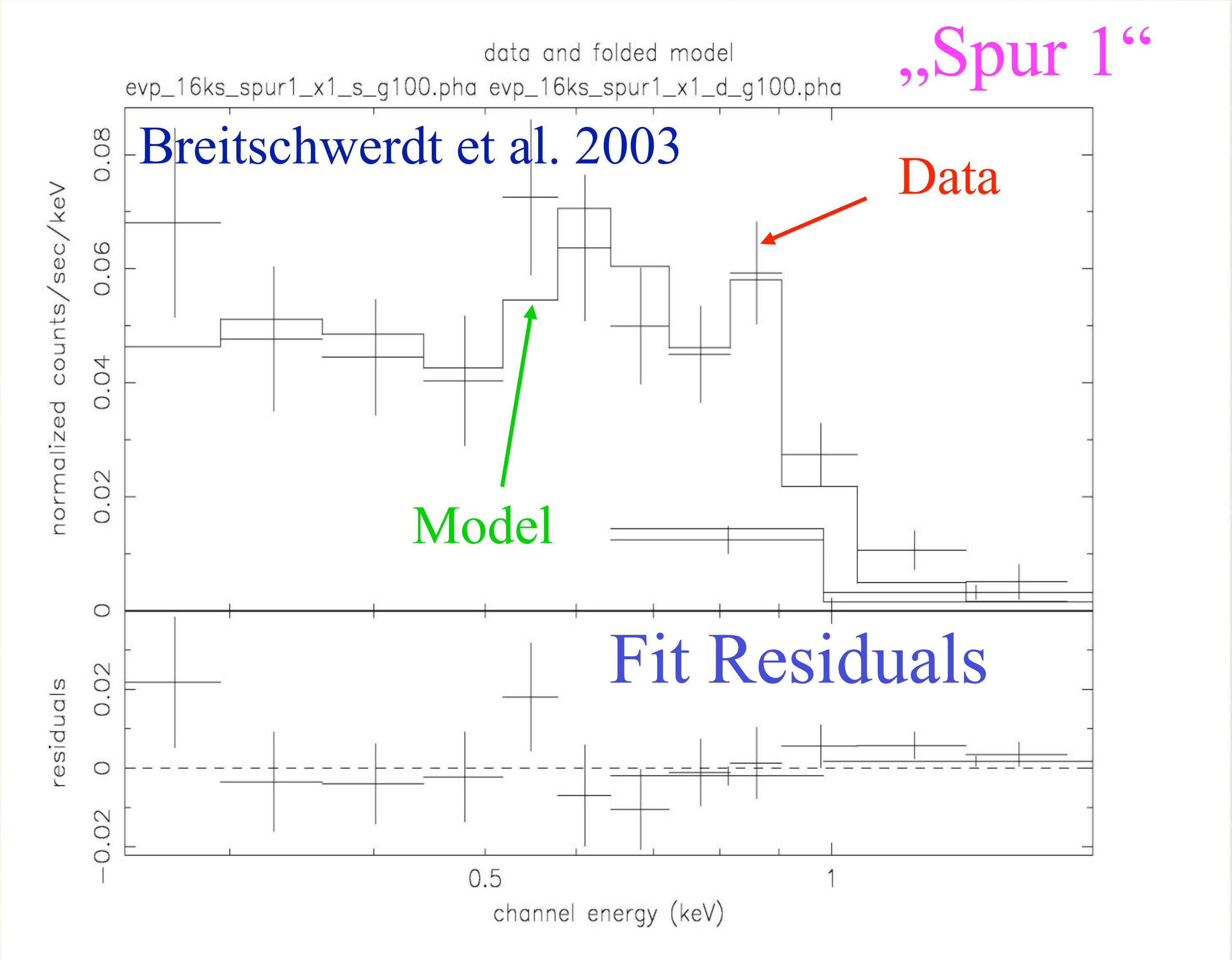

Top: *Comparison between data and dynamically and thermally self-consistent galactic wind model ➔ 5 iterations were necessary to achieve an acceptable fit*

Modeling galactic halos with outflow (V): NCG 3079

- **NGC 3079: smooth subsonic-supersonic transition ➔** critical point (M=1) in the flow at z ~ 5 kpc from the disk
- superbubble gas injected at the inner boundary ($z_0 = 1$ kpc) with initial velocity $u_0 =$ 220 km/s (subsonic, but super-alfvenic)
- terminal velocity ~ 450 km/s

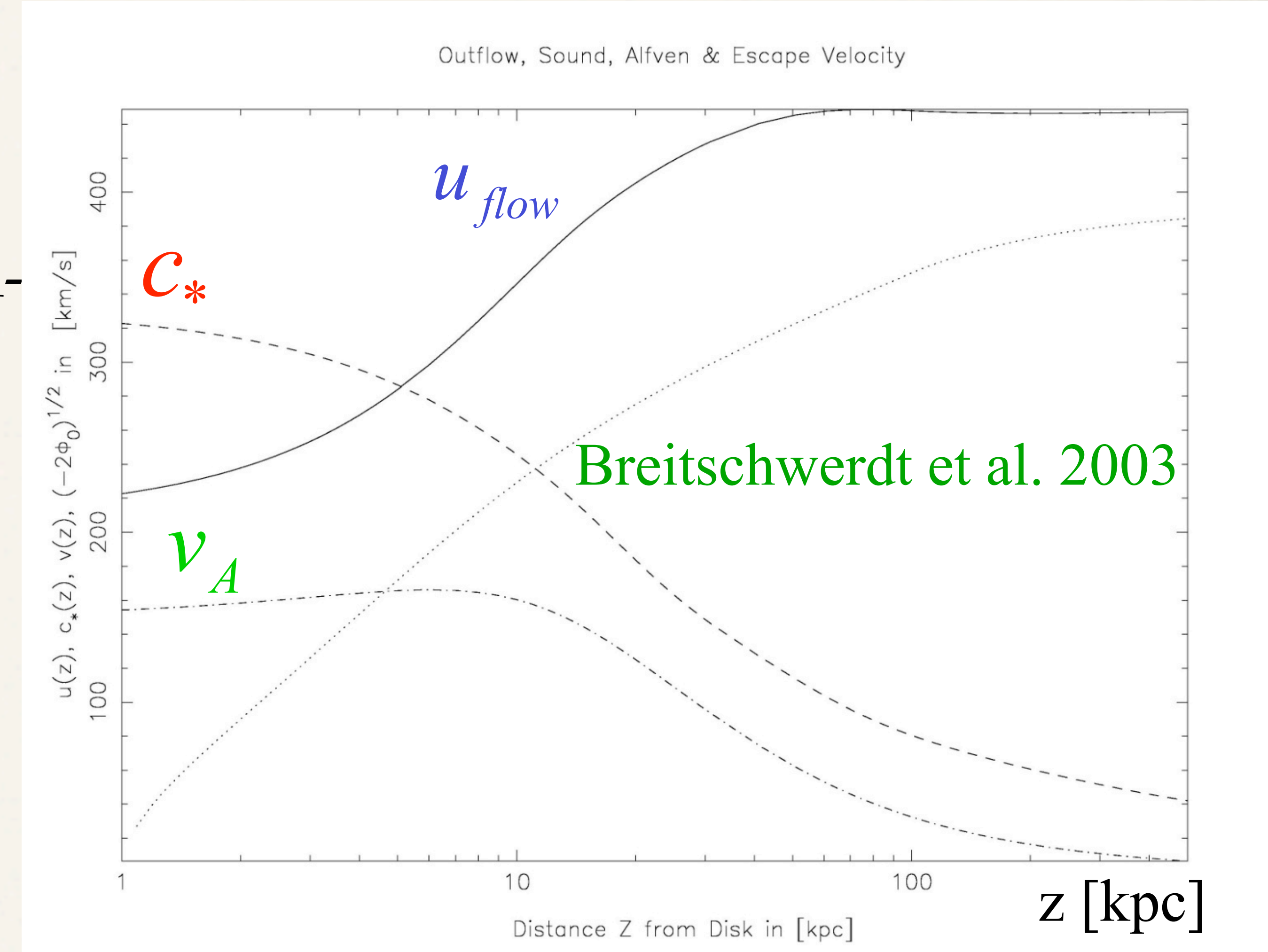

Top: Derived outflow characteristics for the best fit model

Wednesday, June 9, 2010

Modeling galactic halos with outflow (V): NCG 3079

- **Cooling Function**: Cooling curve depends on the ionization state of the plasma
- in case of a fast adiabatically expanding flow the difference between CIE and NEI cooling curves is striking
- whereas the CIE cooling curve peaks at ~ 10^5 K, the NEI curve in this particular model has a maximum ~ 10^6 K, where OVII, OVIII lines are abundant due to **delayed recombination**

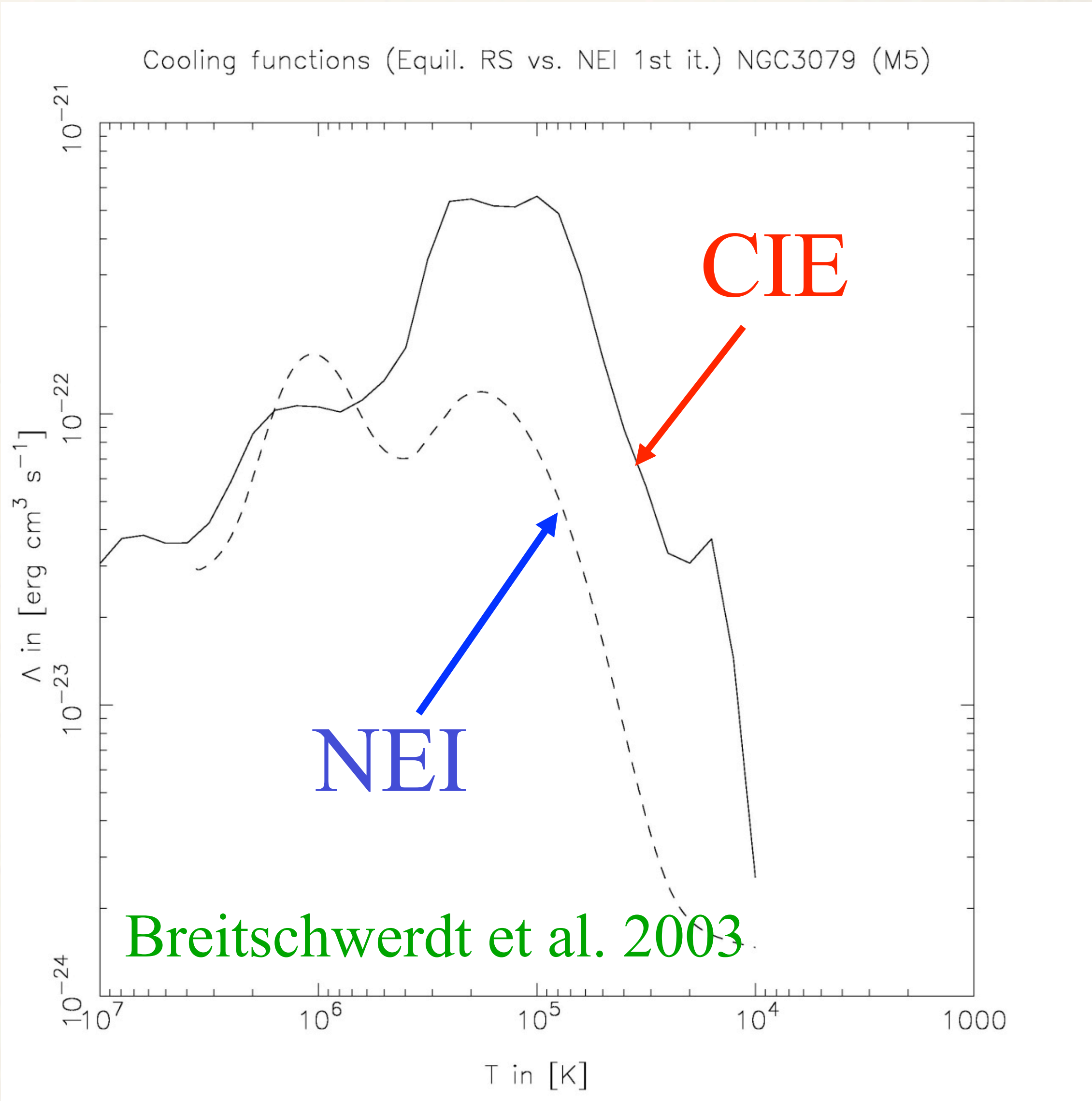

Top: *Comparison between cooling curve for CIE and for a dynamical NEI model for the starburst galaxy NGC 3079*

Cosmic Ray driven Wind in the Milky Way?

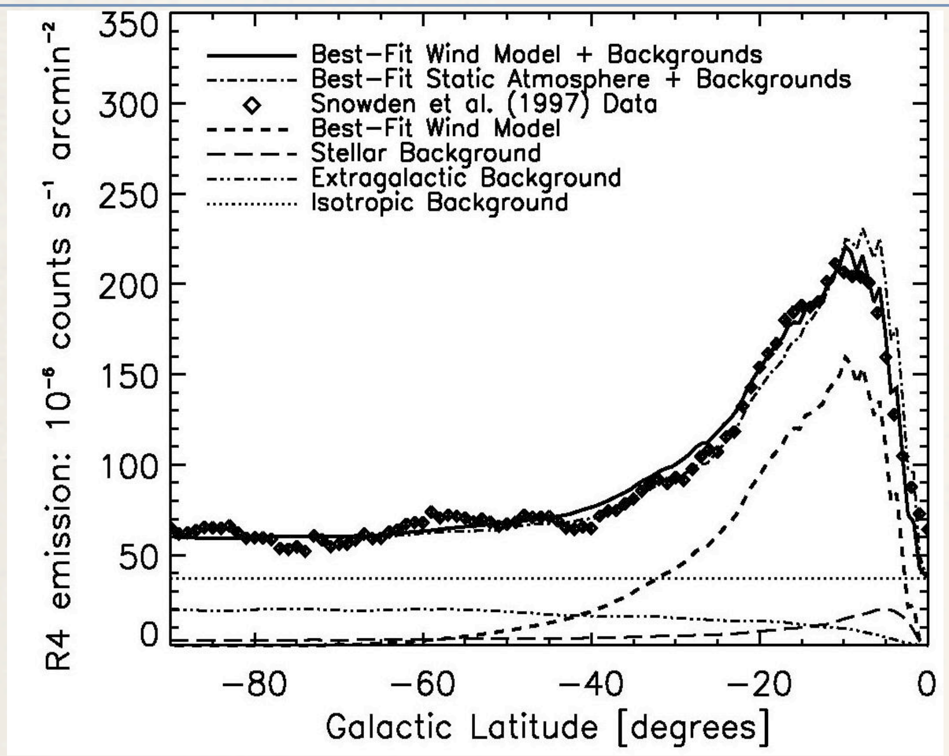

Top: *ROSAT PSPC observations (Snowden et al. 1997); shown is ROSAT R4 band (0.64 keV)*

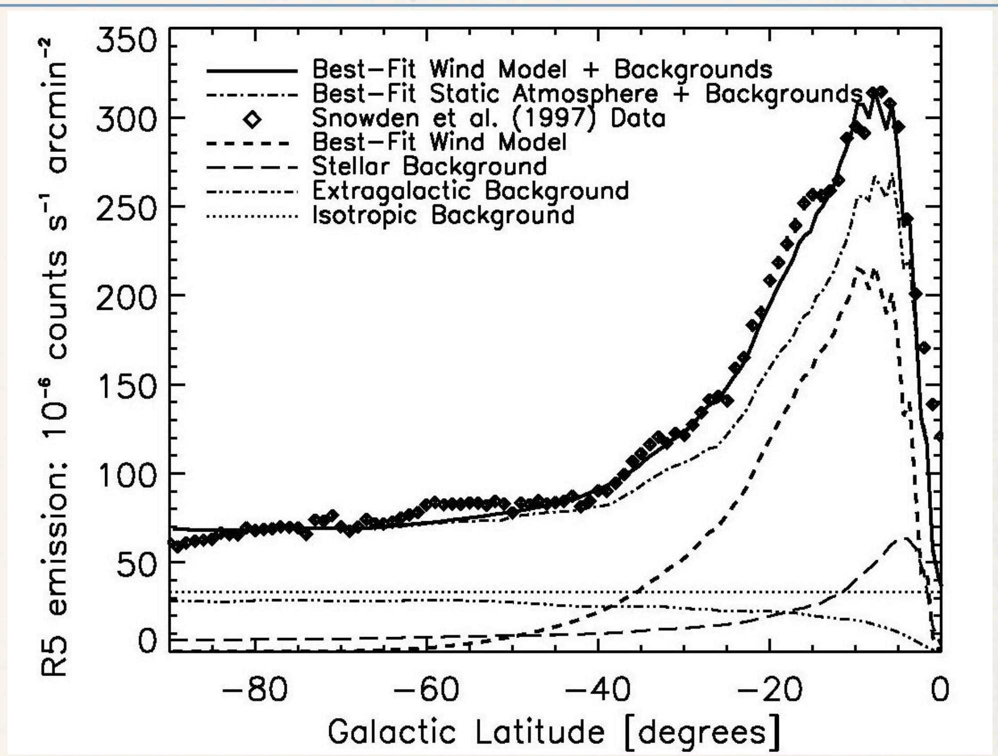

Top: *ROSAT PSPC observations (Snowden et al. 1997); shown is ROSAT R5 band (0.85 keV)*

- To fit ROSAT PSPC data in a given region of the MW sky, Everett et al. (2008) show that a **CR driven wind** gives a statistically much better fit than a hydrostatic halo (especially for ROSAT R5 band)
- for lower halo here CIE is a good approximation, since deviation from NEI still small
- fiducial wind model for Milky Way: $\mathbf{n_0 = 6.9\ 10^{-3}\ cm^{-3}, T_0 = 2.9\ 10^6\ K, u_0 = 173\ km/s}$

CR electron transport in galactic halos (I): NCG 4631

- **Non-thermal radio emission of NGC 4631:** significant linear polarization for $z \leq 5$ kpc
- noticeable B-field component perpendicular to galactic disk
- **Modelling**: solve **diffusion-advection transport equation for electrons** incl. **synchrotron** and **inverse Compton** losses
- **radio spectral index** variation is a measure of dominant transport process: flat curve is indicative of accelerating **advection** flow, compensating for increasing losses with time ➔ galactic wind

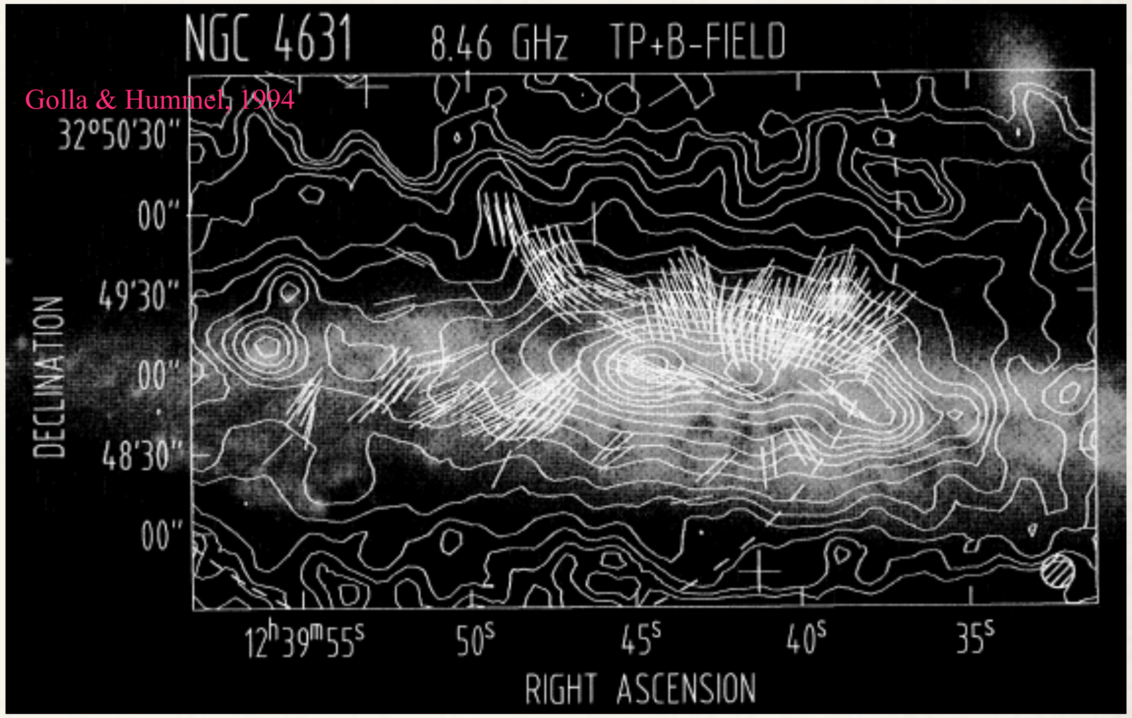

Top: radio map superimposed with polarization vectors on optical image
Right: self-consistent spectral index variation in galactic wind model

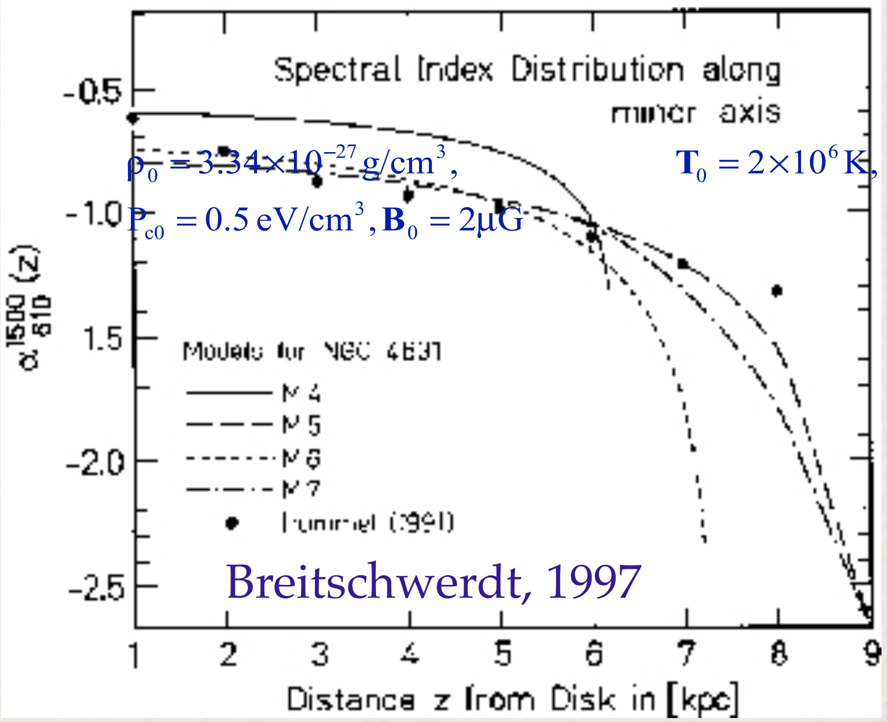

CR electron transport in galactic halos (II): NCG 253

- **Non-thermal radio emission of NGC 253:**
- CR electron transport equation

$$
\begin{aligned}
& - \frac{\partial}{\partial z}\left(D(E,z)\frac{\partial N(E,z)}{\partial z} - u(z)N(E,z)\right) \\
& - \frac{\partial}{\partial E}\left(\frac{1}{3}\frac{du}{dz}EN(E,z) - \frac{dE}{dt}N(E,z)\right) = Q(E,z) \\
Q(E,z) &= K_0 E^{-\gamma_0} h_g \delta(z)
\end{aligned}
$$

- spectral index close to sources up to vertical distances from disk of z ~ 1-2 kpc dominated by **diffusion**
- for z ≥ 1-2 kpc transport dominated by **advection**
- transport mechanism varies locally in agreement with local superbubble break-out from galactic disk

NGC 253

Heesen et al. (2007)

α(4.80,0.33)

minor axis offset [kpc]

Advection Diffusion Diffusion-Advection

Top: Comparison between the model (including a galactic wind) and observations (blue dots with error bars) of the starburst galaxy NGC 253; data from Heesen et al.

In collaboration with:
R. Beck, R.-J. Dettmar,
M. Krause, V. Heesen

CR electron transport in galactic halos (II): NCG 253

- **Non-thermal radio emission of NGC 253:**
- CR electron transport equation

$$
\begin{aligned}
& - \frac{\partial}{\partial z}\left(D(E,z)\frac{\partial N(E,z)}{\partial z} - u(z)N(E,z)\right) \\
& - \frac{\partial}{\partial E}\left(\frac{1}{3}\frac{du}{dz}EN(E,z) - \frac{dE}{dt}N(E,z)\right) = Q(E,z) \\
Q(E,z) &= K_0 E^{-\gamma_0} h_g \delta(z)
\end{aligned}
$$

- spectral index close to sources up to vertical distances from disk of z ~ 1-2 kpc dominated by **diffusion**
- for z ≥ 1-2 kpc transport dominated by **advection**
- transport mechanism varies locally in agreement with local superbubble break-out from galactic disk

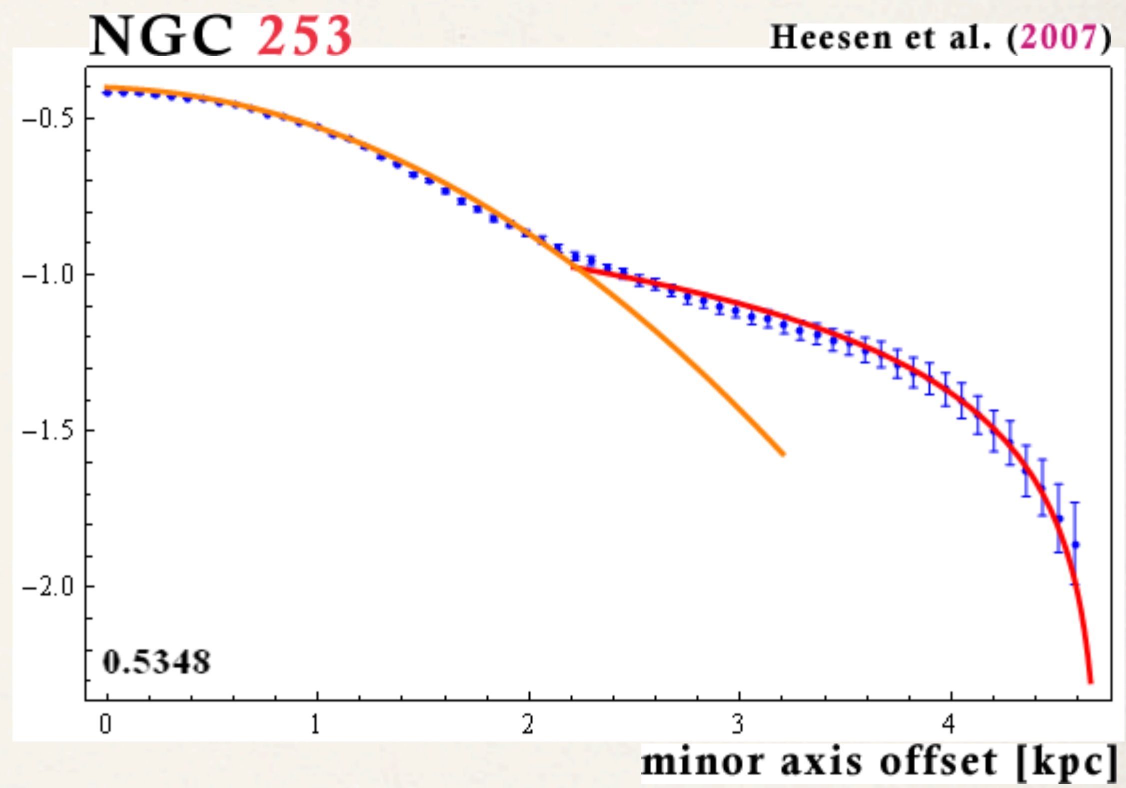

Advection Diffusion Diffusion-Advection

Top: *Comparison between the model (including a galactic wind) and observations (blue dots with error bars) of the starburst galaxy NGC 253; data from Heesen et al.*

In collaboration with:
R. Beck, R.-J. Dettmar,
M. Krause, V. Heesen

ZAA

CR electron transport in galactic halos (II): NCG 253

- **Non-thermal radio emission of NGC 253:**
- CR electron transport equation

$$
\begin{aligned}
& - \frac{\partial}{\partial z}\left(D(E,z)\frac{\partial N(E,z)}{\partial z} - u(z)N(E,z)\right) \\
& - \frac{\partial}{\partial E}\left(\frac{1}{3}\frac{du}{dz}EN(E,z) - \frac{dE}{dt}N(E,z)\right) = Q(E,z) \\
Q(E,z) & = K_0 E^{-\gamma_0} h_g \delta(z)
\end{aligned}
$$

- spectral index close to sources up to vertical distances from disk of z ~ 1-2 kpc dominated by **diffusion**
- for z ≥ 1-2 kpc transport dominated by **advection**
- transport mechanism varies locally in agreement with local superbubble break-out from galactic disk

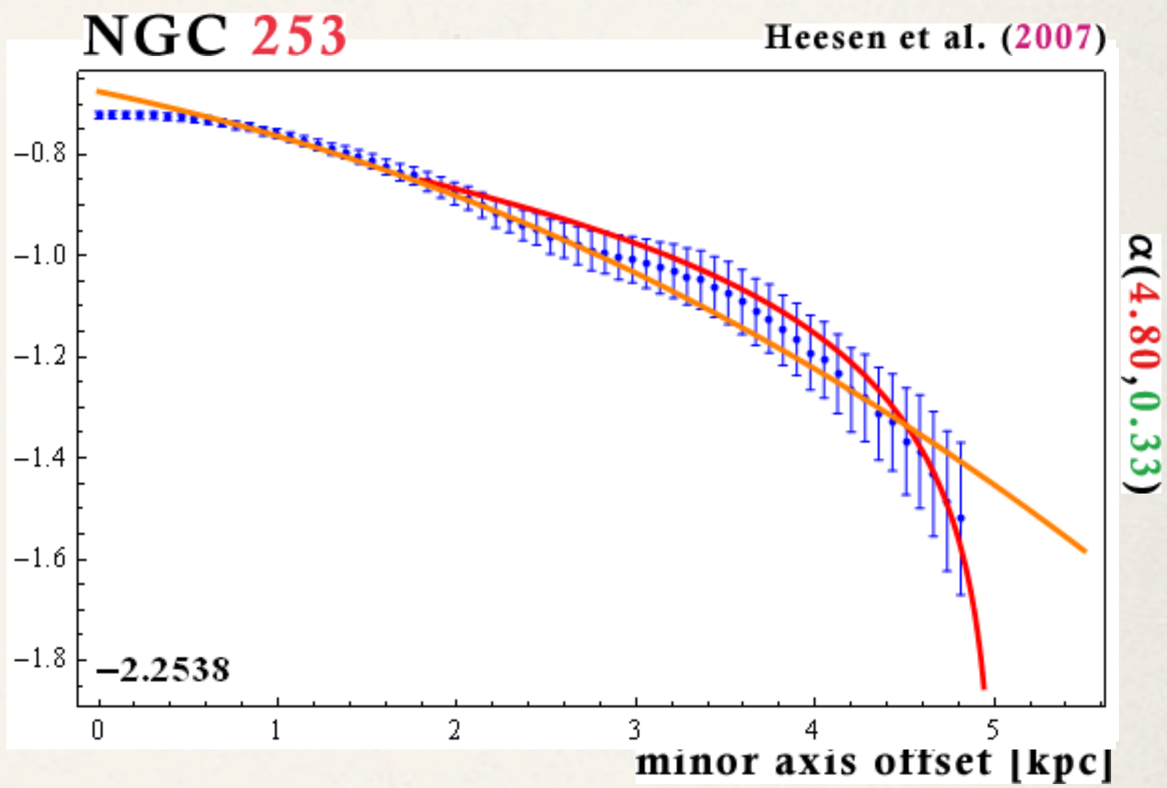

Advection Diffusion Diffusion-Advection

Top: Comparison between the model (including a galactic wind) and observations (blue dots with error bars) of the starburst galaxy NGC 253; data from Heesen et al.

In collaboration with:
R. Beck, R.-J. Dettmar,
M. Krause, V. Heesen

ZAA

CR electron transport in galactic halos (II): NCG 253

- **Non-thermal radio emission of NGC 253:**
- CR electron transport equation

$$
\begin{aligned}
& - \frac{\partial}{\partial z}\left(D(E,z)\frac{\partial N(E,z)}{\partial z} - u(z)N(E,z)\right) \\
& - \frac{\partial}{\partial E}\left(\frac{1}{3}\frac{du}{dz}EN(E,z) - \frac{dE}{dt}N(E,z)\right) = Q(E,z) \\
Q(E,z) &= K_0 E^{-\gamma_0} h_g \delta(z)
\end{aligned}
$$

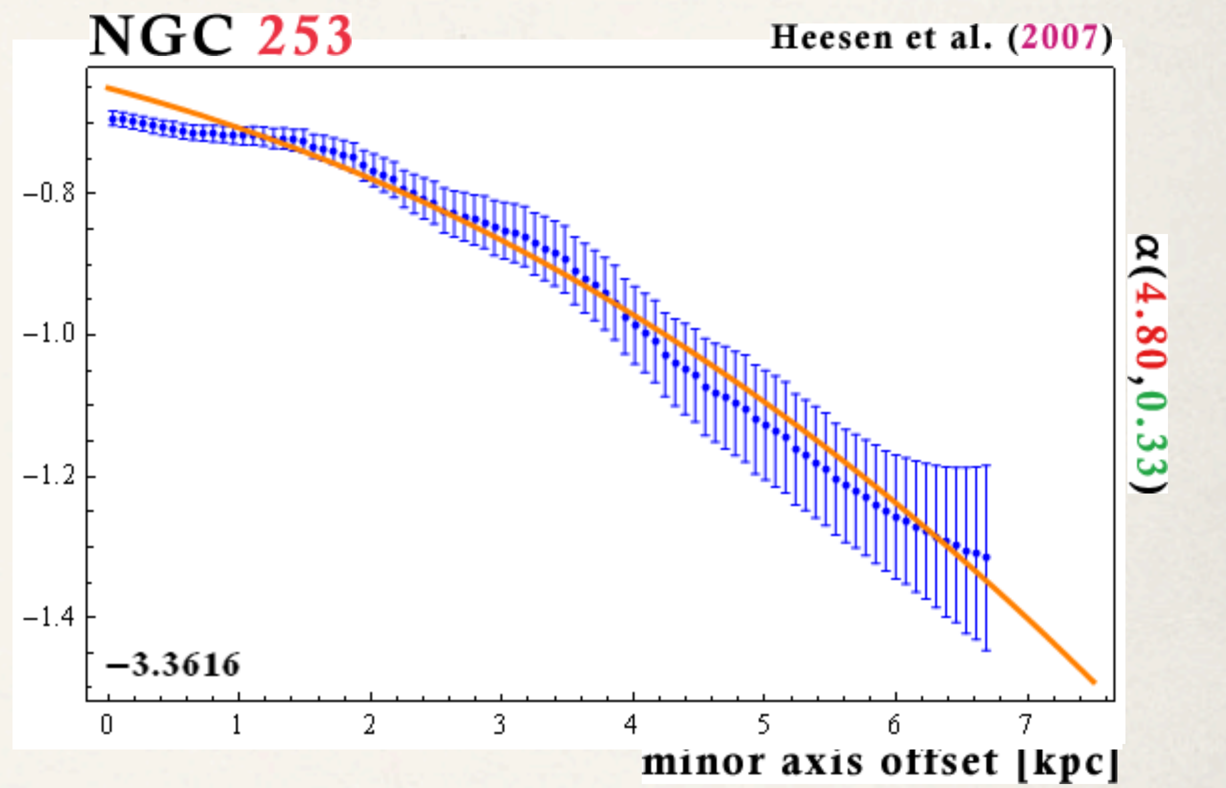

Advection Diffusion Diffusion-Advection

Top: *Comparison between the model (including a galactic wind) and observations (blue dots with error bars) of the starburst galaxy NGC 253; data from Heesen et al.*

- spectral index close to sources up to vertical distances from disk of z ~ 1-2 kpc dominated by **diffusion**
- for z ≥ 1-2 kpc transport dominated by **advection**
- transport mechanism varies locally in agreement with local superbubble break-out from galactic disk

In collaboration with:
R. Beck, R.-J. Dettmar,
M. Krause, V. Heesen

ZAA

CR electron transport in galactic halos (II): NCG 253

- **Non-thermal radio emission of NGC 253:**
- CR electron transport equation

$$
\begin{aligned}
& - \frac{\partial}{\partial z}\left(D(E,z)\frac{\partial N(E,z)}{\partial z} - u(z)N(E,z)\right) \\
& - \frac{\partial}{\partial E}\left(\frac{1}{3}\frac{du}{dz}EN(E,z) - \frac{dE}{dt}N(E,z)\right) = Q(E,z) \\
Q(E,z) &= K_0 E^{-\gamma_0} h_g \delta(z)
\end{aligned}
$$

- spectral index close to sources up to vertical distances from disk of z ~ 1-2 kpc dominated by **diffusion**
- for z ≥ 1-2 kpc transport dominated by **advection**
- transport mechanism varies locally in agreement with local superbubble break-out from galactic disk

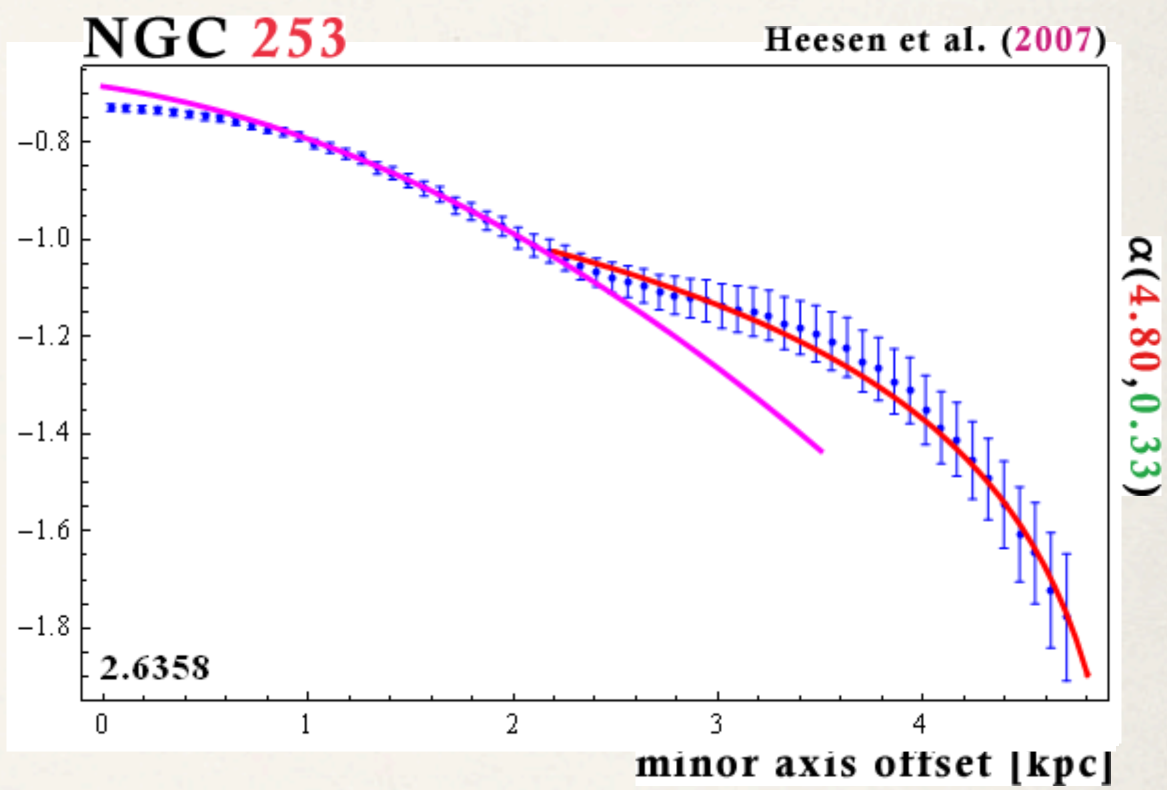

Advection Diffusion Diffusion-Advection

Top: Comparison between the model (including a galactic wind) and observations (blue dots with error bars) of the starburst galaxy NGC 253; data from Heesen et al.

In collaboration with:
R. Beck, R.-J. Dettmar,
M. Krause, V. Heesen

ZAA

CR electron transport in galactic halos (II): NCG 253

- **Non-thermal radio emission of NGC 253:**
- CR electron transport equation

$$
\begin{aligned}
& - \frac{\partial}{\partial z}\left(D(E,z)\frac{\partial N(E,z)}{\partial z} - u(z)N(E,z)\right) \\
& - \frac{\partial}{\partial E}\left(\frac{1}{3}\frac{du}{dz}EN(E,z) - \frac{dE}{dt}N(E,z)\right) = Q(E,z) \\
Q(E,z) &= K_0 E^{-\gamma_0} h_g \delta(z)
\end{aligned}
$$

- spectral index close to sources up to vertical distances from disk of z ~ 1-2 kpc dominated by **diffusion**
- for z ≥ 1-2 kpc transport dominated by **advection**
- transport mechanism varies locally in agreement with local superbubble break-out from galactic disk

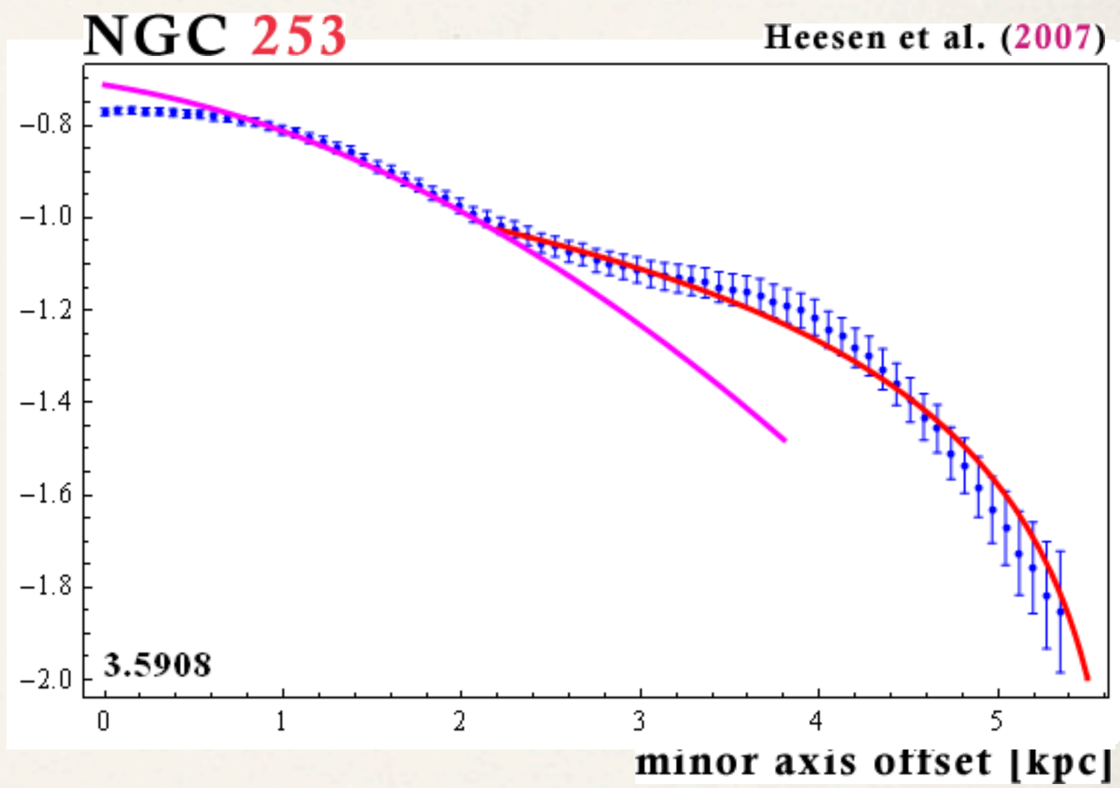

Advection Diffusion Diffusion-Advection

Top: *Comparison between the model (including a galactic wind) and observations (blue dots with error bars) of the starburst galaxy NGC 253; data from Heesen et al.*

In collaboration with:
R. Beck, R.-J. Dettmar,
M. Krause, V. Heesen

CR electron transport in galactic halos (II): NCG 253

- **Non-thermal radio emission of NGC 253:**
- CR electron transport equation

$$
\begin{aligned}
& - \frac{\partial}{\partial z}\left(D(E,z)\frac{\partial N(E,z)}{\partial z} - u(z)N(E,z)\right) \\
& - \frac{\partial}{\partial E}\left(\frac{1}{3}\frac{du}{dz}EN(E,z) - \frac{dE}{dt}N(E,z)\right) = Q(E,z) \\
Q(E,z) &= K_0 E^{-\gamma_0} h_g \delta(z)
\end{aligned}
$$

- spectral index close to sources up to vertical distances from disk of z ~ 1-2 kpc dominated by **diffusion**
- for z ≥ 1-2 kpc transport dominated by **advection**
- transport mechanism varies locally in agreement with local superbubble break-out from galactic disk

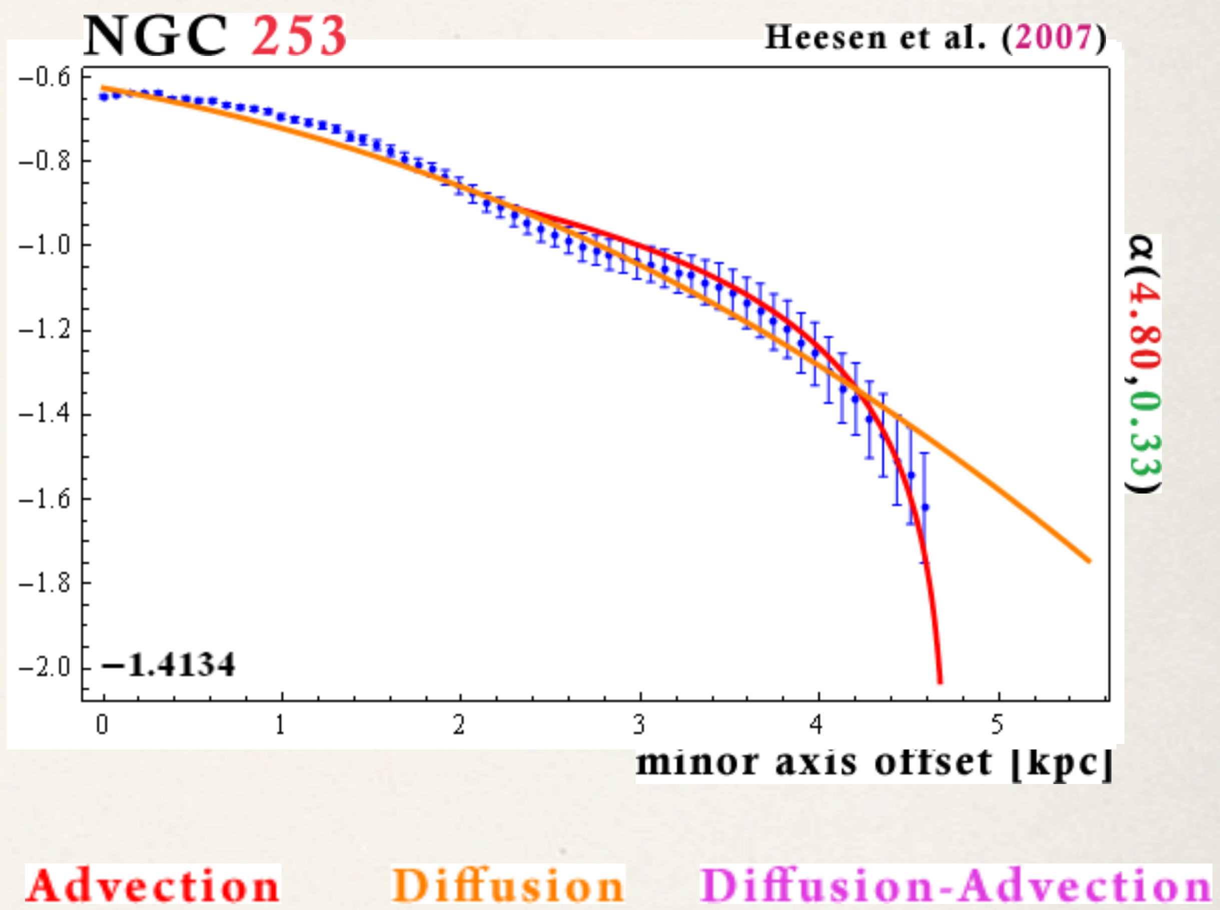

Top: Comparison between the model (including a galactic wind) and observations (blue dots with error bars) of the starburst galaxy NGC 253; data from Heesen et al.

In collaboration with:
R. Beck, R.-J. Dettmar,
M. Krause, V. Heesen

ZAA

CR electron transport in galactic halos (II): NCG 253

- **Non-thermal radio emission of NGC 253:**
- CR electron transport equation

$$
\begin{aligned}
& - \frac{\partial}{\partial z}\left(D(E,z)\frac{\partial N(E,z)}{\partial z} - u(z)N(E,z)\right) \\
& - \frac{\partial}{\partial E}\left(\frac{1}{3}\frac{du}{dz}EN(E,z) - \frac{dE}{dt}N(E,z)\right) = Q(E,z) \\
Q(E,z) & = K_0 E^{-\gamma_0} h_g \delta(z)
\end{aligned}
$$

- spectral index close to sources up to vertical distances from disk of z ~ 1-2 kpc dominated by **diffusion**
- for z ≥ 1-2 kpc transport dominated by **advection**
- transport mechanism varies locally in agreement with local superbubble break-out from galactic disk

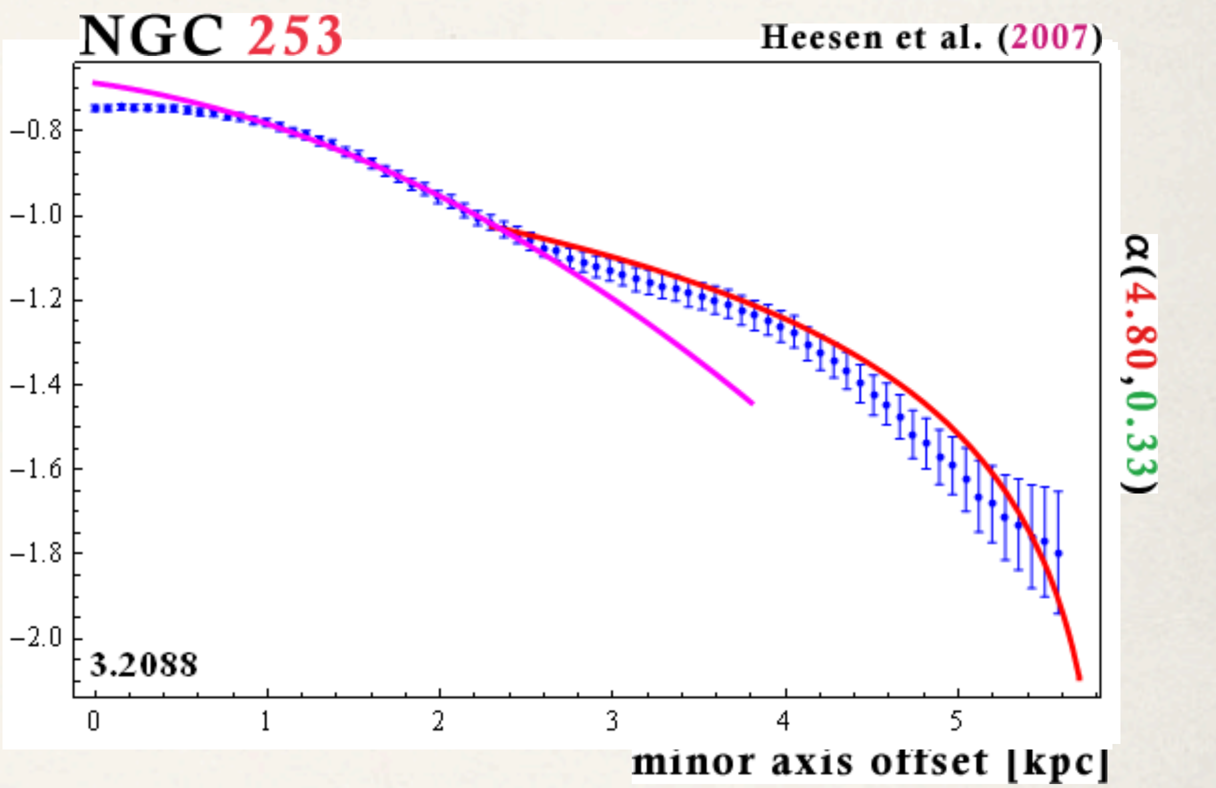

Advection Diffusion Diffusion-Advection

Top: *Comparison between the model (including a galactic wind) and observations (blue dots with error bars) of the starburst galaxy NGC 253; data from Heesen et al.*

In collaboration with:
R. Beck, R.-J. Dettmar,
M. Krause, V. Heesen

CR electron transport in galactic halos (II): NCG 253

- **Non-thermal radio emission of NGC 253:**
- CR electron transport equation

$$
\begin{aligned}
& - \frac{\partial}{\partial z}\left(D(E,z)\frac{\partial N(E,z)}{\partial z} - u(z)N(E,z)\right) \\
& - \frac{\partial}{\partial E}\left(\frac{1}{3}\frac{du}{dz}EN(E,z) - \frac{dE}{dt}N(E,z)\right) = Q(E,z) \\
Q(E,z) &= K_0 E^{-\gamma_0} h_g \delta(z)
\end{aligned}
$$

- spectral index close to sources up to vertical distances from disk of z ~ 1-2 kpc dominated by **diffusion**
- for z ≥ 1-2 kpc transport dominated by **advection**
- transport mechanism varies locally in agreement with local superbubble break-out from galactic disk

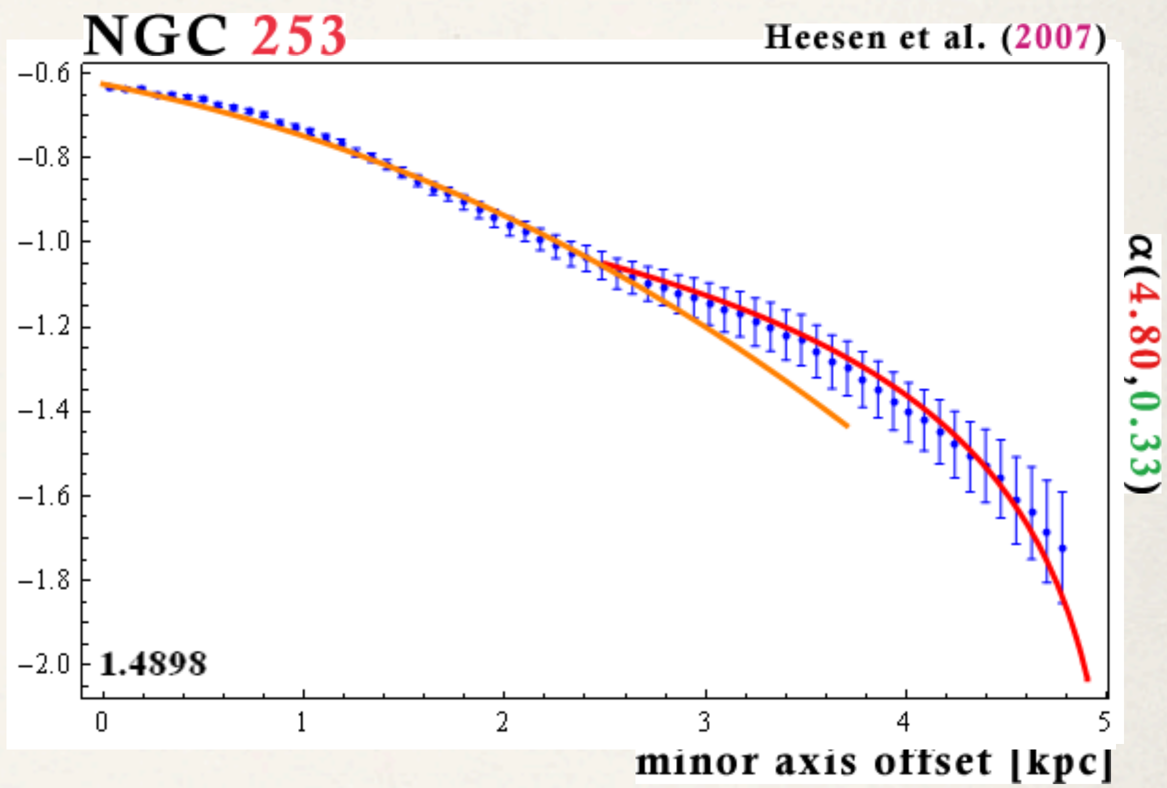

Advection Diffusion Diffusion-Advection

Top: Comparison between the model (including a galactic wind) and observations (blue dots with error bars) of the starburst galaxy NGC 253; data from Heesen et al.

In collaboration with:
R. Beck, R.-J. Dettmar,
M. Krause, V. Heesen

ZAA

CR electron transport in galactic halos (II): NCG 253

- **Non-thermal radio emission of NGC 253:**
- CR electron transport equation

$$
\begin{aligned}
& - \frac{\partial}{\partial z}\left(D(E,z)\frac{\partial N(E,z)}{\partial z} - u(z)N(E,z)\right) \\
& - \frac{\partial}{\partial E}\left(\frac{1}{3}\frac{du}{dz}EN(E,z) - \frac{dE}{dt}N(E,z)\right) = Q(E,z) \\
Q(E,z) &= K_0 E^{-\gamma_0} h_g \delta(z)
\end{aligned}
$$

- spectral index close to sources up to vertical distances from disk of z ~ 1-2 kpc dominated by **diffusion**
- for z ≥ 1-2 kpc transport dominated by **advection**
- transport mechanism varies locally in agreement with local superbubble break-out from galactic disk

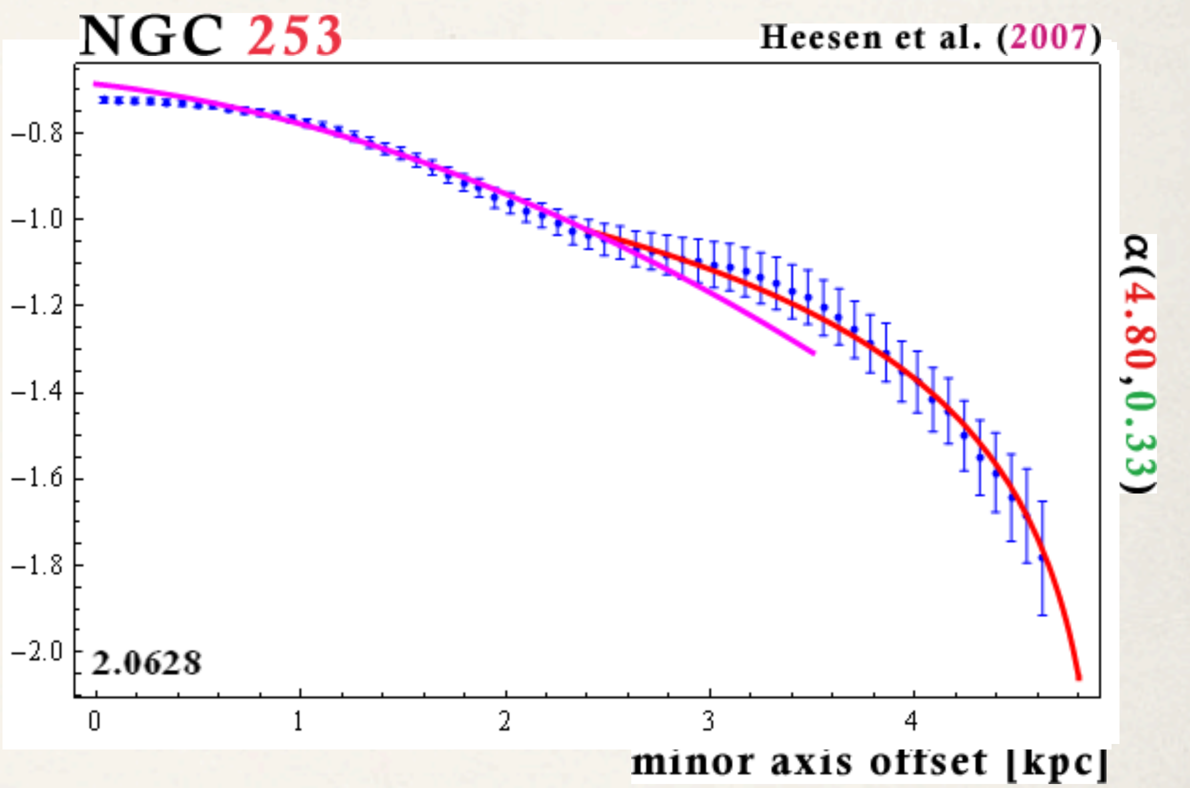

Advection Diffusion Diffusion-Advection

Top: *Comparison between the model (including a galactic wind) and observations (blue dots with error bars) of the starburst galaxy NGC 253; data from Heesen et al.*

In collaboration with:
R. Beck, R.-J. Dettmar,
M. Krause, V. Heesen

CR electron transport in galactic halos (II): NCG 253

- **Non-thermal radio emission of NGC 253:**
- CR electron transport equation

$$
\begin{aligned}
& - \frac{\partial}{\partial z}\left(D(E,z)\frac{\partial N(E,z)}{\partial z} - u(z)N(E,z)\right) \\
& - \frac{\partial}{\partial E}\left(\frac{1}{3}\frac{du}{dz}EN(E,z) - \frac{dE}{dt}N(E,z)\right) = Q(E,z) \\
Q(E,z) &= K_0 E^{-\gamma_0} h_g \delta(z)
\end{aligned}
$$

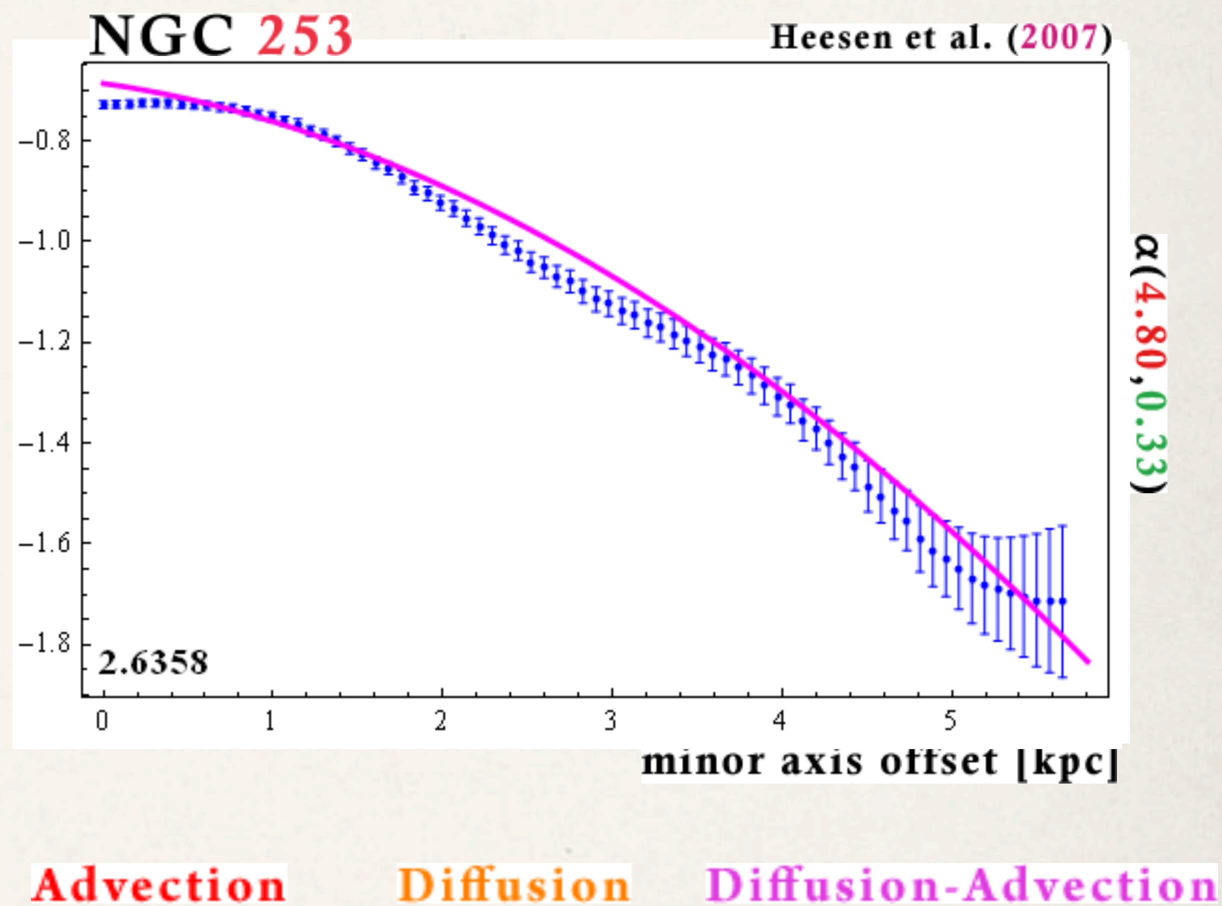

Top: Comparison between the model (including a galactic wind) and observations (blue dots with error bars) of the starburst galaxy NGC 253; data from Heesen et al.

- spectral index close to sources up to vertical distances from disk of z ~ 1-2 kpc dominated by **diffusion**
- for z ≥ 1-2 kpc transport dominated by **advection**
- transport mechanism varies locally in agreement with local superbubble break-out from galactic disk

In collaboration with:
R. Beck, R.-J. Dettmar,
M. Krause, V. Heesen

ZAA

CR electron transport in galactic halos (II): NCG 253

- **Non-thermal radio emission of NGC 253:**
- CR electron transport equation

$$
\begin{aligned}
& - \frac{\partial}{\partial z}\left(D(E,z)\frac{\partial N(E,z)}{\partial z} - u(z)N(E,z)\right) \\
& - \frac{\partial}{\partial E}\left(\frac{1}{3}\frac{du}{dz}EN(E,z) - \frac{dE}{dt}N(E,z)\right) = Q(E,z) \\
Q(E,z) &= K_0 E^{-\gamma_0} h_g \delta(z)
\end{aligned}
$$

- spectral index close to sources up to vertical distances from disk of z ~ 1-2 kpc dominated by **diffusion**
- for z ≥ 1-2 kpc transport dominated by **advection**
- transport mechanism varies locally in agreement with local superbubble break-out from galactic disk

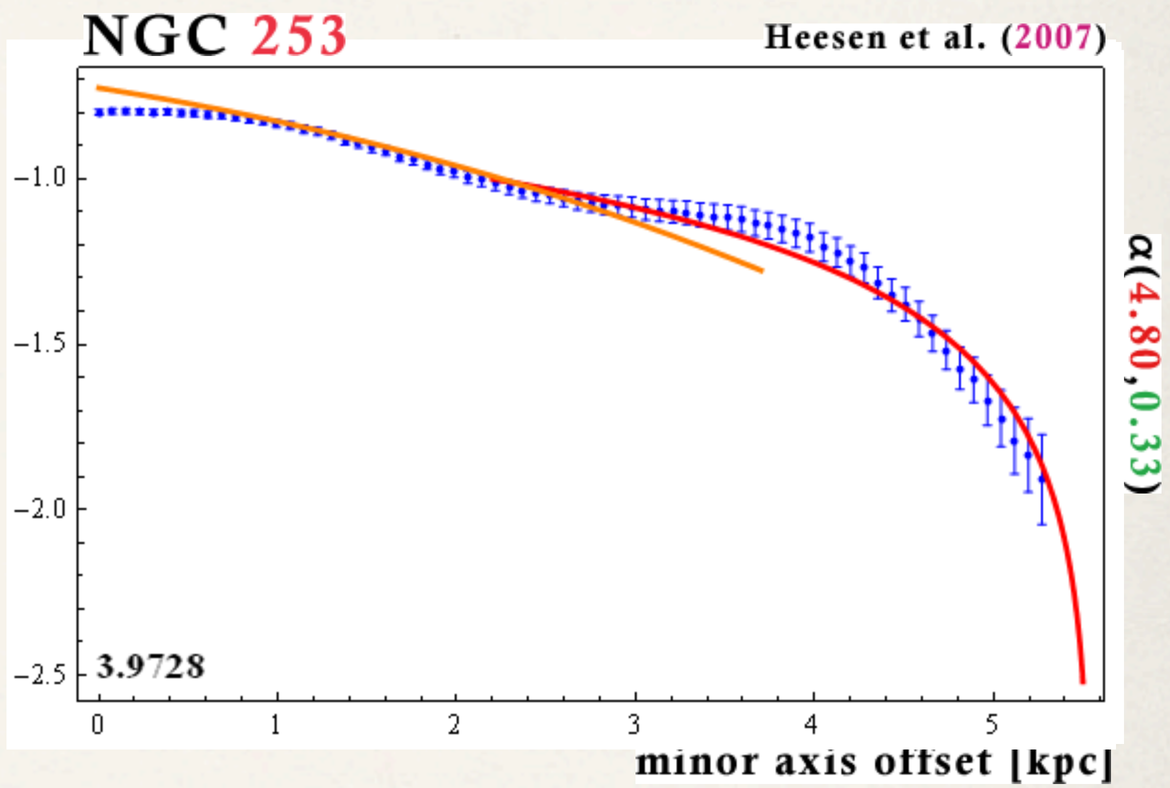

Advection Diffusion Diffusion-Advection

Top: *Comparison between the model (including a galactic wind) and observations (blue dots with error bars) of the starburst galaxy NGC 253; data from Heesen et al.*

In collaboration with:
R. Beck, R.-J. Dettmar,
M. Krause, V. Heesen

CR electron transport in galactic halos (II): NCG 253

- **Non-thermal radio emission of NGC 253:**
- CR electron transport equation

$$
\begin{aligned}
& - \frac{\partial}{\partial z}\left(D(E,z)\frac{\partial N(E,z)}{\partial z} - u(z)N(E,z)\right) \\
& - \frac{\partial}{\partial E}\left(\frac{1}{3}\frac{du}{dz}EN(E,z) - \frac{dE}{dt}N(E,z)\right) = Q(E,z) \\
Q(E,z) &= K_0 E^{-\gamma_0} h_g \delta(z)
\end{aligned}
$$

- spectral index close to sources up to vertical distances from disk of z ~ 1-2 kpc dominated by **diffusion**
- for z ≥ 1-2 kpc transport dominated by **advection**
- transport mechanism varies locally in agreement with local superbubble break-out from galactic disk

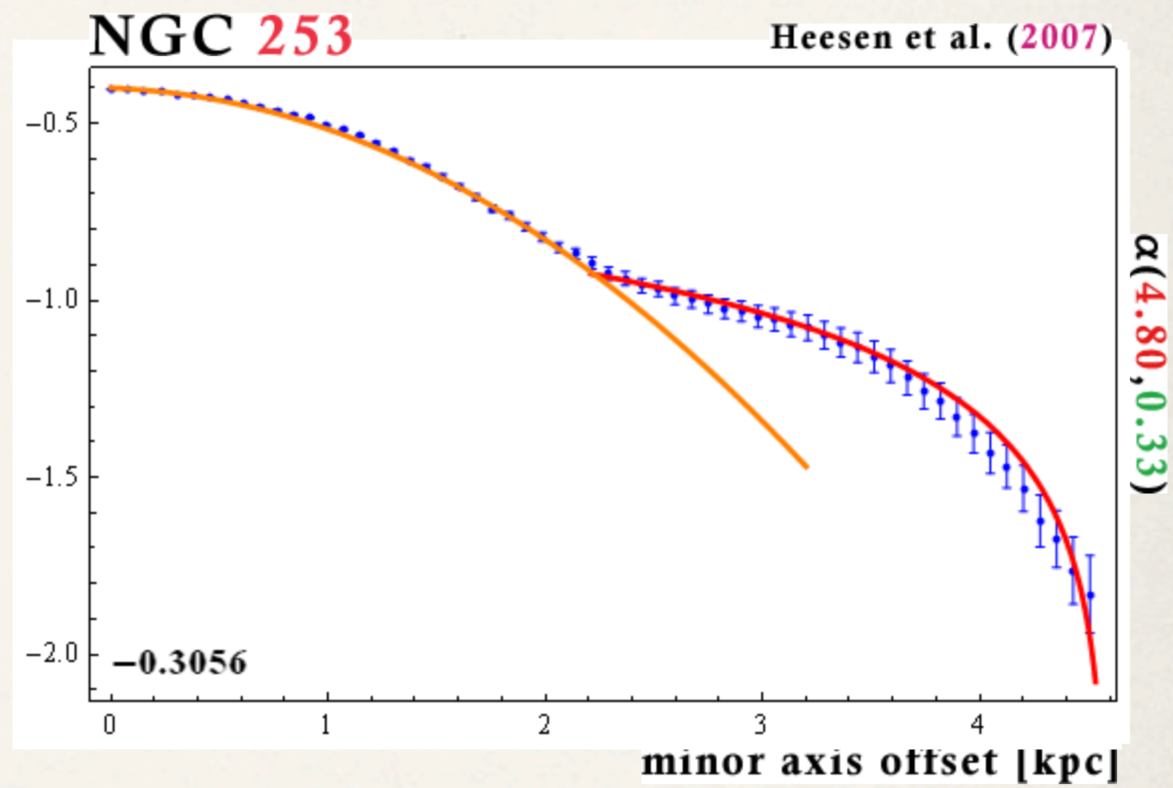

Advection Diffusion Diffusion-Advection

Top: Comparison between the model (including a galactic wind) and observations (blue dots with error bars) of the starburst galaxy NGC 253; data from Heesen et al.

In collaboration with:
R. Beck, R.-J. Dettmar,
M. Krause, V. Heesen

ZAA

Radial Diffuse γ-ray Gradient in the Galaxy

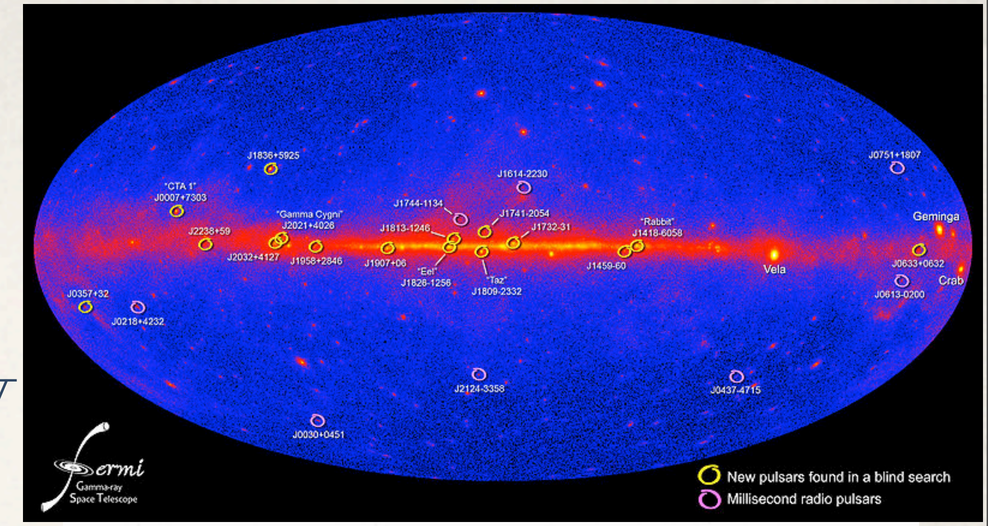

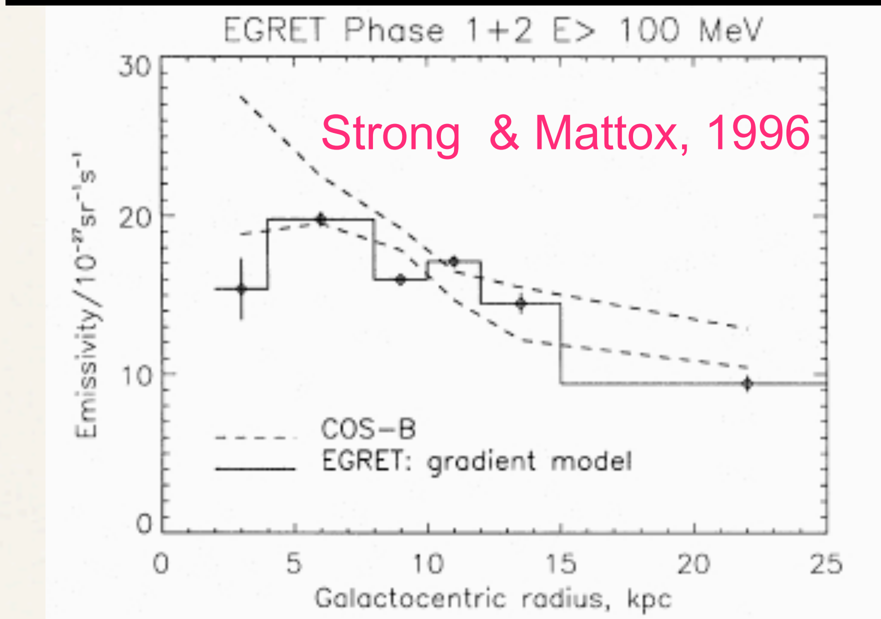

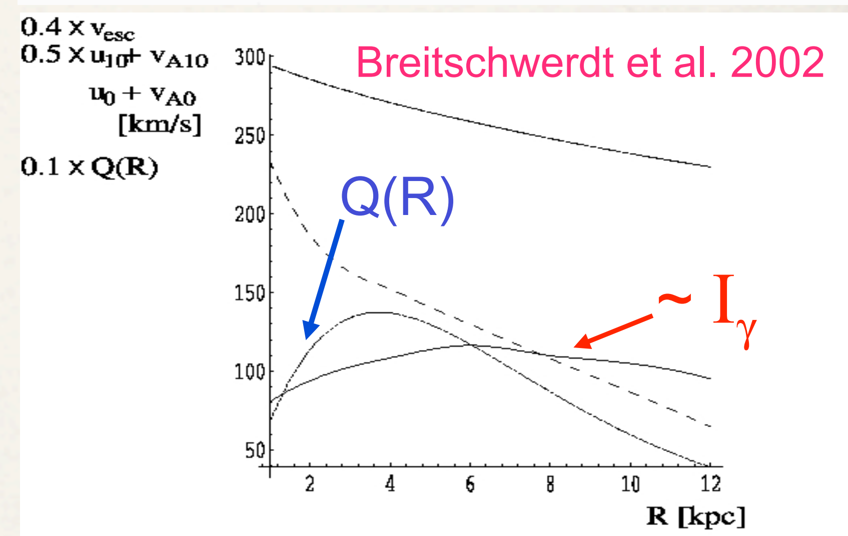

- **Diffuse γ-ray gradient in the Milky Way:** Cos-B, EGRET measured **shallow** gradient of diffuse γ-emission
- for E > 100 MeV γ-rays are mainly due to **π_0-decay**, which are due to interaction between CR protons and HI atoms ➔ γ-emission should follow **CR source** distribution (SNRs and pulsars), which peaks at R ~ 4 kpc
- diffusion model can only marginally reproduce γ-ray gradient for huge CR halo
- **simple model**: radially dependent **diffusion-advection** boundary due to local radial variations in **star formation**

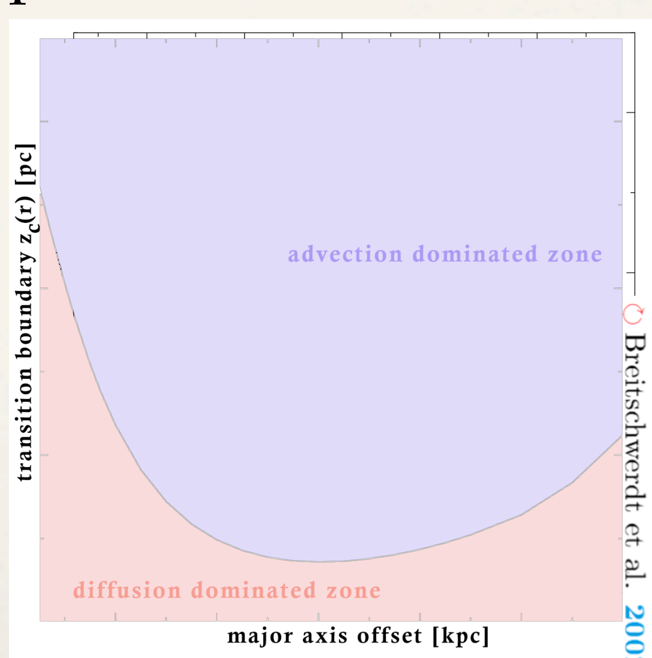

Top: *Fermi γ-ray all-sky survey*
Middle: *diffuse γ-ray gradient according to COS-B and EGRET observations*
Bottom: *model (galactic wind) of diffuse γ-ray emission*

CR acceleration be-yond the “Knee” (I)

- **Time-dependent galactic wind** calculations (Dorfi & Breitschwerdt 2010) confirm **stationary** wind solutions as time-asymptotic flow
- for starburst galaxies we use **time-dependent boundary conditions**, reflecting the duration of a starburst ➔ increase of CR & gas pressures by a factor of 10 at $z=z_0$
- double shock structure in the galactic wind region ➔ **post-acceleration** of galactic CRs (**1st order Fermi**)
- particles are convected downstream of **forward shock**, i.e. towards the galactic disk
- particle acceleration modifies shock ➔ **sub-shock** ➔ shock strengthens as propagating down a density gradient
- within a few 10^6 - 10^7 yr, particles can reach energies up to **10^{17} - 10^{18} eV**

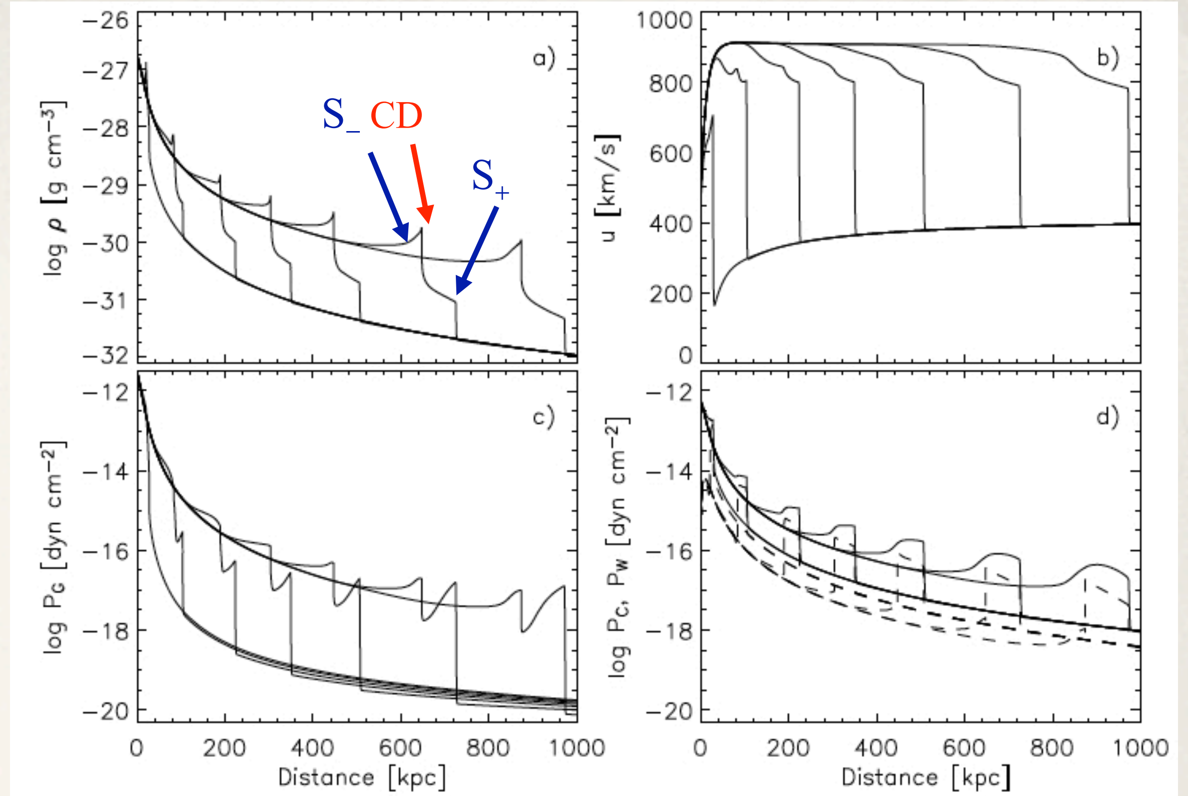

Dorfi & Breitschwerdt (2010)

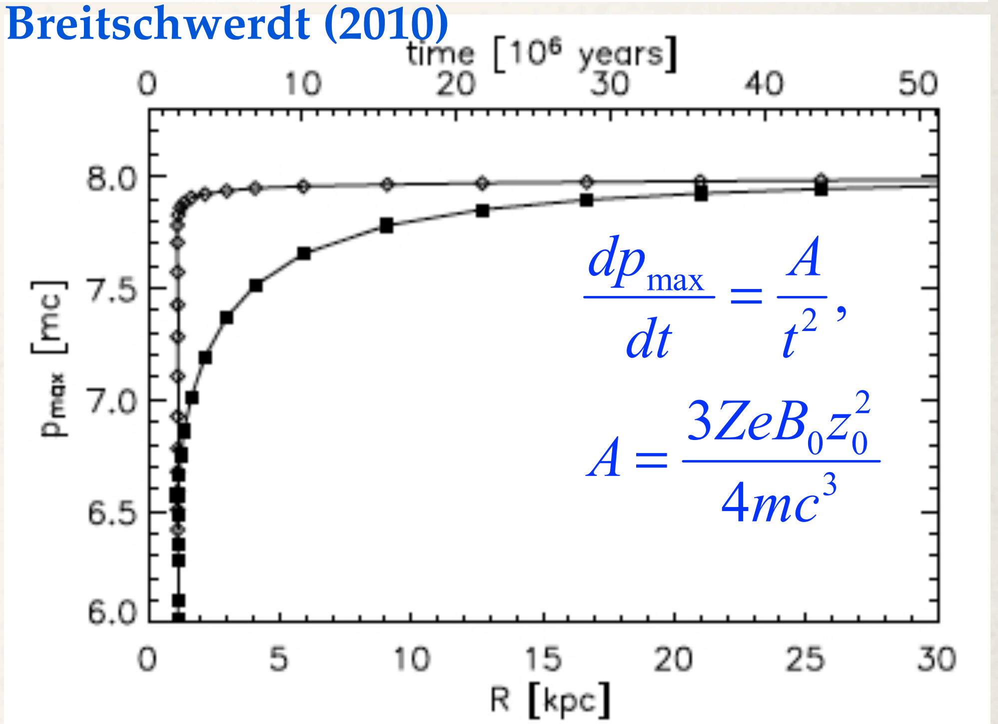

Top: density (a), velocity (b), gas (c), CR and wave pressures (d) for shocks in a galactic wind of the Milky Way for 3 $10^7 \leq t \leq 10^9$ yr
***Bottom**: maximum momentum of particles post-accelerated in galactic wind for forward (filled squares) and forward + reverse shock (diamonds)*

CR acceleration beyond the “Knee” (II)

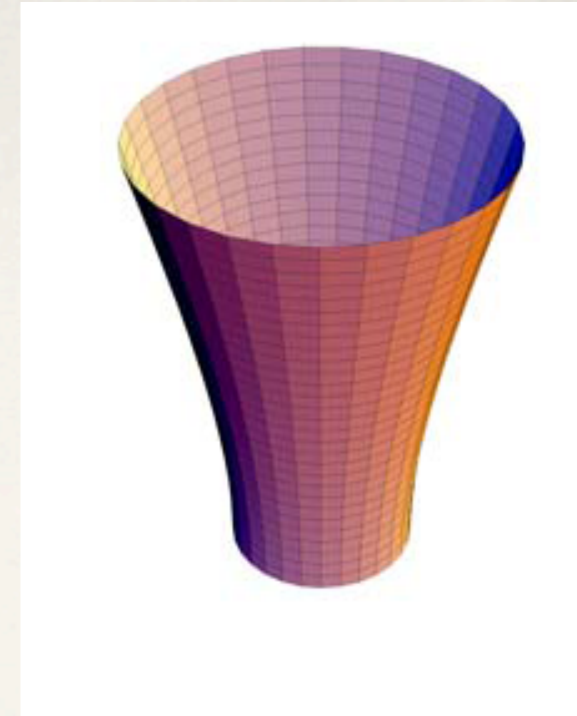

$$A(z) = A_0 \left[1 + \left(\frac{z}{H}\right)^2\right]$$

- **galactic wind post-acceleration of CRs** in the halo, i.e. **Halo CRs** (**HCRs**) guarantee a **smooth transition** to the spectrum of Galactic Cosmic Rays (GCRs)
- How do we get spectral hardening at the knee? For energy-dependent CR diffusion ~ $E^{-0.6}$, we need a spectral index for CR momentum of 2 (3.1-0.6) = 5
- Solve **Fokker-Planck Equation** in Flux Tube coordinates:

$$\frac{\partial f}{\partial t} + u(z)\frac{\partial f}{\partial z} = \frac{\partial}{\partial z}\left(\kappa\frac{\partial f}{\partial z}\right) + \frac{2z}{H^2+z^2}\kappa\frac{\partial f}{\partial z} + \frac{1}{3}p\frac{\partial f}{\partial p}\left(\frac{\partial u(z)}{\partial z} + \frac{2z}{H^2+z^2}u(z)\right)$$

- assume self-similar velocity field:
- u(z)=V(ξ) ξ dR/dt, ξ=z/R(t)

Metric Tensor

$$r = r_0\sqrt{1+\frac{z^2}{H^2}}$$

$$\Rightarrow g_{ij} = \begin{pmatrix} 1 & 0 & \frac{zr_0^2}{rH^2} \\ 0 & r^2 & 0 \\ \frac{zr_0^2}{rH^2} & 0 & 1+\frac{z^2r_0^4}{r^2H^4} \end{pmatrix}$$

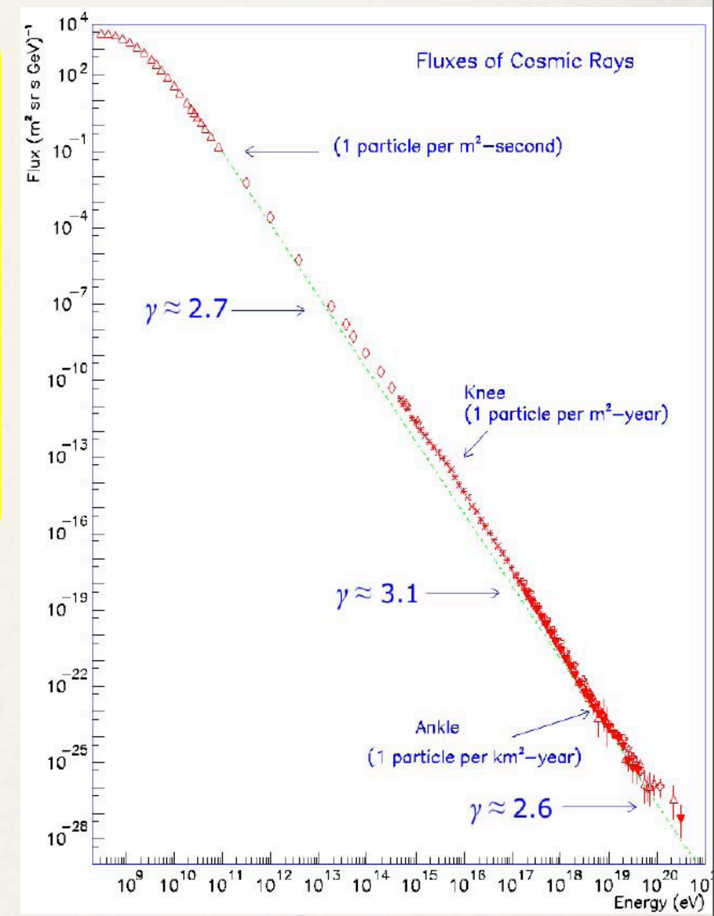

Top*: Flux tube geometry for a galactic wind perpendicular to the disk; shown is the area cross section; H is the opening distance of the flux tube from the disk*
Bottom*: observed CR differential energy spectrum*

CR acceleration beyond the "Knee" (III)

- **singular perturbation analysis:**
- use a power law ansatz: f ~ $p^{-a} R(t)^{b}$
- use ε=ϰ/(R dR/dt) as perturbation parameter
- match "inner" to "outer" solution, e.g. expand
$$f(\xi) = \sum_i f_i(\xi)\epsilon^i$$
- we obtain a correction term to the CR power law index *a (for R → 0 pert. theory breaks down)*
- *a* tends rapidly to *a*=5 for increasing R (or z) as required
- **Conclusion**: increased star formation in the disk can cause shock waves to propagate into the halo and **post-accelerate** GCRs
- HCRs can explain observed energies **and** the steepening of the spectrum

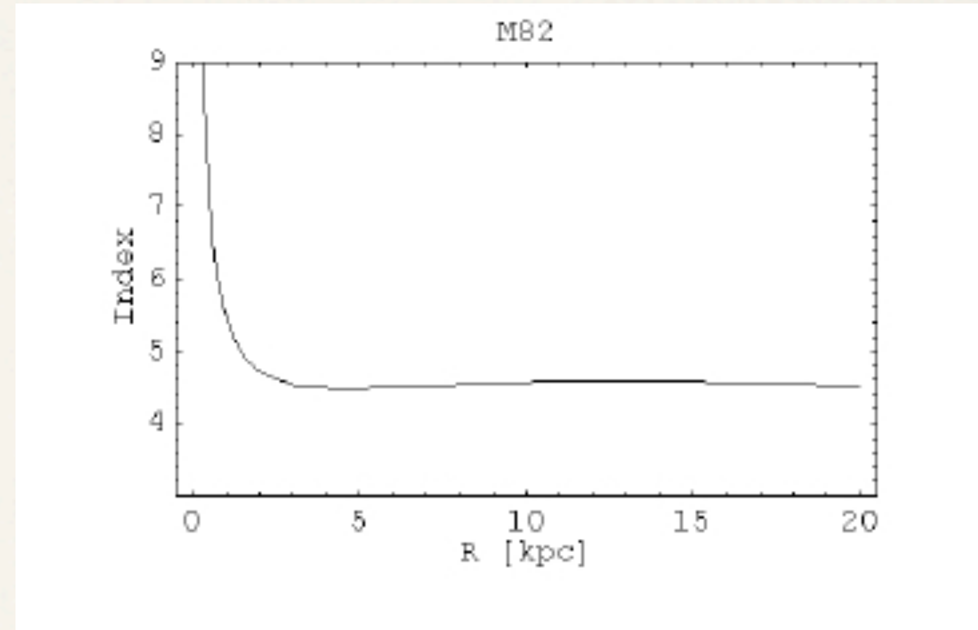

Zwettler & Breitschwerdt (2010)

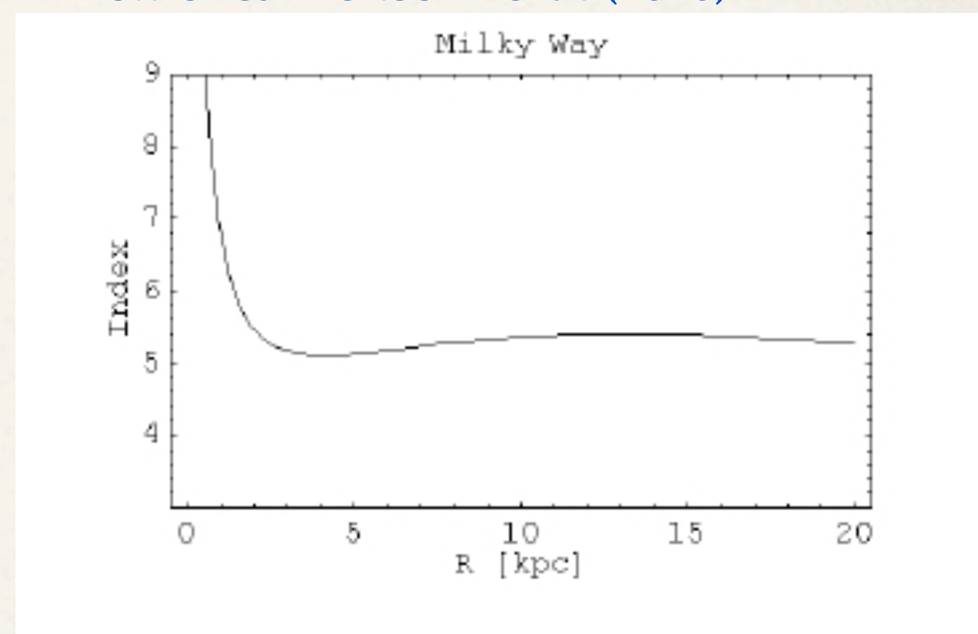

Top: *Power law index of CR particle momentum spectrum in a galactic wind outflow (in flux tube coordinates) modified by increasing star formation*
Bottom: *same, but for Milky Way parameters*

Summary & Conclusions

- ISM is a highly **turbulent** compressible medium ➔ **nonlinear** dynamics
- **High resolution** (parallel computers, AMR) simulations necessary
- **Requirements**: (i) box sufficiently **large** not to be dominated by boundary conditions, (ii) time evolution **long** enough to wipe out memory of initial conditions, (iii) ensure that results are **resolution independent**
- SN dominated ISM shows structures on **all** scales (**turbulent coupling**)
- **Turbulence** fed by **on-going star formation**
- **galactic fountain** acts as pressure release valve, reducing pressure in the disk ➔ volume filling factor of hot gas is reduced
- ISM is not in pressure equilibrium, flow is **ram pressure** dominated
- interstellar clouds are **shock compressed** (transient) layers
- substantial amount of ISM in **thermally unstable** temp. range (e.g. 50% of HI mass)
- enhanced star formation and **superbubbles** drive **galactic winds**
- winds can explain **X-ray and radio halos** ➔ **thermally & dynamically self-consistent** models ➔ flattening of **radio spectral index** due to **advection flow**
- **CR acceleration** beyond the "**knee**" ➔ wind shocks can explain energies & spectrum!

Thank you for your attention!

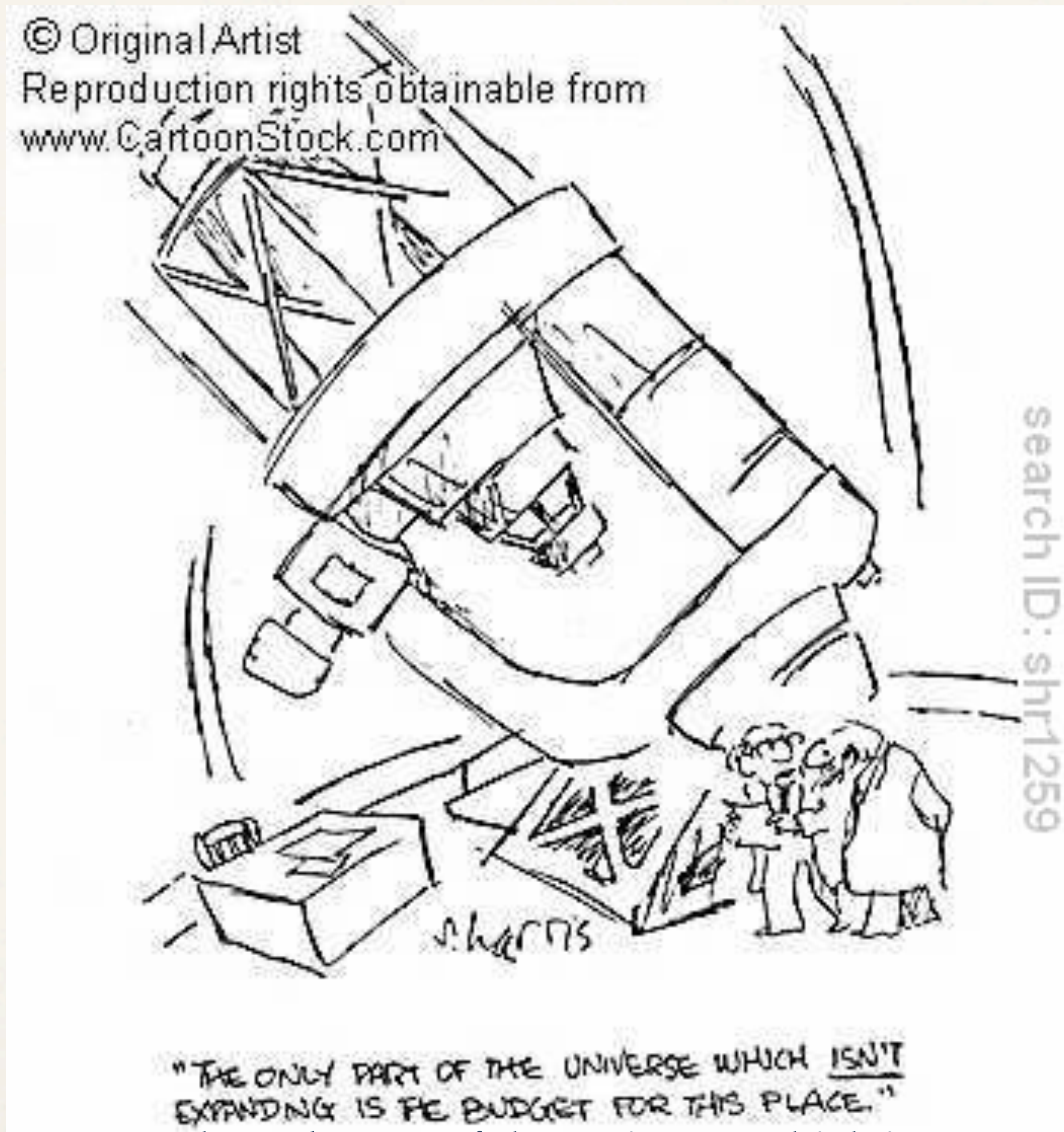

"The only part of the Universe which isn't expanding is the budget for this place."